# 博士論文

Development and Mechanistic Investigations of Oxo-Catalyst
Using Ruthenium as a Key Component

(ルテニウムを鍵とする新しいオキソ触媒の開発と反応機構研究)

Kohei Takahashi

高橋　講平

# Table of Contents

**Chapter 4 Tandem Hydroformylation/Hydrogenation of Terminal Alkenes to *Normal*-Alcohols Using a Rh/Ru Dual Catalyst System**

# List of abbreviations

**A4N3**
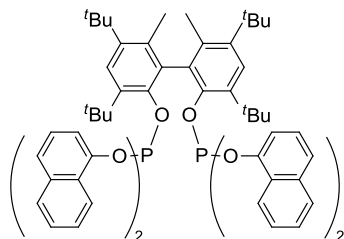


**Ac**  acetyl

**BISBI**

2,2'-bis(diphenylphosphinomethyl)-

1,1'-biphenyl
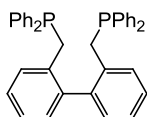


**Cp**  cyclopentadienyl

**Cp\***

1,2,3,4,5-pentamethylcyclopentadienyl

**CO**  carbon monoxide

**DFT**  Density functional theory

**Diglyme**  1,2-dimethoxyethane

**DMPE**

1,2-bis(dimethylphosphino)ethane

**DMA**  *N,N*-dimethylacetamide

**DPPE**

1,2-bis(diphenylphosphino)ethane

**DPPP**

1,3-bis(diphenylphosphino)propane

**Et**  ethyl

**equiv.**  equivalent

**ESI**  electrospray ionization

**GC**  gas chromatography

**$^i$Pr**  isopropyl

**IR**  infrared

**M**  mol per liter

**MCC**

Mitsubishi Chemical Corporation

**N. D.**  not determined

**NMP**  *N*-methylpyrrolidone

**NMR**  nuclear magnetic resonance

**$^t$Bu**  tert-butyl

**Ph**  phenyl

**PPN**

bis(triphenylphosphoranilidene)-

ammonium

$Ph_3P=\overset{\oplus}{N}=PPh_3$
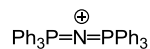
**R**  alkyl or aryl

**r.t.**  room temperature

| | |
|---|---|
| **S/N** | signal-to-noise ratio |
| **TBS** | tert-butyldimethylsilyl |
| **TCI** | Tokyo Chemical Industry Co., Ltd. |
| **THF** | tetrahydrofuran |
| **THP** | tetrahydropyranyl |
| **TOF** | turnover frequency |
| **UCC** | Union Carbide Corporation |

**XANTPHOS**

4,5-bis(diphenylphosphino)-9,9-

dimethylxanthene
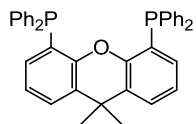
# 1 Introduction

**Introduction**

**1-1 Hydroformylation**

Mankind has been enormously benefitted from chemical industry over 100 years. Now, it is based on fossil resources such as petroleum oil, natural gas, or coal. One of the chief building blocks is carbon monoxide. Carbon monoxide is available in an admixture with dihydrogen, which is referred to as synthesis gas. As a mixture or after separation from dihydrogen, it is utilized in a number of syntheses of chemical compounds such as hydrocarbons (Fischer-Tropsch synthesis), esters, carboxylic acids, aldehydes, etc. Hydroformylation is a reaction giving aldehyde from an alkene and $H_2$/CO in the presence of transition metal catalyst (Scheme 1-1).

**Scheme 1-1.** Hydroformylation of an alkene
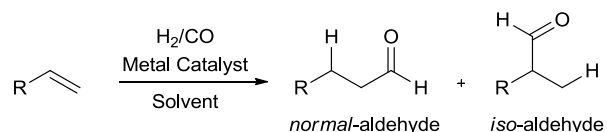


This reaction was originally reported by Roelen in 1938,[1] and commercialized as a method to produce aldehyde. Currently, hydroformylation is the most widely used method for aldehyde synthesis, and more than 10 million tons of aldehydes are annually produced in the world. Representative examples of industrial uses and consumptions of aldehydes are summarized in the Tables 1-1 and 1-2. Since *normal*-aldehyde is more desired than *iso*-aldehyde, extensive devotions have been paid on the development of *normal*-selective hydroformylation catalyst. Another target of hydroformylation is the enantio-selective hydroformylation since α-carbon of carbonyl of *i*-aldehyde could be a chiral center. That is potentially a useful tool for fine chemical synthesis.[2]

4

**Table 1-1** Summary of industrial use of aldehydes produced by hydroformylation

| aldehyde | Uses |
|---|---|
| propanal[3] | Trimethylolethane |
| butanals[4] | 1-butanol[5] for solvent, plastisizer etc. |
| | 2-ethylhexanol[6] for plastisizer |
| pentanals[7] | 1-pentanol for solvent, plasticizers, lubricants etc. |
| $C_6$ aldehydes[7] | alcohol, carboxylic acid |
| $C_7$ aldehydes[7] | α-amylcinnamaldehyde for perfume |
| | heptanoic acids or esters for lubricants |
| $C_8$ aldehydes[7] | citrus oils or α-hexylcinnamaldehyde for perfume |
| | alcohols for plasticizer |
| | *N*-(2-ethylhexyl)aniline for vulcanizing agents and antioxidants for rubber |
| | sodium 2-propylpentanoate for antiepileptic |
| $C_9$ aldehydes[7] | perfume |
| | intermediate for plasticizer |
| $C_{10}$ aldehydes[7] | intermediates for *iso*-decanol and *iso*-decanoic acid |
| | intermediates for perfume, medicine, polymer, and pesticide. |
| $C_{11}$ aldehydes[7] | intermediates for perfume |
| | intermediates for medicine, fungicides, plant growth regulators, |
| | bactericides, and disinfectants. |
| $C_{12}$-$C_{18}$ aldehydes[8] | alcohols for detergent |

**Table 1-2** Summary of consumption of aldehydes produced by hydroformylation in 1998 ($10^3$ t/y)[7]

| | Western Europe | United States | Japan |
|---|---|---|---|
| Propanal | 12 | 183 | 1 |
| *n*-butanal | 1274 | 1178 | 622 |
| *i*-butanal | 128 | 263 | 72 |
| Pentanals | 12 | 35 | 105 |
| $C_6$-$C_{13}$ aldehydes | 460 | 430 | 53 |
| (the amounts are those of alcohols for plasticizers) | | | |
| $C_{12}$-$C_{18}$ aldehydes | 174 | 215 | 53 |
| (the amounts are those of alcohols for detergents) | | | |
| $C_7$-$C_9$ oxo fatty acids | 12 | 44 | - |
| Others | 80 | 20 | - |

## 1-1-1 Industrially used catalyst for hydroformylation

Rolen's first discovery of hydroformylation was cobalt-based catalyst and chemical plant by using cobalt was initially commercialized. Since then, many kinds of transition metal elements such as rhodium,[9a] iridium,[9b] iron,[9c] ruthenium,[9d] osmium,[9e] palladium,[9f] and platinum[9g] have been reported to have activity for hydroformylation. One of the most important advances was the

development of phosphine-modified cobalt and rhodium catalysts patented in 1966 by Shell Oil Company.[10] It claimed that when a phosphine ligand was used as a catalytic additive with cobalt or rhodium, activities and selectivities of hydroformylation were significantly changed depending on the structure of the phosphine ligand. Importantly, phosphine-modified systems tend to exhibit higher selectivity to *normal*-aldehyde over *iso*-aldehyde (the ratio is defined as *n/i* ratio here), which meets industrial demand. Since the phosphine-modified rhodium system is superior to the cobalt system in terms of selectivity and activity, it became used more widely and partially replaced the traditional cobalt-based processes. Currently, phosphine-modified rhodium catalysts are most commonly used, but still some processes are operated by using cobalt-based catalysts.[11a]

## 1-1-2 Mechanistic aspects of hydroformylation

Reaction mechanism of rhodium catalyzed hydroformylation is illustrated in Scheme 1-2.[11] As a precursor, $Rh(I)XL_3$ (X: anionic ligand, L: neutral ligand) type complex is commonly used and tetracarbonylhydridorhodium is produced by losing HX and 3L under $H_2$/CO pressure. Dissociation of one carbon monoxide molecule allows coordination-insertion of an alkene to the Rh–H bond to form an alkylrhodium intermediate. Then, insertion of CO takes place and successive hydrogenolysis of the resulting Rh(acyl) species releases aldehyde and regenerates Rh–H.

**Scheme 1-2.** Reaction mechanism of hydroformylation catalyzed by rhodium
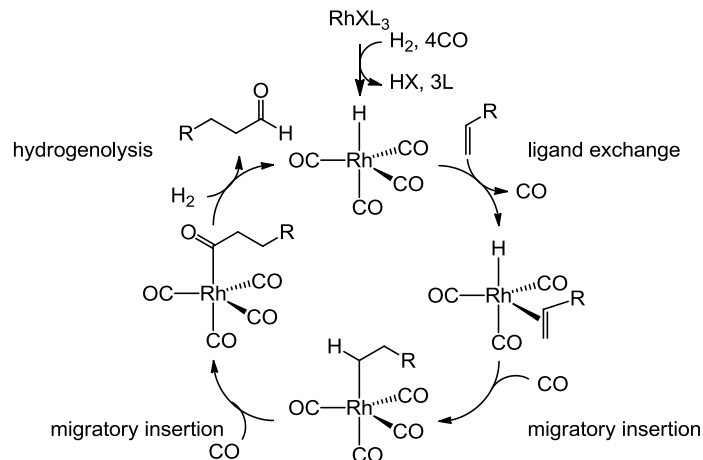


Under typical condition ($P_{H_2}$ and $P_{CO}$ ~1.0 MPa, temperature ~100 °C), initial loss of CO and coordination-insertion of an alkene is the rate-determining step. When the insertion of an alkene to the Rh–H bond takes place in 1,2-form as described in Scheme 1-2, the resulting aldehyde will be *normal*-aldehyde. On the other hand, when the insertion occurs in 2,1-form, *iso*-aldehyde is obtained (Scheme 1-3). With the unmodified rhodium catalyst, the *n/i* ratio is roughly one for 1-hexene.

**Scheme 1-3.** Mechanism to afford *iso*-aldehyde
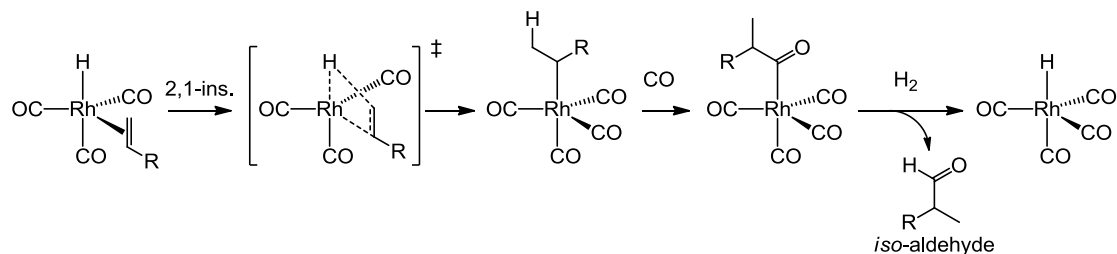
On the other hand, in phosphine-modified systems with an excess amount of phosphine ligands to rhodium (2 to 100 equivalent to rhodium), *n/i* ratios are improved. This effect is roughly explained by the larger steric repulsion between the phosphorus ligands and *iso*-alkyl or acyl group on rhodium than *normal*-counterparts (Scheme 1-4).[12] However, it is not clear which step in the catalytic cycle (Scheme 1-2) is the selectivity determining step.[11b]

**Scheme 1-4.** Insertion of an alkene to rhodium hydride in the presence of phosphorus ligands
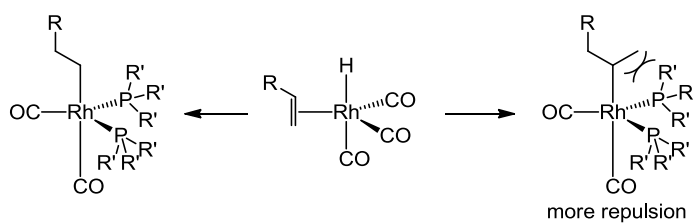


Among the various phosphorus ligands, triphenylphosphine-modified hydroformylation was first commercialized in 1970s, and still now commonly used. Investigations for developing better *normal*-selective catalyst were still paid significant attention. As a result, two important scaffolds of bidentate phosphorus ligands were developed, namely, BISBI[12] and XANTPHOS in 1987 and 1995 respectively (Figure 1-1).[14]
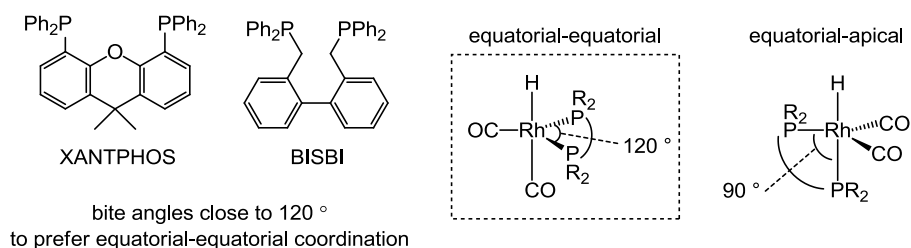


**Figure 1-1.** XANTPHOS and BISBI, and their preferred coordination geometry

When combined with rhodium, both of these ligands and their derivatives exhibited very high $n/i$ ratio (> 50) and high reaction rate (TOF > 500 h$^{-1}$). The high $n/i$ ratios were found to be explained by introducing a parameter of "natural bite angle",[15] which represents a range of favorable chelating angle of bisphosphorus ligand. In exact definition, it is a computationally calculated most favorable P-M-P angle for bidentate phosphorus ligands, where M is a dummy metal atom having no preference for any coordination geometry. Casey *et al*. and van Leeuwen *et al*. independently reported correlation between the bite-angle and the $n/i$ ratio.[13, 14] A more stable coordination geometry of pentacoordinated hydridoRh(I) is generally trigonal bipyramidal (tbp) rather than square pyramidal (sp) geometry. Insertion of an alkene takes place via RhH(alkene)L$_3$ (L = phosphine or CO). In this complex, the hydride ligand was always found at apical position and the alkene has to be at equatorial position to undergo insertion.[13b,14a] For bidentate phosphorus ligands, two chelation modes are possible, which are equatorial-equatorial and equatorial-apical. The ideal angle of L-M-L is 120° in the former case and 90° in the latter (Figure 1-2). Casey *et al*. reported that BISBI, which has a natural bite-angle of 113° preferably coordinates with an equatorial-equatorial form.[13b] With isotope experiments, they confirmed that coordination of an alkene to rhodium by ligand exchange and concerted migratory insertion of the alkene to Rh-H to give alkylrhodium intermediate (Scheme 1-2) were irreversible under typical conditions.[13c] Therefore, the $n/i$ ratio should be determined in this step. They proposed that when the bisphosphine is chelating with equatorial-equatorial form, both of the phosphorus atoms are close to the coordinating alkene and the hydride ligand. Therefore, steric effect to destabilize *iso*-alkyl Rh intermediate or transition state leading to *iso*-alkyl Rh intermediate is larger with equatorial-equatorial chelating bisphosphorus ligand (Figure 1-1).[13c] However, they also reported that molecular mechanics calculations failed to support the proposal.[13c]

a) equatorial-equatorial

both of the substituents on phosphorus atoms are close to the alkyl goup in the transition state or resulting intermediate

b) apical-equatorial

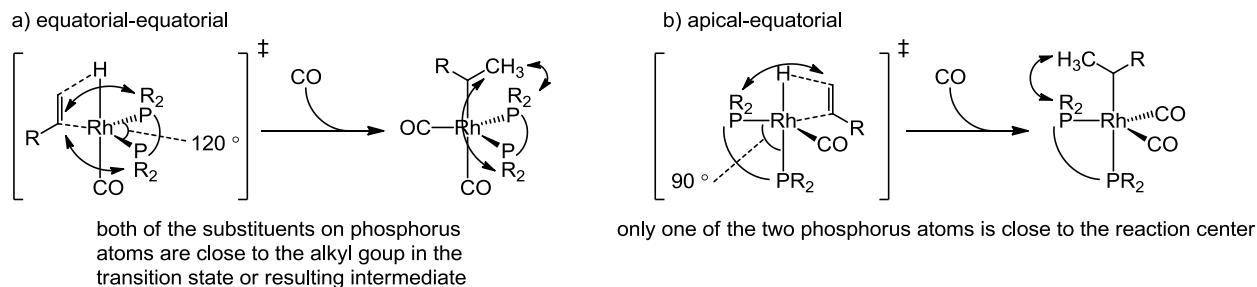only one of the two phosphorus atoms is close to the reaction center

**Figure 1-2.** Two possible transition states of the insertion of an alkene into a rhodium hydride with a bidentate phosphorus ligand

On the other hand, van Leeuwen *et al*. reported that equatorial-equatorial coordination is not the prerequisite for the high *n/i* ratio in the case of XANTPHOS and its derivatives.[14d] Their conclusion was that high *normal*-selectivity was simply a result of the steric congestion induced by the large bite angle to form a sterically less demanding linear alkyl rhodium species. They also performed DFT calculations to prove that the difference of the relative energies of the transition states to give *normal*- and *iso*-alkylrhodium species from Rh(CO)(alkene)(diphosphine) agrees with the high *n/i* selectivity of XNATPHOS derivatives.[14f]

In terms of catalytic activity, phosphite ligands are superior to phosphines. Since the dissociation of carbon monoxide is incorporated in the rate-determining step, acceleration of this step will increase the catalytic activity. Phosphite is more electron-withdrawing ligand compared to phosphine. Therefore, the electron density of the metal center coordinated by phosphites is relatively low compared to that of the phosphine complex. This results in weaker back donation from metal to carbon monoxide, which facilitates the dissociation of carbon monoxide. Consequently, rhodium complexes bearing bisphosphite ligands with BISBI-type backbone

exhibit high *n/i* ratio and catalytic activity. Two examples[16 17] are shown in Figure 1-3. With those systems, *n/i* ratio is higher than 50 and TOF is more than 1000 h$^{-1}$.
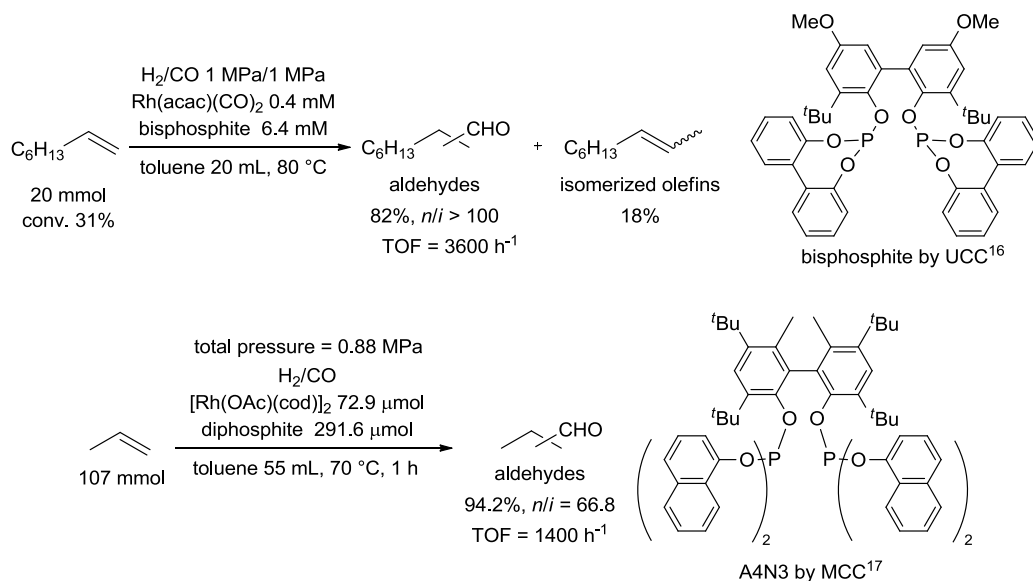


**Figure 1-3.** Representative examples of BISBI-type bisphosphite ligand

In summary, hydroformylation has been paid significant attention for decades as a method to prepare aldehydes since the discovery by Roelen. Industrial application was accomplished more than 50 years, while the development of better catalyst systems is still desired. Now the selectivities *normal*-aldehyde and catalytic activities of recent systems are satisfactory for the industrial use.

## 1-2 Hydrogenation of carbonyl groups by metal–ligand bifunctional catalysts

Metal-catalyzed hydrogenation of unsaturated compounds is among the most important synthetic reactions in view of not only academic interests but also industrial applications.[18] One of the earliest example of transition metal-based hydrogenation catalyst is Adam's catalyst derived from platinum oxide, which catalyzed the reaction in the solid-liquid surface.[19] Wilkinson introduced RhL$_3$Cl (L = neutral ligand), well known as "Wilkinson's catalysts", which were reported as well defined homogeneous hydrogenation catalyst for alkenes and alkynes.[20] Reaction mechanism was well investigated to establish the catalytic cycle drawn in Scheme 1-5.[20c, 20d]

**Scheme 1-5.** Hydrogenation of an alkene catalyzed by Wilkinson's catalyst
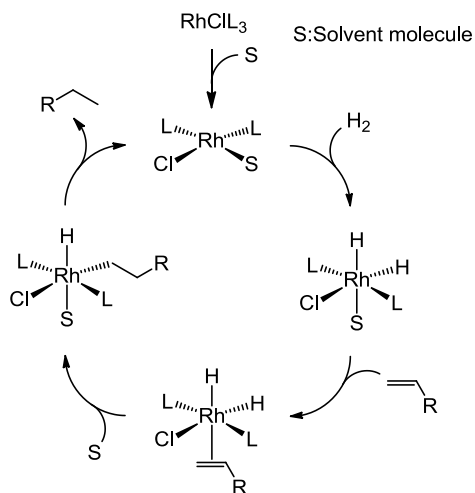


Since then, a number of homogeneous catalysts utilizing various tansition metals have been reported for hydrogenation of a variety of unsaturated substrates and many kinds of reaction mechanisms have been proposed for these systems. Among them, one of the relatively new type
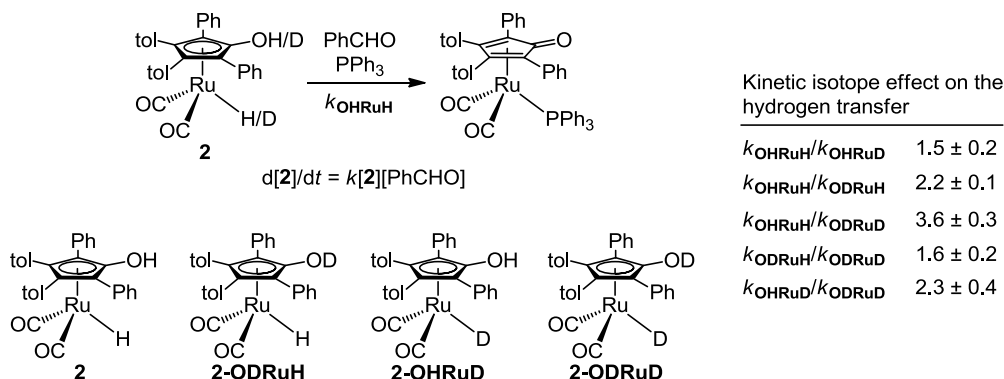
of hydrogenation catalysts is "metal–ligand bifunctional hydrogenation catalysts", in which dihydrogen is cooperatively activated by the metal center and its ligand. This type of hydrogenation catalyst was first reported by Shvo *et al.* (Scheme 1-6).[21] They reported that tricarbonyl(tetraphenylcyclopentadienone)ruthenium (**1**) affords dicarbonyl(tetraphenylhydroxycyclopentadienyl)hydridoruthenium (**2**) under dihydrogen pressure, and that mediates hydrogenation by transfer of its protic hydrogen on oxygen atom and hydridic hydrogen on the ruthenium center (Scheme 1-6).[21c] As a resting state, isolable ruthenium dimer (**3**) is formed, which supported the proposed mechanism,[21c] and this dimer is known as "Shvo's catalyst". The mechanism was thoroughly studied by Casey *et al.*[21e-21h] They proposed that the hydrogen transfer from (hydroxycyclopentadienyl)hydridoruthenium to carbonyl takes place in a concerted manner as illustrated in Scheme 1-6. In this type of mechanism, coordination of the substrate to ruthenium center is not necessary to undergo hydrogenation, and thus it is referred to as "outer-sphere mechanism". This mechanism was supported by various experiment.

For example, Casey prepared deuterated **2** having deuteriam both or either on the oxygen and ruthenium center, and observed the difference of the rate of the hydrogen transfer to an aldehyde.[21e] As a result, kinetic isotope effect was observed for both of the two hydrogen atoms. This fact indicates the concerted mechanism, where two hydrogen atoms are transferred to the aldehyde via single transition state.

**Scheme 1-6.** Proposed mechanism for the hydrogenation of an aldehyde by Shvo's hydrogenation catalyst in an outer-sphere mechanism
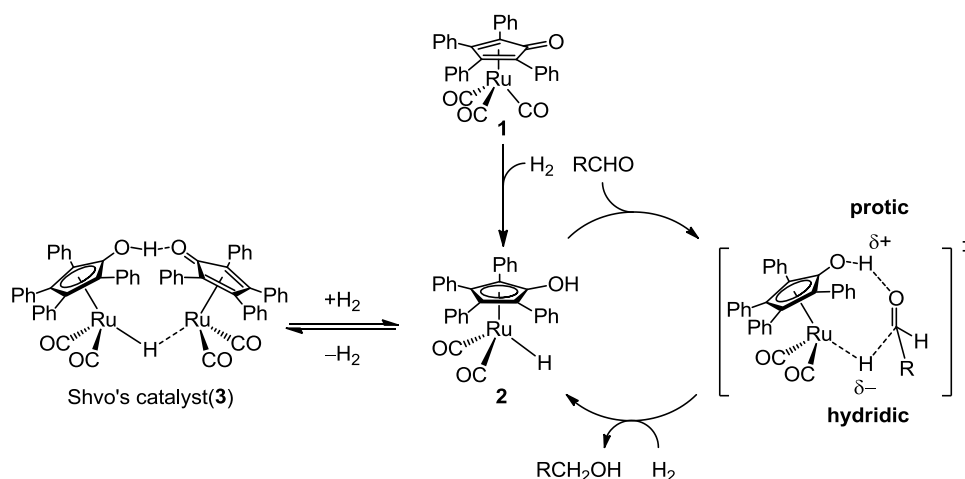


**Scheme 1-7.** Kinetic isotope effect on the hydrogen transfer from **2** to an aldehyde



$$d[\mathbf{2}]/dt = k[\mathbf{2}][\text{PhCHO}]$$

| Kinetic isotope effect on the hydrogen transfer | |
| --- | --- |
| $k_{OHRuH}/k_{OHRuD}$ | 1.5 ± 0.2 |
| $k_{OHRuH}/k_{ODRuH}$ | 2.2 ± 0.1 |
| $k_{OHRuH}/k_{ODRuD}$ | 3.6 ± 0.3 |
| $k_{ODRuH}/k_{ODRuD}$ | 1.6 ± 0.2 |
| $k_{OHRuD}/k_{ODRuD}$ | 2.3 ± 0.4 |

Another possible reaction mechanism is inner-sphere mechanism as drawn in Scheme 1-8. In this mechanism, aldehyde coordinates to ruthenium center with its oxygen and then the transfer of the two hydrogen atoms takes place. This mechanism was proposed by Shvo[21d] and Backväll.[21i] Backväll *et al.* supported this mechanism by the experiment indicated in Scheme 1-9. They performed stoichiometric reaction of **2** with imine having amino group. As a result, complexes **4** (mixture of isomers, *cis-* and *trans-* disubstituted cyclohexane, *cis*:*trans* ~ 1:1)

having coordinated amine was generated as the kinetic products at −80 °C. The coordinating

nitrogen atoms were the ones originated from the imino nitrogen. When the solution was warmed

up to −8 °C, another complex **5** (mixture of *cis-* and *trans-* disubstituted cyclohexane, *cis:trans* =

1.2:1) was formed as the thermodinamic products, where the other nitrogen atom was

coordinated to ruthenium center. The fact that the thermodinamically unfavorable isomers **4**

were obtained at low temperature indicated the initial hydryde transfer from the ruthenium center

to the imino carbon is accompanied by the coordination of the imino nitrogen to the ruthenium

center, which mean a inner-sphere mechanism. If the reaction was proceeded via an outer-sphere

mechanism without coordination of the imino nitrogen, the thermodinamically favorable isomer

**5** should be initially generated. However, they failed to obtain the corresponding alcohol

coordinated complex shown in the Scheme 1-8.

**Scheme 1-8.** Proposed mechanism for the hydrogenation of an aldehyde by Shvo's

hydrogenation catalyst in an inner-sphere mechanism
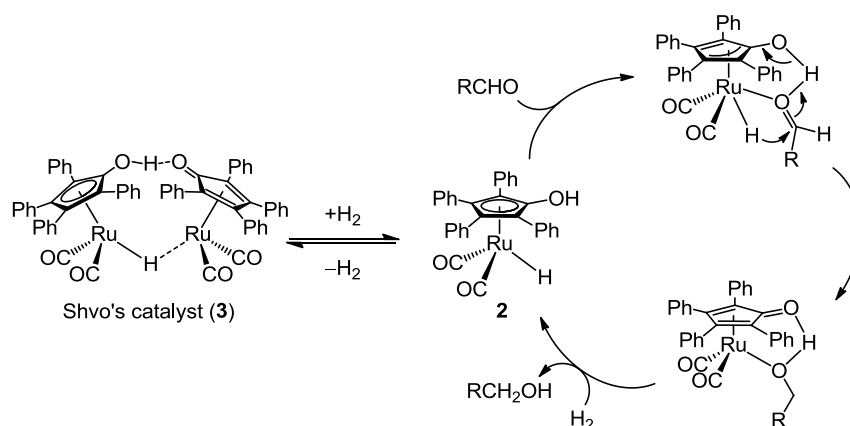
**Scheme 1-9.** Stoichiometric reaction of **2** with imine having amino group
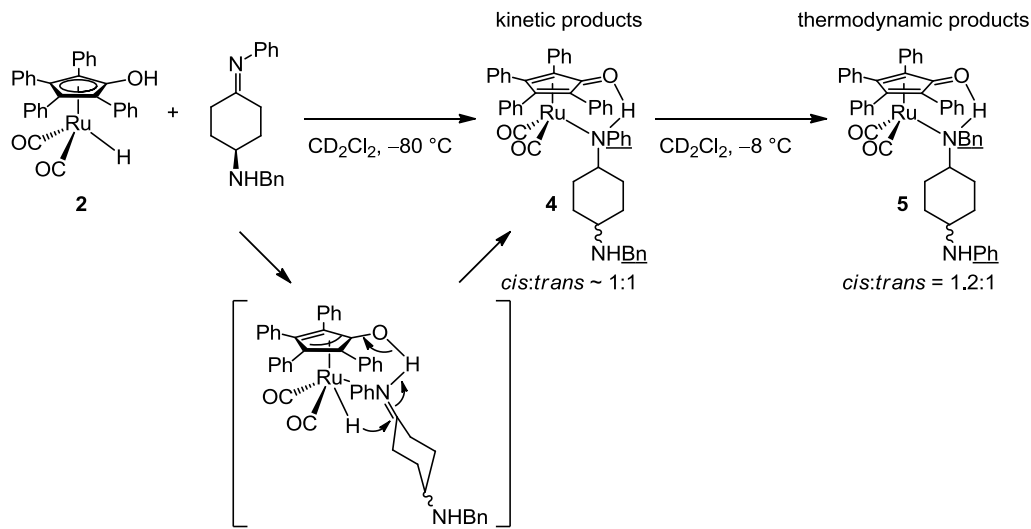


Computational studies about the reaction mechanism were carried out by Lledós *et al*. at density functional theory level by means of the hybrid B3LYP functional (basis sets were 6-31 for H, Lanl2dz for Ru, and 6-31(d,p) for other elements).[21j] They calculated the energy profiles of the hydrogenation of formaldehyde by a model coumpound for Shvo's catalyst (the phenyl groups on the Cp-ring were substituted with hydrogens) via an outer-sphere and an inner-sphere mechanism (Figure 1-4).
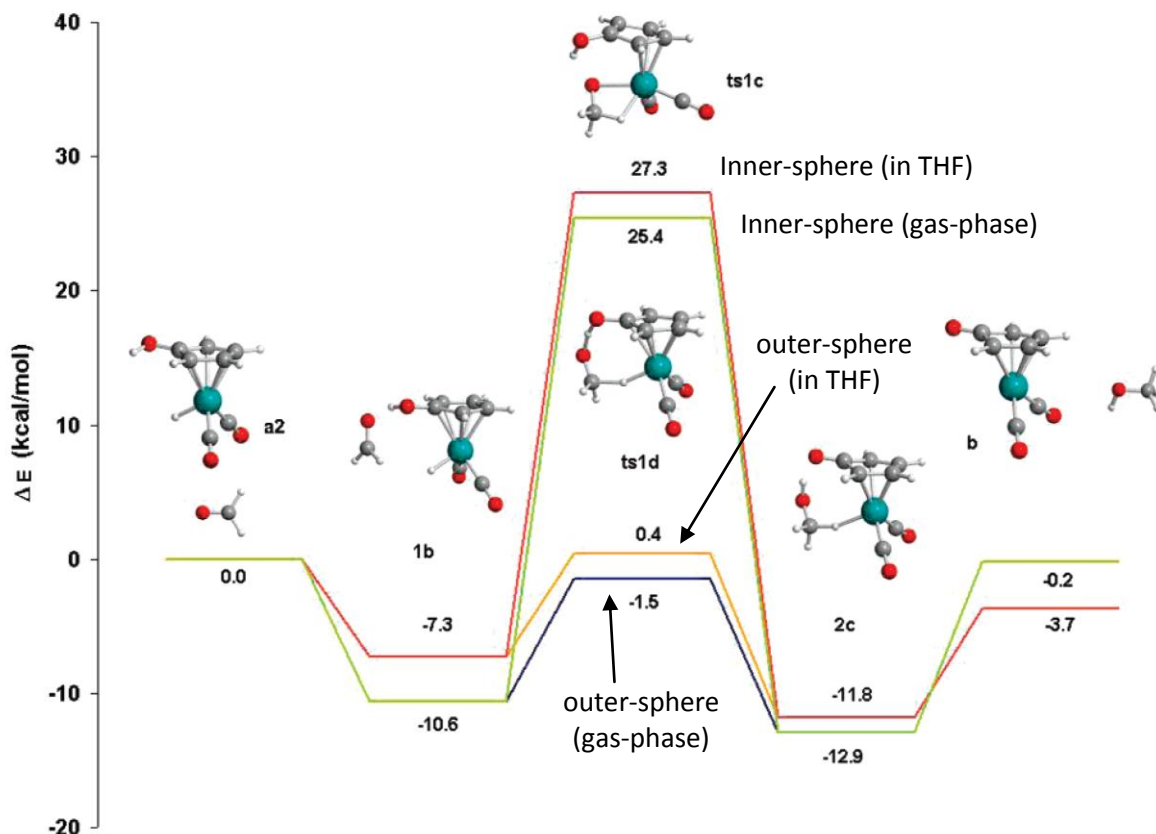
**Figure 1-4.** Computationally calculated energy profiles of hydrogenation via outer-sphere and inner-sphere hydrogen transfer in gas-phase or THF.

The result clearly showed outer-sphere mechanism is the preferable pathway in hydrogen transfer. They also performed computational calculations for the hydrogenations of imine, ethene, and acetylene.[21k] Outer-sphere mechanisms were suggested to be more favorable for these substrates.

Metal–ligand bifunctional type catalysts played important roles as highly enantioselective hydrogenation catalysts for carbonyl compounds as developed by Noyori *et al.*[18,22] They reported ruthenium complexes coordinated by a chiral diamine and/or a chiral bisphosphine, which are metal–ligand bifunctional type hydrogenation catalyst (Figure 1-5). Similar to Shvo's

hydrogenation catalyst, the protic hydrogen on the nitrogen and hydridic hydrogen on ruthenium center were experimentally[23] and computationally[24] proven to be transferred to C=O of ketone in an outer-sphere mechanism.
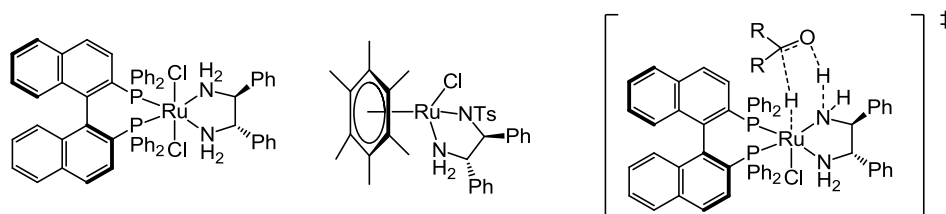


**Figure 1-5.** Examples of enantioselective hydrogenation catalysts reported by Noyori *et al*. and proposed transition state of hydrogen transfer

As for chemoselectivity, hydrogenation catalysts of outer-sphere mechanisms are known to be more active for hydrogenation of polar double bonds such as C=O or C=N than C=C.[25] For example, Noyori reported selective hydrogenation of carbonyl compounds bearing a C=C bond to corresponding unsaturated alcohols in high yields.[25a]

**Scheme 1-10.** Chemoselective hydrogenation of C=O in the presence of C=C
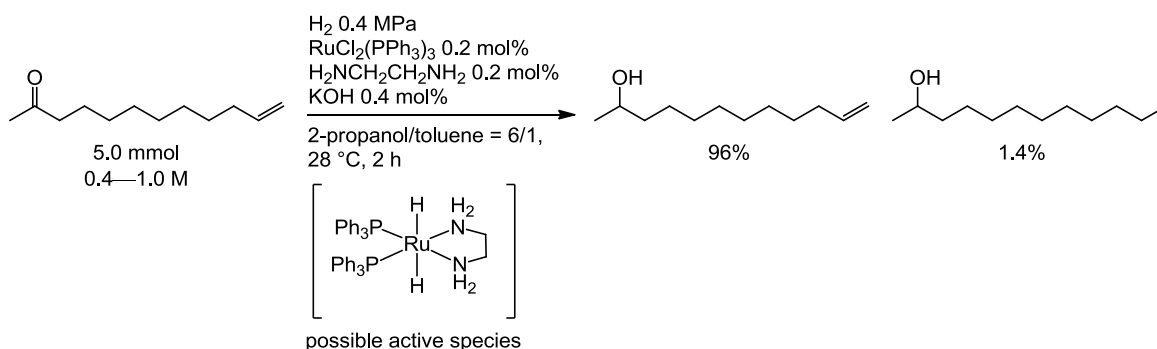
The theoretical calculations by Lledós explained the chemoselectivity. Based on model complex for Shvo's catalyst,[21j, k] barrier of transition state of the concerted hydrogen transfer to formaldehyde, imine, ethene, and acetylene were calculated as 9.1, 11, 17.9, and 18.5 kcal/mol respectively (Figure 1-6). Altough it is not clearly mentioned in the literature, the lower activation energies for polar double bonds than less polar double bonds might be ascribed to dipole–dipole interactions between the $H^{\delta+}$ and $H^{\delta-}$ on **2** and the $C^{\delta+}=X^{\delta-}$ bond of substrates.
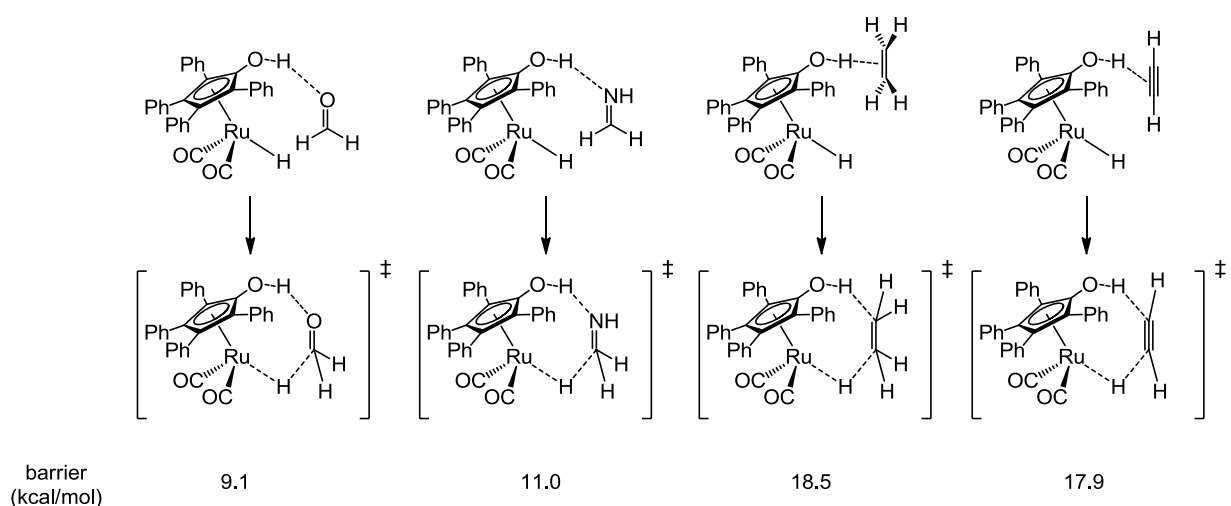


**Figure 1-6.** Barriers for concerted hydrogen transfer to unsaturated double bond via outer-sphere mechanisms

Another recent example of a metal–ligand bifunctional hydrogenation catalyst (not via outer-sphere mechanism) is PNN-pincer ruthenium complex (**4**) developed by Milstein *et al.*[26] The proposed catalytic cycle for hydrogenation of aldehyde is shown in Scheme 1-11. Activation of dihydrogen is cooperatively accomplished by the ruthenium center and the carbon on the ligand backbone. Coordination insertion of C=O bond takes place via dissociation of the tethered amino group from ruthenium center. Alcohol was released with deprotonation from methylene linker of

phosphinomethyl group and **4** is regenerated. This catalyst is effective for hydrogenation of ester,[26a] amide,[26b] formate,[26c] and carbonate[26c] under relatively mild conditions.

**Scheme 1-11.** Proposed reaction mechanism of hydrogenation of carbonyl compounds by Milstein's catalyst
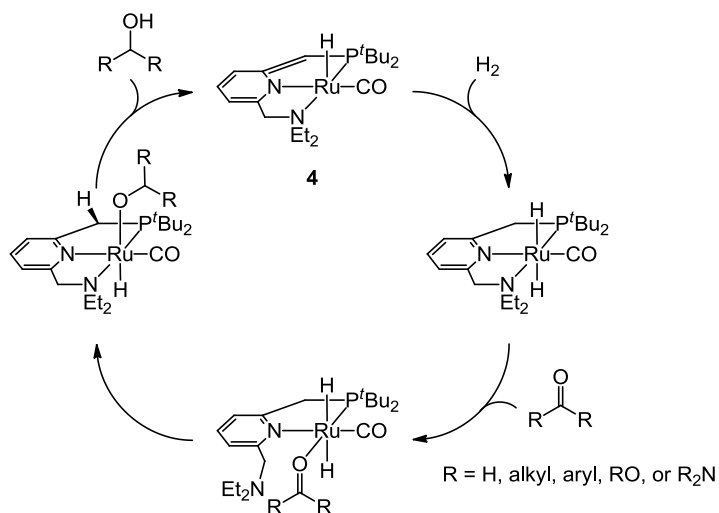


In summary, metal–ligand bifunctional-type hydrogenation catalysts exhibit unique activities and chemoselectivities. Close investigations on the reaction mechanisms have contributed to understand the origins of such features. Metal–ligand bifunctional hydrogenation catalysts are still paid much attention, and further applied to hydrogenation of other classes of unsaturated compounds such as carbon dioxide.[27]

**1-3 Applications of Shvo's catalyst in multiple catalyst systems for tandem reaction**

In the conventional organometallic catalysis, a single active species mediates one specific conversion. In contrast, combination of multiple catalysts for one-pot multistep conversion would provide more advantageous synthetic process by reducing required energy, processing times, and waste.[28] In this purpose, Shvo's catalyst and its derivatives are recently paid more attention as a good candidate. For example, Bäckvall *et al.* combined Shvo's catalyst with enzyme for dynamic kinetic resolution of secondary alcohols (Scheme 1-12).[29] In this catalysis, *R* and *S* enantiomers of a secondary alcohol are equilibrated by the racemization activity of Shvo's catalyst, and the enzymatic acetylation takes place selectively to one of the enantiomers. As a result, both enantiomers of the starting secondary alcohol are converted to the single enantiomer product. The requirements for the metal catalyst is exhibiting racemization activity under suitable conditions for enzymatic acetylation, which is relatively neutral, at low temperature, in the presence of water, etc., and Shvo's catalyst meets these requirements. One of the examples utilizing Novozym,[30] which is a enantioselective acetylation catalyst, is shown in Scheme 1-12. [29b]

**Scheme 1-12.** Dynamic kinetic resolution of racemic secondary alcohol to enantiomerically pure acetate
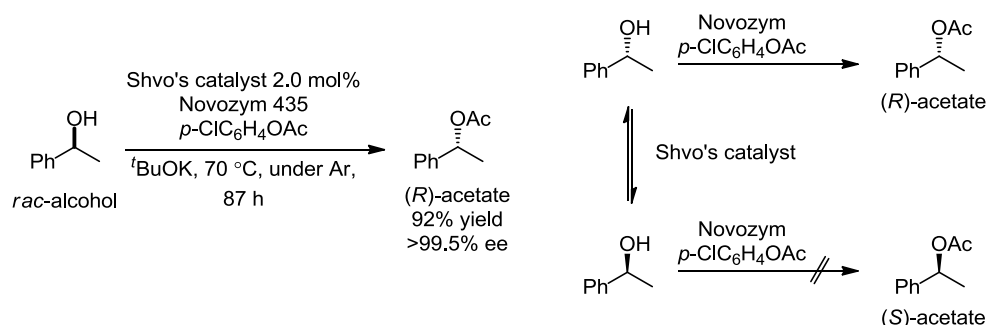


Very recently, Grubbs *et al.* combined palladium and copper-based Wacker oxidation catalyst and Shvo's catalyst for one-pot tandem Wacker oxidation/transfer hydrogenation of alkenes to alcohols (Scheme 1-13).[30] Since this catalyst system selectively gives *normal*-alcohols, it is formally a catalytic anti-Markovnikov hydration of an alkene, which is a very important challenge facing transition metal catalysis. The key to success was that Shvo's catalyst was compatible with the oxidizing condition for Wacker oxidation.

**Scheme 1-13.** Tandem aldehyde selective Wacker oxidation/hydrogenation of an alkene to *normal*-alcohol
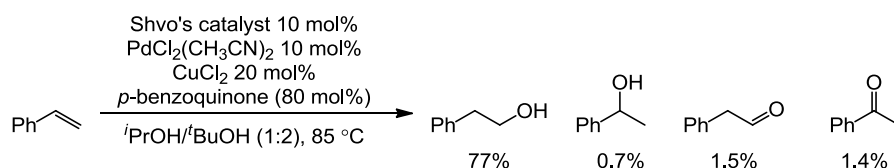


Similarly, Herzon *et al.* combined ruthenium-based aldehyde selective hydration catalyst for alkyne[32] and Shvo's catalyst to achieve one-pot tandem hydration/transfer hydrogenation of alkynes to *n*-alcohols (Scheme 1-14).[33]

**Scheme 1-14.** Tandem aldehyde selective hydration/hydrogenation of alkyne to *normal*-alcohol
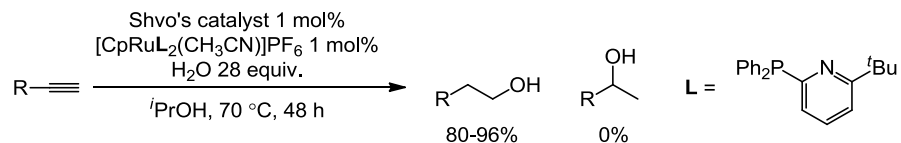


In these examples, Shvo's catalyst hydrogenates aldehydes, but did not react with alkenes or alkynes, which represents the chemoselectivity of hydrogenation towards polar unsaturated bonds, mentioned in the previous section.

In summary, Shvo's catalyst is a promising candidate for multiple catalyst system for tandem reactions including a hydrogenation step. This utility is ascribed to the better chemoselectivity to C=O hydrogenation over C=C and C≡C, independency from base, robustness against water or oxidant, relatively high activity at low temperatures, etc. Further investigation of Shvo's catalyst would provide a new synthetic method superior to conventional ones.

23

## 1-4 Research subjects of this dissertation

For hydroformylation, the selectivity to $n$-aldehyde and reaction rate are almost saturated by Rh/bisphosphine or bisphosphite systems, and thus, recent research interests are more focused on the improvement of other aspects. For example, recent increase of global demand for rhodium metal is enhancing the price of this already expensive metal. Therefore, hydroformylation catalyst employing other metal is desired. The use of cobalt has longer history than rhodium. Although the selectivity to $n$-aldehyde and the reaction rate is generally lower than rhodium, it is still industrially used. As for other metals, ruthenium,[9d] iridium, [9b] and palladium[9f] are recently paid more attention than before. Iron, platinum,[9b] and osmium[9e] were also reported but activities are low.

Another issue is simplification of the process operation. As mentioned above, parts of synthesized $n$-aldehydes by hydroformylation are converted to $n$-alcohols via successive hydrogenation (Scheme 1-15). This hydrogenation step is performed by copper or nickel heterogeneous catalyst using dihydrogen as a hydrogen source. One-pot conversion of an alkene to $n$-alcohol by the reaction with two equivalents of dihydrogen and carbon monoxide, namely, *tandem normal-selective hydroformylation/hydrogenation* would be advantageous in two reasons; 1) the number of reactor and distillation tower for hydrogenation will be reduced. 2) membrane separation of dihydrogen from synthesis gas will be omitted.[34] Although there has been many reports on such catalyst systems, none of them are efficient enough for industrial application.

**Scheme 1-15.** Research subjects of dissertation

**alternative to Rh?**



**One-pot?**
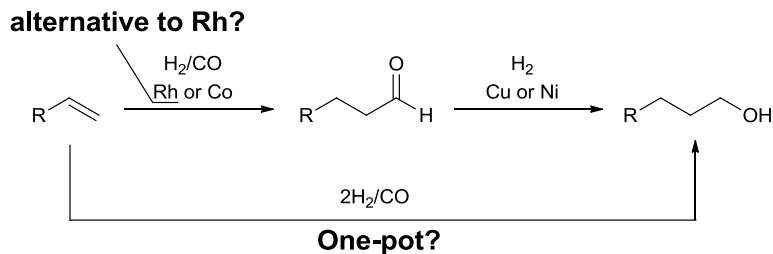
In this dissertion, the author developed three catalyst systems to solve these problems using cyclopentadienylruthenium as a key structure.

1) The author developed cyclopentadienylruthenium/bisphosphine or bisphosphite systems for *normal*-selective hydroformylation (Chapter 2).[35]

**Scheme 1-16.** *Normal*-selective hydroformylation catalyzed by cyclopentadienylruthenium/bisphosphine systems
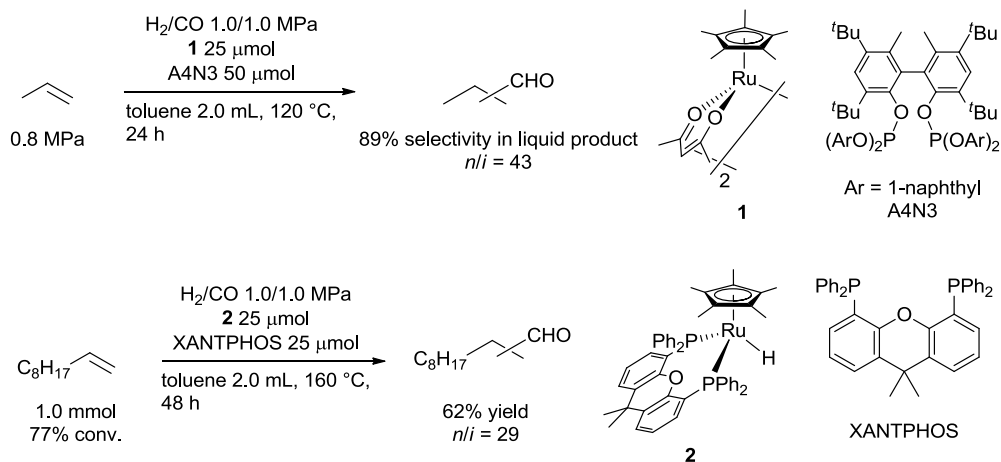


2) The author found hydroxycyclopentadienylruthenium/bisphosphine system for tandem *normal*-selective hydroformylation/hydrogenation (Chapter 3).[36b]

**Scheme 1-17.** Tandem *normal*-selective hydroformylation/hydrogenation catalyzed by cyclopentadienylruthenium/bisphosphine systems
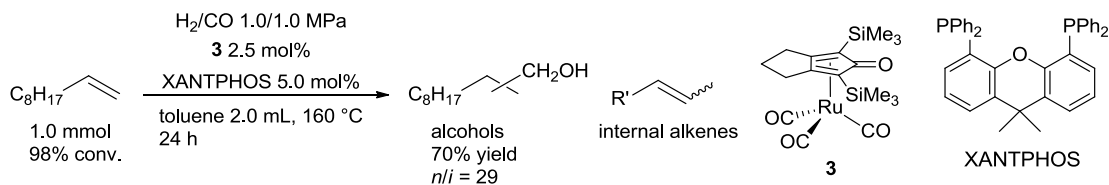


3) The author established rhodium/ruthenium dual catalyst system for high yielding and more facile tandem *normal*-selective hydroformylation/hydrogenation (Chapter 4).[36]

**Scheme 1-18.** Tandem *normal*-selective hydroformylation/hydrogenation catalyzed by Rh/Ru dual catalyst system
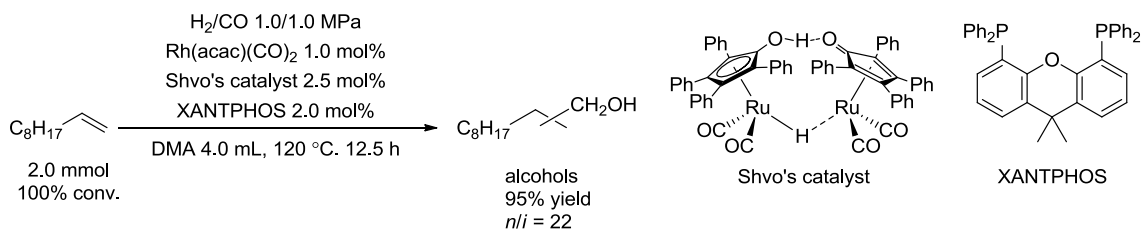


Mechanistic investigations for these systems were performed to obtain a clue for further improvement of the catalyst system.

## References

1) Roelen, O. US2127127, 1938.

2) a) Agbossou, F.; Carpentier, J. F.; Mortreux, A. *Chem. Rev.* **1995**, *95*, 2485. b) Klosin, J.; Landis, C. R. *Acc. Chem. Res.* **2007**, *40*, 1251.

3) Papa, A. J., Propanal: *Ullmann's Encyclopedia of Industrial Chemistry*; Wiley-VCH Verlag GmbH & Co. KGaA: 2000.

4) Cornils, B.; Fischer, R. W.; Kohlpaintner, C., Butanals: *Ullmann's Encyclopedia of Industrial Chemistry*; Wiley-VCH Verlag GmbH & Co. KGaA: 2000.

5) Hahn, H. D.; Dämbkes, G.; Rupprich, N.; Bahl, H., Butanols: *Ullmann's Encyclopedia of Industrial Chemistry*; Wiley-VCH Verlag GmbH & Co. KGaA: 2000.

6) Bahrmann, H.; Hahn, H.-D.; Mayer, D., 2-Ethylhexanol: *Ullmann's Encyclopedia of Industrial Chemistry*; Wiley-VCH Verlag GmbH & Co. KGaA: 2000.

7) Kohlpaintner, C.; Schulte, M.; Falbe, J.; Lappe, P.; Weber, J., Aldehydes, Aliphatic: *Ullmann's Encyclopedia of Industrial Chemistry*; Wiley-VCH Verlag GmbH & Co. KGaA: 2000.

8) Falbe, J.; Bahrmann, H.; Lipps, W.; Mayer, D., Alcohols, Aliphatic: *Ullmann's Encyclopedia of Industrial Chemistry*; Wiley-VCH Verlag GmbH & Co. KGaA: 2011.

9) (a) Evans, D.; Osborn, J. A.; Wilkinson, G. *J. Chem. Soc. A.* **1968**, 3133. (b) Schiller, G. DE953605, 1956. (c) Gresham, W. F.; Brooks, R. E.; Del, W. US2497303, 1945. (d) Evans, D.; Osborn, J. A.; Jardine, F. H.; Wilkinson, G. *Nature*, **1965**, 1203. (e) Alvila, L.; Pakkanen, T. A.; Pakkanen, T. T. *J. Mol. Cat.* **1992**, *73*, 325. (f) Konya, D.; Almedia, L. K. Q.; Drent, E. *Organometallics* **2006**, *25*, 3166. (g) Slaugh, L. H.; Hill, P.; Mullineaux, R. D. US3239571, 1966.

10) (a) Slaugh, L. H.; Hill, P.; Mullineaux, R. D. US3239569, 1966. (b) Slaugh, L. H.; Hill, P.; Mullineaux, R. D. US3239566, 1966.

11) (a) van Leeuwen, P. W. N. M.; Claver, C., *Rhodium Catalyzed Hydroformylation*. Springer - Verlag: 2000. (b) van Leeuwen, P. W. N. M., *HOMOGENIOUS CATALYSIS Understanding the Art*. Springer: 2004.

12) Brown, C. K.; Wilkinson, G. *J. Am. Chem. Soc. A.* **1968**, 2753.

13) (a) Devon, T. J. P., G. W.; Puckette, T. A.; Stavinoha, J. L.; Vanderbilt, J. J. US4694109, 1987. (b) Casey, C. P.; Whiteker, G. T.; Melville, M. G.; Petrovich, L. M.; Gavney, J. A.; Powell, D. R. *J. Am. Chem. Soc.* **1992**, *114*, 5535. (c) Casey, C. P.; Petrovich, L. M. *J. Am. Chem. Soc.* **1995**, *117*, 6007.

14) (a) Kranenburg, M.; van der Burgt, Y. E. M.; Kamer, P. C. J.; van Leeuwen, P. W. N. M.; Goubitz, K.; Fraanje, J. *Organometallics* **1995**, *14*, 3081. (b) van der Veen, L. A.; Boele, M. D. K.; Bregman, F. R.; Kamer, P. C. J.; van Leeuwen, P. W. N. M.; Goubitz, K.; Fraanje, J.; Schenk, H.; Bo, C. *J. Am. Chem. Soc.* **1998**, *120*, 11616. (c) Dierkes, P.; W. N. M. van Leeuwen, P. *J. Chem. Soc., Dalton Trans.* **1999**, 1519. (d) van der Veen, L. A.; Keeven, P. H.; Schoemaker, G. C.; Reek, J. N. H.; Kamer, P. C. J.; van Leeuwen, P. W. N. M.; Lutz, M.; Spek, A. L. *Organometallics* **2000**, *19*, 872. (e) Bronger, R. P. J.; Kamer, P. C. J.; van Leeuwen, P. W. N. M. *Organometallics* **2003**, *22*, 5358. (f) Carbo, J. J.; Maseras, F.; Bo, C.; van Leeuwen, P. W. M. N. *J. Am. Chem. Soc.* **2001**, *123*, 7630.

15) Casey, C. P.; Whiteker, G. T. *Isr. J. Chem.* **1990**, *30*, 299.

16) van der Veen, L. A.; Kamer, P. C. J.; van Leeuwen, P. W. N. M. *Angew. Chem. Int. Ed.* **1999**, *38*, 336.

17 Urata, H.; Itagaki, H.; Takahashi, E.; Wada, Y.; Tanaka, T.; Ogino, Y. JPH1045776, 1998.

18) (a) Zhang, X.; Chi, Yongxiang, Tang, W. C-H Bond Formation by Asymmetric and Stereoselective Hydrogenation. *Comprehensive Organometallic Chemistry*, III; Elsevier Ltd.:

Oxford, 2007; vol. 10, 1. (b) Kitamura, M.; Noyori, R. Hydrogenation and Transfer Hydrogenation. *Ruthenium in Organic Synthesis*, Wiley-VCH Verlag GmbH & Co. KGaA: Weinheim, 2004; 3. (c) *The Handbook of Homogeneous Hydrogenation*, de Vries, J. G. Elsevier, C. J., Eds.; Wiley-VCH Verlag GmbH & Co. KGaA: Weinheim, 2006. (d) Homogeneous Hydrogenation. *Organotransition Metal Chemistry: From Bonding to Catalysis*, Hartwig, J. F. Eds.; University Science Books: Sausalito, 2010, 575.

19) Voorhees, V. V.; Adams, R. *J. Am. Chem. Soc.* **1922**, *44*, 1397.

20) (a) Young, J. F.; Osborn, J. A.; Jardine, F. H.; Wilkinson, G. *Chem. Commun. (London)*, **1965**, 131. (b) Evans, D.; Osborn, J. A.; Jardine, F. H.; Wilkinson, G. *Nature* **1965**, *208*, 1203. (c) Osborn, J. A.; Jardine, F. H.; Young, J. F.; Wilkinson, G. *J. Chem. Soc. A* **1966**, 1711. (d) Baird, M. C.; Mague, J. T.; Osborn, J. A.; Wilkinson, G. J. *J. Chem. Soc.* **1967**, 1347.

21) (a) Blum, Y.; Shvo, Y. *Inorg. Chim. Acta* **1985**, *97*, L25. (b) Shvo, Y.; Czarkie, D. *J. Organomet. Chem.* **1986**, *315*, C25. (c) Shvo, Y.; Czarkie, D.; Rahamim, Y.; Chodosh, D. F. *J. Am. Chem. Soc.* **1986**, *108*, 7400. (d) Menashe, N.; Shvo, Y. *Organometallics* **1991**, *10*, 3885. (e) Casey, C. P.; Singer S.; Powell, D. R.; Hayashi, R. K.; Kavana, M. *J. Am. Chem. Soc.* **2001**, *123*, 1090. (f) Casey, C. P.; Johnson, J. B.; Singer, W. S.; Cui, Q. *J. Am. Chem. Soc.* **2005**, *127*, 3100. (g) Casey, C. P.; Strotman, N. A.; Beetner, S. E.; Johnson, J. B.; Priebe, D. C.; Guzei, I. A. *Organometallics,* **2006**, *25*, 1236. (h) Casey, C. P.; Beetner, S. E.; Johnson, J. B. *J. Am. Chem. Soc.* **2008**, *130*, 2285. (i) Samec, J. S. M.; Éll, A. H.; Åberg, J. B.; Privalov, T.; Eriksson, L.; Backväll, J.-E. *J. Am. Chem. Soc.,* **2006**, *128*, 14293. (j) Comas-Vives, A.; Ujaque, G.; Lledós, A. *Organometallics* **2007**, *26*, 4135. (k) Comas-Vives, A.; Ujaque, G.; Lledós, A. *Organometallics* **2008**, *27*, 4854.

22) (a) Ohkuma, T.; Ooka, H.; Hashiguchi, S.; Ikariya, T.; Noyori, R. *J. Am. Chem. Soc.* **1995**, *117*, 2675. (b) Hashiguchi, S.; Fujii, A.; Takehara, J.; Ikariya, T.; Noyori, R. *J. Am. Chem. Soc.* **1995**, *117*, 7562.

23) Casey, C. P.; Johnson, J. B. *J. Org. Chem.* **2002**, *68*, 1998.

24) (a) Yamakawa, M.; Ito, H.; Noyori, R. *J. Am. Chem. Soc.* **2000**, *122*, 1466. (b) Hedberg, C.; Kallstrom, K.; Arvidsson, P. I.; Brandt, P.; Andresson, P. G. *J. Am. Chem. Soc.* **2005**, *127*, 15083.

25) (a) Ohkuma, T.; Ooka, H.; Ikariya, T.; Noyori, R. *J. Am. Chem. Soc.* **1995**, *117*, 10417. (b) Ohkuma, T.; Koizumi, M.; Doucet, H.; Pham, T.; Kozawa, M.; Murata, K.; Katayama, E.; Yokozawa, T.; Ikariya, T.; Noyori, R. *J. Am. Chem. Soc.* **1998**, *120*, 13529.

26) (a) Zhang, J.; Leitus, G.; Ben-David, Y.; Milstein, D. *Angew. Chem. Int. Ed.* **2006**, *45*, 1113. (b) Balaraman, E.; Gnanaprakasma,B.; Shimon, L. J. W.; Milstein, D. *J. Am. Chem. Soc.* **2010**, *132*, 16756. (c) Balaraman, E.; Gunanathan, C.; Zhang, J.; Shimon, L. J. W.; Milstein, D. *Nat. Chem.* **2011**, *3*, 609.

27) (a) Lee, J. M.; Na, Y.; Han, H.; Chang, S. *Chem. Soc. Rev.* **2004**, *33*, 302. (b) Wasilke, J. C.; Obrey, S. J.; Baker, R. T.; Bazan, G. C. *Chem. Rev.* **2005**, *105*, 1001-1020. (c) Paull, D. H.; Abraham, C. J.; Scerba, M. T.; Alden-Danforth, E.; Lectka, T. *Acc. Chem. Res.* **2008**, *41*, 655-663; (d) Haibach, M. C.; Kundu, S.; Brookhart, M.; Goldman, A. S. *Acc. Chem. Res.* **2012**, *45*, 947-958. (e) Du, Z.; Shao, Z. *Chem. Soc. Rev.* **2013**, *42*, 1337.

28) (a) Pamies, O.; Bäckvall, J. E. *Chem. Rev.* **2003**, *103*, 3247. (b) Larsson, A. L. E.; Persson, B. A.; Bäckvall, J. E. *Angew. Chem. Int. Ed.* **1997**, *36*, 1211.

29) Johnson, C. R.; Sakaguchi, H. *Synlett,* **1992**, 813.

30) Cong, G.; Teo, P.; Wickens, Z. K.; Grubbs, R. H. *Science* **2011**, *333*, 1609.

31) (a) Wenzel, T. *J. Chem. Soc. Chem. Commun.* **1993**, 862. (b) Teo, P.; Wickens, Z. K.; Dong, G.; Grubbs, R. H. *Org. Lett.* **2012**, *14*, 3237.

32) Grotjahn, D. B.; Incarvito, C. D.; Rheingold, A. L. *Angew. Chem. Int. Ed.* **2001**, *40*, 3884.

33) Li, L.; Herzon, S. *J. Am. Chem. Soc.* **2012**, *134*, 17376.

34) Hiller, H.; Reimert, R.; Marschner, F.; Renner, H.-J.; Boll, W.; Supp, E.; Brejc, M.; Liebner, W.; Schaub, G.; Hochgesand, G.; Higman, C.; Kalteier, P.; Müller, W.-D.; Kriebel, M.; Schlichting, H.; Tanz, H.; Stönner, H.-M.; Klein, H.; Hilsebein, W.; Gronemann, V.; Zwiefelhofer, U.; Albrecht, J.; Cowper, C. J.; Driesen, H. E., Gas Production: *Ullmann's Encyclopedia of Industrial Chemistry*; Wiley-VCH Verlag GmbH & Co. KGaA: 2000.

35) Takahashi, K.; Yamashita, M.; Tanaka, Y.; Nozaki, K. *Angew. Chem. Int. Ed.* **2012**, *51*, 4383.

36) (a) Takahashi, K.; Yamashita, M.; Ichihara, T.; Nakano, K.; Nozaki, K. *Angew. Chem. Int. Ed.* **2010**, *48*, 4488. (b) Takahashi, K.; Yamashita, M.; Nozaki, K. *J. Am. Chem. Soc.* **2012**, *134*, 18746.
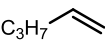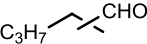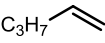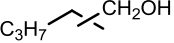
# Chapter 2
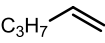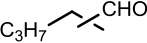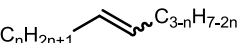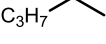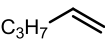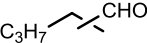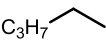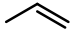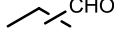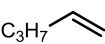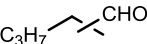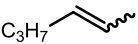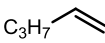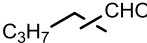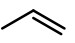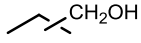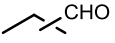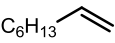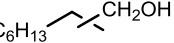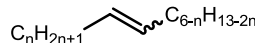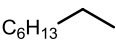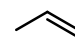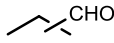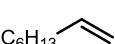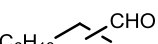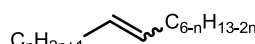
# Hydroformylation of Terminal Alkenes Catalyzed

# by Ru-Based Catalyst Systems

## 2 Hydroformylation of Terminal Alkenes Catalyzed by Ruthenium-Based Catalyst Systems

### 2-1 Background

As introduced in Chapter 1, hydroformylation catalysts not based on rhodium is desired. Among the other metals, there are relatively many reports about ruthenium-based system. However, in the previously reported systems, activities and selectivities of ruthenium catalysts are significantly lower than those of rhodium catalysts. Representative catalysts are summarized in Table 2-1.[1] The first well-defined ruthenium-based hydroformylation catalyst was Ru(CO)$_3$(PPh$_3$)$_2$,[1a] which was reported in 1965 by Wilkinson *et al*. In this report, 1-pentene was converted to a mixture of *n*- and *i*-aldehydes in 80% yield. There was no description about *n*/*i* ratio and side products. This discovery was followed by Shell Oil Company's patent, which claimed P$^n$Bu$_3$-modified ruthenium catalyst dominantly gave alcohols with low *n*/*i* ratio (93.6% conversion, *n*/*i* = 2).[1b] Although cyclopentadienyl ruthenium complexes were reported as a catalyst for hydroformylation, low yield of aldehyde (12%) and predominant formation of isomerized alkenes (53%) were reported.[1c] Most investigated scaffold of ruthenium hydroformylation catalyst was multinuclear ruthenium carbonyl complex. When dodecacarbonyltriruthenium (Ru$_3$(CO)$_{12}$) was used as a catalyst precursor, *n*/*i* ratio was increased up to 4.3, accompanied by hydrogenation of the alkene to the alkane in 12.8% yield.[1d] For propene, one of the most *normal*-selective catalysts is [NEt$_4$][HRu$_3$(CO)$_{11}$], which affords *n*-butanal almost quantitatively.[1e] On the other hand, for the substrates having a longer alkyl chain (>C$_4$), isomerization of the C=C bond to internal alkenes is problematic with this type of anionic complexes. Among the previously reported systems, [PPN][HRu$_3$(CO)$_{11}$] (PPN = Ph$_3$P=N$^+$=PPh$_3$

**Table 2-1.** Representative ruthenium-based hydroformylation catalysts

| complex (mmol) additive (mmol) | condition | substrate | product (yield, *n/i*) | byproduct (yield) | ref |
|---|---|---|---|---|---|
| Ru(CO)$_3$(PPh$_3$)$_2$1 | H$_2$/CO = 5/5 MPa, benzene, 100 °C, 15 h | C$_3$H$_7$ (alkene) | C$_3$H$_7$–CHO (>80%) | | 1a |
| RuCl$_3$/$^n$Bu$_3$P/NaOAc (0.07 M, 0.14 M, 0.35 M) | H$_2$/CO = 2/1 MPa, octane, 195 °C | C$_3$H$_7$ (alkene) (2.3 M) Conv. 93.6% | C$_3$H$_7$–CH$_2$OH *n/i* = 2 | | 1b |
| [($\eta^5$-C$_5$H$_5$)Ru(CO)$_2$]$_2$ (0.1 mmol) | H$_2$/CO = 4.3/4.3 MPa, toluene 5 mL, 135 °C | C$_3$H$_7$ (alkene) (3.5 mmol) | C$_3$H$_7$–CHO (12%, 2.9) | C$_n$H$_{2n+1}$–CH=CH–C$_{3-n}$H$_{7-2n}$ (53%); C$_3$H$_7$ (alkane) (4.7%) | 1c |
| Ru$_3$(CO)$_{12}$ (4.2 mmol) | H$_2$/CO = 4.5/5.0 MPa, benzene 25 mL, 150 °C | C$_3$H$_7$ (alkene) (25 mmol) | C$_3$H$_7$–CHO (83.0%, 4.3) | C$_3$H$_7$ (alkane) (12.8%) | 1d |
| [NEt$_4$][HRu$_3$(CO)$_{12}$] (0.17 mmol) | H$_2$/CO = 0.17/0.33 MPa, diglyme 10 mL, 70 °C, 66 h | (alkene) (0.5 MPa) | CHO (TON 49.2, 70.8) | | 1e |
| [PPN][HRu$_3$(CO)$_{12}$] (0.99 mmol) | H$_2$/CO = 15/15 MPa, DMF 10 mL, 150 °C, 16.5 h | C$_3$H$_7$ (alkene) (20 mmol) | C$_3$H$_7$–CHO (60.6%, 18) | C$_3$H$_7$ (isomerized alkene) (22.8%) | 1f |
| K[Ru(EDTA-H)Cl]•H$_2$O (3 mmolL$^{-1}$) | H$_2$/CO = 2.5/2.5 MPa, ethanol 113mL, water 28 mL, 130 °C, 12.0 h | C$_3$H$_7$ (alkene) (0.426 molL$^{-1}$) | C$_3$H$_7$–CHO (100%, >99) | | 1g |
| Ru$_3$(CO)$_{12}$ (6.0 mmol) 2,2'-bipyridyl (6.0 mmol) Bu$_4$PBr (29 mmol) | H$_2$/CO = 5.6/2.8 MPa, neat, 160 °C, 4 h | (alkene) (0.4 mol) | CH$_2$OH (89.5% of liquid, >99) | CHO (6.4%) | 1h |
| Ru$_3$(CO)$_{12}$ (6.0 mmol) 2,2'-bipyridyl (6.0 mmol) Bu$_4$PBr (29 mmol) | H$_2$/CO = 5.6/2.8 MPa, neat, 180 °C, 4 h | C$_6$H$_{13}$ (alkene) (0.2 mol) | C$_6$H$_{13}$–CH$_2$OH (79.6%, 6.1) | C$_n$H$_{2n+1}$–CH=CH–C$_{6-n}$H$_{13-2n}$ (9.0%); C$_6$H$_{13}$ (alkane) (9.0%) | 1h |
| Ru$_3$(CO)$_{12}$ (0.11 mmol) 1,10-phenanthroline (1.33 mmol) | H$_2$/CO = 4.0/4.0 MPa, DMA 10 mL, 130 °C, 20 h | (alkene) (40 mmol) | CHO (93%, 19) | | 1i |
| Ru$_3$(CO)$_{12}$ (0.11 mmol) 1,10-phenanthroline (1.33 mmol) | H$_2$/CO = 5.0/5.0 MPa, DMA 5 mL, 120 °C, 20 h | C$_6$H$_{13}$ (alkene) (40 mmol) | C$_6$H$_{13}$–CHO (49%, 32) | C$_n$H$_{2n+1}$–CH=CH–C$_{6-n}$H$_{13-2n}$ (32%) | 1i |

bis(triphenylphosphoranylidene)ammonium)[1f] is the most effective (total aldehyde 60.6%, $n/i$ = 18), but accompanied by formation of 22.8% of isomerized alkenes. Exclusive formation of $n$-aldehyde was reported for K[Ru(edtaH)Cl] · $H_2O$ (edta = ethylenediaminetetraacetate).[1g] However, the author could not replicate the result. Another important system is $RuO_2/2,2$'-bipyridyl/$Bu_4PBr$, which mediated *normal*-selective hydroformylation/hydrogenation under somewhat harsh condition (for 1-octene at 180 °C, 79.6% alcohols yield, $n/i$ = 6.1).[1h] $Ru_3(CO)_{12}$/phenanthroline exhibits high $n/i$ ratio of 19 for propene and 32 for 1-octene respectively.[1i]

## 2-2 Design of the catalyst system of this work

Our design of Ru-based *normal*-selective hydroformylation catalyst is described in Figure 2-1.
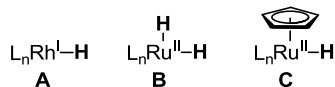


**Figure 2-1.** Comparison of rhodium and ruthenium hydride species

In the conventional rhodium-catalyzed hydroformylation, monohydridorhodium(I) (**A**) mediates the reaction (Scheme 2-1), by the insertion of an alkene to produce alkylrhodium species. Successive coordination insertion and hydrogenolysis give aldehyde as a product and regenerate **A**. On the other hand, corresponding hydride complex for ruthenium is dihydridoruthenium(II) (**B**). Catalytic cycle could be drawn for **B** similarly to monohydridorhodium(I) as described in Scheme 2-2. However, reductive elimination of alkane from alkylhydridoruthenium intermediate is a problematic side reaction in this cycle. Hydrogenation of aldehyde via similar mechanism is also a problematic side reaction when the

desired compound is aldehyde. Although active species in hydroformylation using multinuclear carbonylruthenium(0) as precursor were not well characterized, oxidative addition of dihydrogen to ruthenium(0) to form $Ru_xH_y(CO)_z$ was proposed.[1j]

**Scheme 2-1.** Hydroformylation catalyzed by monohydridorhodium(I) (**A**)
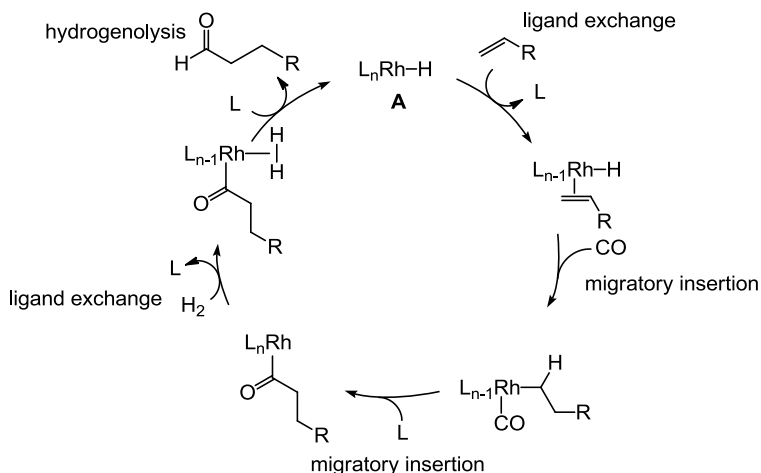


**Scheme 2-2.** Hydroformylation catalyzed by dihydridoruthenium(II) (**B**)
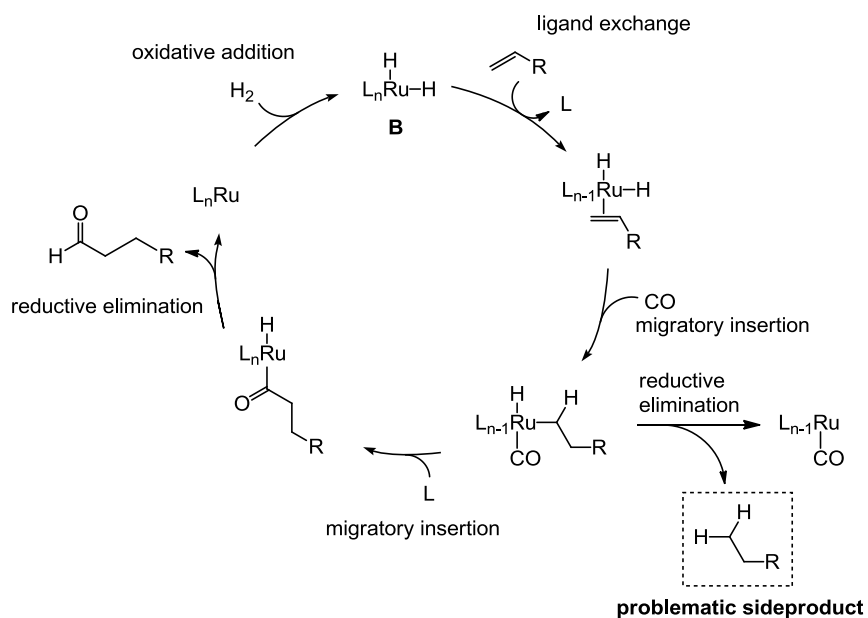
On the other hand, cyclopentadienylhydridoruthenium(II) (**C**) is expected to be less active in hydrogenation of an alkene because there is only one hydride on the ruthenium center. This effect was implied in the previous report utilizing $[CpRu(CO)_2]_2$ for hydroformylation, where the yield of alkane was as low as 4.7%.[1c] Expected catalytic cycle is drawn in Scheme 2-3. Since $CpRuHL_2$ is coordinatively saturated 18-electron complex, two mechanisms are possible to afford open coordination site for substrates. One is the slippage of cyclopentadienyl ring from $\eta^5$ to $\eta^3$-coordination mode shown in the cycle. Another possibility is dissociation of one of the ligands L as shown in the dotted box in Scheme 2-3.

**Scheme 2-3.** Expected reaction mechanism of hydroformylation by cyclopentadienylruthenium
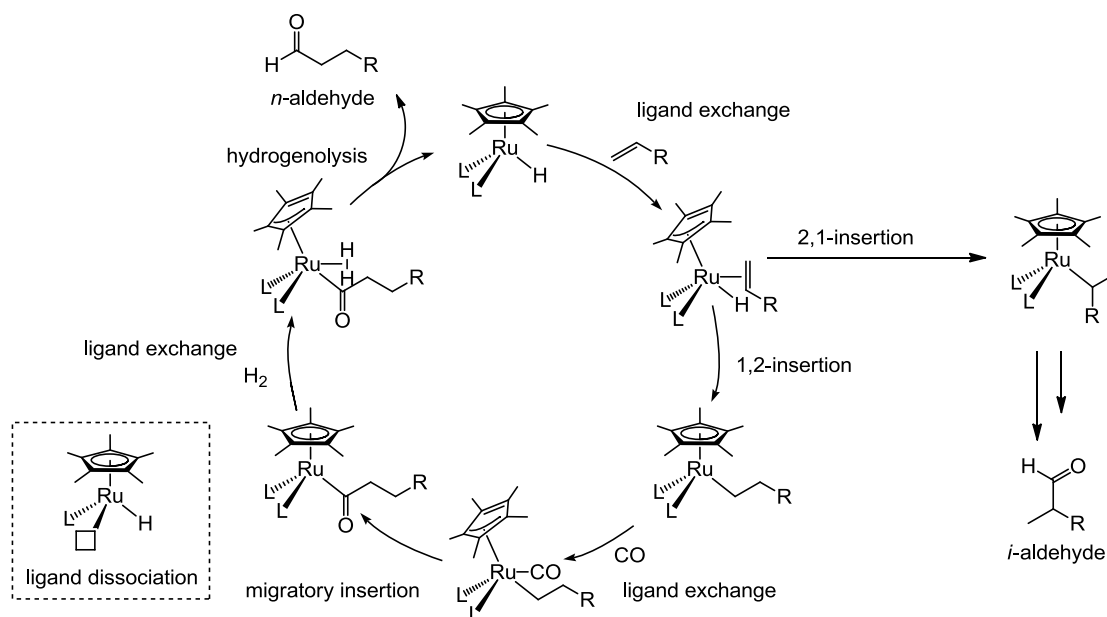


In the rhodium catalyzed hydroformylation, bulky bisphosphine or bisphosphite ligands are known to enhance the selectivity to *normal*-aldehyde by inducing sterically crowded environment around rhodium center (summarized in Chapter 1). Similar effect could be expected for ruthenium-based system (Scheme 2-4). When the species formed after insertion was

37

compared between 1,2- and 2,1-insertion of an alkene to Ru–H bond, steric repulsion between the substituent on the phosphorus atom and the alkyl group on ruthenium is expected to be larger in 2,1-inserted complex.

**Scheme 2-4.** Expected steric effect of phosphorus ligand
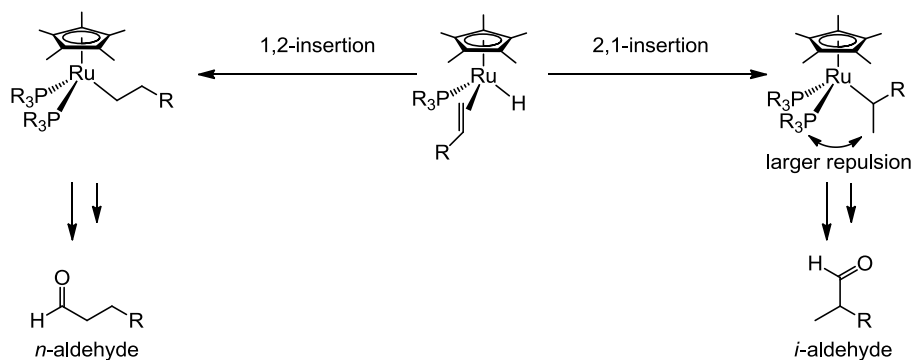


## 2-3 Hydroformylation of propene catalyzed by ruthenium complex in this work

Based on these speculations above, hydroformylation of propene using (acetylacetonato)(1,2,3,4,5-pentamethylcyclopentadienyl)ruthenium dimer ([Cp*Ru(acac)]$_2$) and phosphorus ligand as precursor was investigated. Results were summarized in Table 2-2. When the reaction was performed with [Cp*Ru(acac)]$_2$/A4N3,[2] aldehydes were obtained with a total conversion rate (to liquid product observed by gas chromatography) of 1.7 h$^{-1}$, with 78% selectivity to aldehydes, and *n/i* ratio of aldehyde was 17 (run 1). On the other hand, use of Ru$_3$(CO)$_{12}$/A4N3 resulted in predominant formation of alcohols (48%) and other side products (50%) (run 2). Those results could be interpreted that the cyclopentadienyl moiety is essential for suppressing side reactions. When the result by only [Cp*Ru(acac)]$_2$/A4N3 is compared with that of only [Cp*Ru(acac)]$_2$ (run 3), sharp increase of *n/i* ratio is evident (17 compared to 1.8). This fact indicates A4N3 is required for higher *n/i* ratio. The reaction rate with only by Ru$_3$(CO)$_{12}$

(run 4) is much higher (TOF = 19.8 h$^{-1}$), but low selectivity to aldehydes and $n/i$ ratios were problematic (42% aldehyde selectivity and $n/i$ = 1.7). Effect of phosphorus ligands is demonstrated in runs 5-10. XANTPHOS[3] (run 5) and BISBI[4] (run 6) exhibited similar selectivity to aldehydes and slightly lower $n/i$ ratios compared to A4N3 (97%, $n/i$ = 13 and 94%, $n/i$ = 14 respectively). Use of triphenylphosphine resulted in lower activity and $n/i$ ratio (TOF = 0.3, $n/i$ = 5.4, run 7). Bisphosphines having small bite angle gave relatively larger amounts of alcohols (runs 8-10). When the reaction was performed at 120 °C using [Cp*Ru(acac)]$_2$/A4N3, selectivity to aldehyde and $n/i$ ratios were increased up to 89% and 43 respectively at the expense of reaction rate (TOF = 0.54 h$^{-1}$, run 11). The $n/i$ ratio obtained in run 11 is comparable to that of the previously reported most *normal*-selective hydroformylation catalyst under its best condition (run 12). Sharp increase of reaction rate was observed when indenyl and trimethylindenyl ruthenium complexes were used as catalyst (runs 13 and 14, TOF = 2.3 and 4.4 h$^{-1}$ respectively). Since indenyl derivatives are known to have lower barrier to give the $\eta^3$-Cp type intermediate, this acceleration effect suggestes involvement of this intermediate in the reaction mechanism.[5]

**Table 2-2.** Hydroformylation of propene catalyzed by ruthenium based catalysts[a]
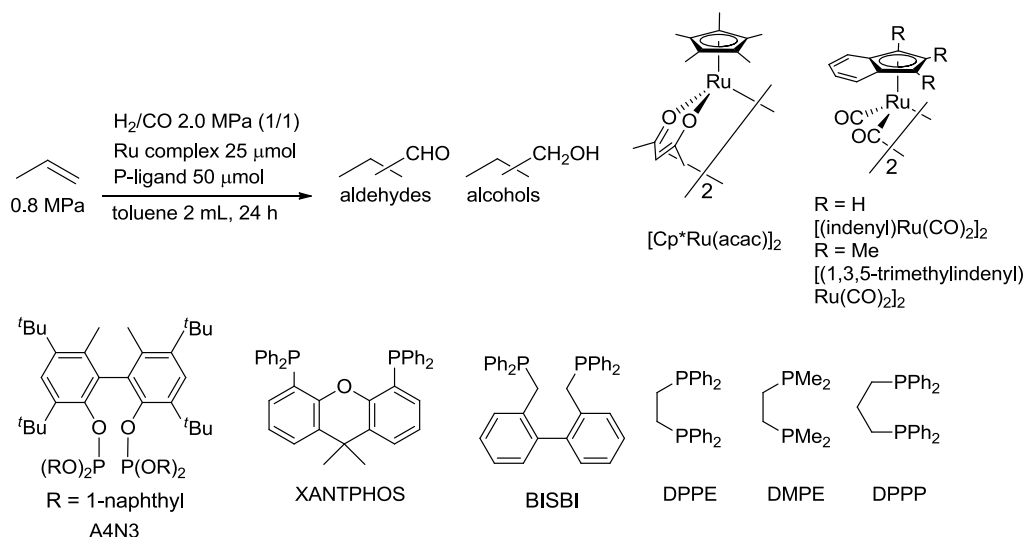
| run | catalyst | temp. (°C) | conv. to liquid product (TOF, h$^{-1}$) | aldehydes (%), (n/i) | alcohols (%), (n/i) | others (%) |
|---|---|---|---|---|---|---|
| 1 | [Cp*Ru(acac)]$_2$/A4N3 | 160 | 1.7 | 78 (17) | 17 (14) | 5 |
| 2 | Ru$_3$(CO)$_{12}$/A4N3 | 160 | 1.8 | 2 (8.0) | 48 (8.0) | 50 |
| 3 | [Cp*Ru(acac)]$_2$ | 160 | 1.1 | 86 (1.8) | 7 (2.5) | 7 |
| 4 | Ru$_3$(CO)$_{12}$ | 160 | 19.8 | 42 (1.7) | 43 (1.9) | 14 |
| 5[b] | [Cp*Ru(acac)]$_2$ /XANTPHOS | 160 | 1.8 | 97 (13) | 3 (> 100) | trace |
| 6[b] | [Cp*Ru(acac)]$_2$/BISBI | 160 | 0.6 | 94 (14) | 6 | trace |
| 7 | [Cp*Ru(acac)]$_2$ /PPh$_3$ (100 μmol) | 160 | 0.3 | 66 (5.4) | 20 (8.7) | 14 |
| 8 | [Cp*Ru(acac)]$_2$/DPPE | 160 | 1.2 | 38 (56) | 45 (17) | 17 |
| 9 | [Cp*Ru(acac)]$_2$/DMPE | 160 | 0.4 | 5 (0.5) | 46 (16) | 49 |
| 10 | [Cp*Ru(acac)]$_2$/DPPP | 160 | 0.9 | 29 (0.8) | 64 (9.1) | 7 |
| 11[c] | [Cp*Ru(acac)]$_2$/A4N3 | 120 | 0.54 | 89 (43) | 11 (>100) | trace |
| 12 | [NEt$_4$][HRu$_3$(CO)$_{11}$][d] | 70 | 0.11 | 100 (45) | trace | trace |
| 13 | [(indenyl)Ru(CO)$_2$]$_2$/A4N3 | 120 | 2.3 | 94 (32) | 6 (12) | trace |
| 14 | [1,2,3-trimethylindenyl Ru(CO)$_2$]$_2$/A4N3 | 120 | 4.4 | 97 (41) | 0.14 (>100) | trace |

[a]The molar quantity of Ru complexes are based on the total mol of Ru atoms. TOF = (mol of products observed by GC)/[(mol of Ru atom)×(reaction time)]. The amounts of charged H$_2$ and CO were so high that the changes of their partial pressure during the reaction time were negligible. The amounts of other side products were roughly estimated by the integration of the signals on the GC chart compared to that of n-aldehyde. Those side products were probably dimers or trimers of aldehydes and alcohols by aldol reaction of acetalization.[b]1,4-dioxane was used as solvent. [c] 120 °C [d]The condition was the same as the best one reported in literature (ref. 1d). Ru complex (102 μmol), propene (0.5 MPa), H$_2$ (0.17 MPa), CO (0.34 MPa) in dimethoxyethane (2 mL), 70 °C, 66 h.

## 2-4 Hydroformylation of 1-decene

Next, the system was applied for hydroformylation of 1-decene. Results are summarized in the

Table 2-3. When the reaction was performed by [Cp*Ru(acac)]$_2$/A4N3 or

[Cp*Ru(acac)]$_2$/XANTPHOS (runs 1 and 2), n-aldehyde was obtained with moderate yield and

high n/i ratio of 79 and 29 respectively. However, low reproducibilities of those reactions were

problematic because the amount of formation of isomerized alkenes was fluctuating. In the reaction using [Cp*Ru(acac)]$_2$ as a catalyst precursor without ligands, rapid isomerization of decene was observed (run 3). It suggests that ruthenium species without phosphorus ligands can catalyze rapid isomerization of decene. This problem was avoided by using well-defined complex (1,2,3,4,5-pentamethylcyclopentadienyl)hydrido(xantphos)ruthenium (**1**), which was prepared as shown in Scheme 2-5. The intermediate Cp*Ru(xantphos)Cl was characterized by X-ray crystallographic analysis, which proved that XANTPHOS can coordinate ruthenium center as a bidentate ligand to form three legged piano-stool structure (Figure 2-2). With this complex, isomerization of 1-decene was suppressed, and the reaction was performed with better reproducibility. As a result, the yield of *n*-aldehyde reached to 60% with *n*/*i* ratio of 29 (run 4). Notably, hydrogenation of the alkene to the alkane and that of the aldehydes to the alcohols were suppressed as low as 3.2% and trace respectively. Although the yield of isomerized alkenes and *n*/*i* ratios were similar to those in the case using in-situ generated system from [Cp*Ru(acac)]$_2$/XANTPHOS, the reaction rate was slower (conv. 40% in 24 h in run 5 versus 86% in 21 h in run 2). Therefore, the real active species may not be Cp*Ru(xantphos)H for in-situ generated system. However, characterization of such species was not successful. It could be expected that internal alkenes would be isomerized back to the terminal alkene and converted to *n*-aldehyde. However, this pathway was confirmed to be negligibly slow by the fact that (*Z*)-2-decene did not afford aldehyde at all (run 6). The reaction was also performed with Ru$_3$(CO)$_{12}$/XANTPHOS and RuH$_2$(CO)(PPh$_3$)$_3$/XANTPHOS (run 7, 8). Both of them resulted in rapid isomerization of the alkene and slow hydroformylation.

**Table 2-3.** Hydroformylation of 1-decene by ruthenium-based hydroformylation catalyst[a]
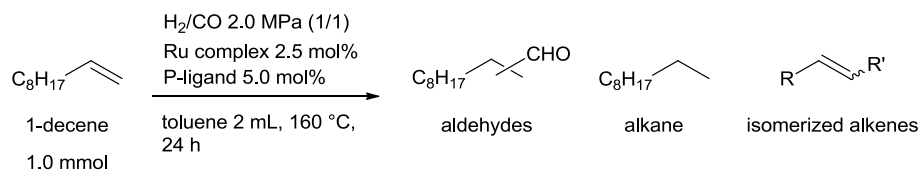


| run | Cat. | conv. | Aldehyde | | n/i | alkane (%) | isomerized alkenes (%)[c] |
|---|---|---|---|---|---|---|---|
| | | | n(%) | i(%)[b] | | | |
| 1[d] | [Cp*Ru(acac)]$_2$/A4N3 | 87 | 65 | 0.8 | 79 | 1.5 | 19 |
| 2 | [Cp*Ru(acac)]$_2$/XANTPHOS | 80 | 61 | 2.1 | 29 | 2.5 | 9.0 |
| 3 | [Cp*Ru(acac)]$_2$ | 100 | 11 | 2 | 5.5 | | 81% in total |
| 4[e] | Cp*Ru(xantphos)H/XANTPHOS | 77 | 58 | 2.1 | 28 | 3.2 | 8.4 |
| 5 | Cp*Ru(xantphos)H/XANTPHOS | 40 | 28 | 0.9 | 31 | 1.2 | 8.5 |
| 6[f] | Cp*Ru(xantphos)H/XANTPHOS | 14 | trace | trace | - | 1.4 | 4.6 |
| 7[g] | Ru$_3$(CO)$_{12}$/XANTPHOS | 92 | 19 | 1.3 | 14 | 10 | 56 |
| 8[g] | RuH$_2$(CO)(PPh$_3$)$_3$/XANTPHOS | 97 | 33 | 1.5 | 22 | 3.2 | 47 |

[a]The molar quantity of Ru complexes are based on the total mol of Ru atoms. Yields were determined by gas chromatography by using dodecane as internal standard otherwise mentioned. [b]Yields were determined by using calibration curve for *normal*-isomer. [c]Yields were determined by using calibration curve for 1-decene. [d]100 °C, 18 h. [e]48 h. [f](Z)-2-decene was used as substrate. [g]18 h.

**Scheme 2-5.** Synthesis of (pentamethylcyclopentadienyl)hydrido(xantphos)ruthenium
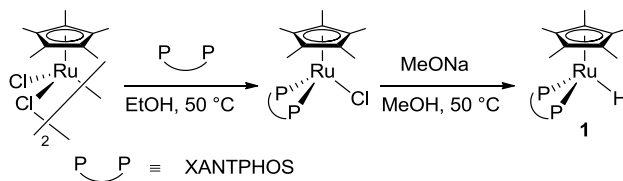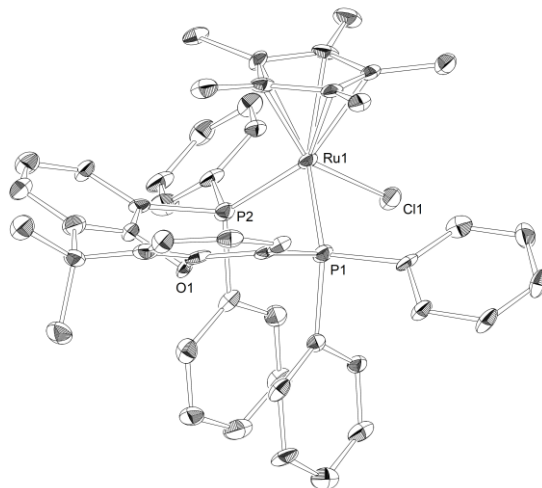
**Figure 2-2.** Ortep drawing of Cp*Ru(xantphos)Cl (50% thermal ellipsoid, hydrogen atoms and solvent molecule $C_6H_6$ were omitted for clarity)

## 2-5 Discussion of the effect of cyclopentadienyl ligand

As for activity of hydrogenation, comparison of [Cp*Ru(acac)]$_2$/A4N3 and Ru$_3$(CO)$_{12}$/A4N3 (supposed to form RuH$_2$(CO)$_2$(A4N3) under H$_2$/CO) clearly indicates suppression of hydrogenation activity for aldehyde with [Cp*Ru(acac)]$_2$ (runs 1 and 2 in Table 2-2), which supports our initial assumption that dihydride intermediate is responsible for hydrogenation of aldehyde. However, when the hydroformylation of 1-decene performed by [Cp*Ru(acac)]$_2$/XANTPHOS and RuH$_2$(CO)(PPh$_3$)$_3$/XANTPHOS were compared, the yields of alcohol were trace in both cases. Therefore, introduction of Cp ligand is not be the only way to suppress hydrogenation of aldehyde.

As for *n*/*i* selectivity, Cp* improves the ratio. For example, *n*/*i* ratio in the hydroformylation of propene catalyzed by [Cp*Ru(acac)]$_2$/A4N3, Ru$_3$(CO)$_{12}$/A4N3 were 16 and 8.0 (total of aldehydes and alcohols) respectively. Similarly considered to the effect of bidentate phosphorus

ligand on rhodium catalyzed hydroformylation, this increase of $n/i$ ratio by introducing Cp*
could be interpreted as the steric effect, which is more destabilizing *iso*-alkylruthenium
intermediate than *n*-alkylruthenium intermediate.

Indenyl and trimethylindenyl ruthenium complexes exhibited higher catalytic activity than
Cp* derivatives. These results imply that an $\eta^3$-Cp type intermediate is involved in the catalytic
cycle. Such effects have been reported as the acceleration of ligand substitution reactions in
coordinatively saturated $\eta^5$-indenyl metal complexes compared to $\eta^5$-Cp.[5] The extent of
acceleration is dependent on systems employed (acceleration is $10 - 10^{10}$ times).

## 2-6 Discussion of the effect of phosphorus ligand

As for $n/i$ selectivity, phosphorus ligand made difference. Similar to rhodium catalyst, bulky
bisphosphite or bisphosphine such as A4N3, XANTPHOS, and BISBI led to higher $n/i$ ratio
(runs 1, 5, 6 in Table 2-2). Also, the isomerization to internal alkenes was suppressed in the
presence of XANTPHOS. This is probably because of the suppression of 2,1-insertion by the
steric bulk of XANTPHOS.

## 2-7 Mechanistic investigations

In order to get information about selectivity-determining step and rate-determining step, the
reaction mechanism was investigated with well-defined complex Cp*Ru(xantphos)H (**1**).

## 2-7-1 Stoichiometric reactions of 1 and 1-decene

First, reversible insertion of 1-decene to the Ru–H bond in **1** was studied by $^1$H and $^{31}$P NMR
spectra by treating complex **1** with 1-decene in toluene-$d_8$ under 1 atm of Ar or CO (Schemes 2-

6 and 2-7). Under Ar, **1** did not give any other ruthenium species by the reaction with 1-decene. On the other hand, irreversible formation of 2-decenes ($E/Z = 85/15$) was observed. No further isomerization to 3-decenes was detected. This isomerization is explained by coordination-2,1-insertion of 1-decene into the Ru–H bond and successive C3-$\beta$-H-elimination. Intermediates such as Ru–alkene or alkyl complexes that supposed to be involved in the catalytic cycle was not detected.

**Scheme 2-6.** Stoichiometric reaction of **1** and 1-decene under Ar
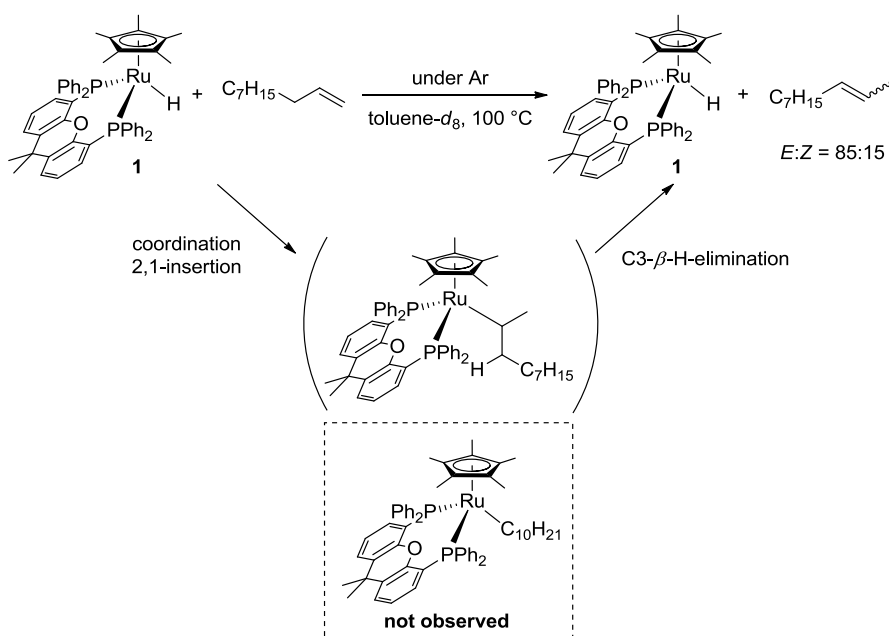


Under CO, no isomerization of 1-decene took place and slow dissosiation of XANTPHOS was observed in the $^{31}$P NMR spectrum. It suggested that at least at this temperature competetive coordination of CO prohibits the coordination of 1-decene. When only **1** was treated under 1.0 MPa of CO at room temperature, no change was observed.

**Scheme 2-7.** Treatment of **1** under CO in the presence or absence of 1-decene
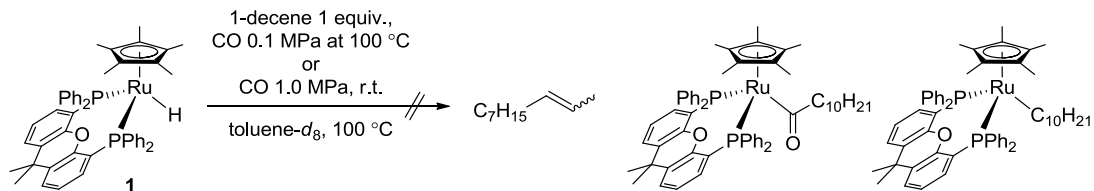


Next, stoichiometric reaction of **1** with C1-dideuterated 1-decene (1-decene-$d_2$, D content 96%) under Ar was followed by $^1$H and $^2$H NMR spectroscopy (Scheme 2-8 and Figure 2-3) to determine the relative rate of 1,2- and 2,1-alkene insertion and $\beta$-H elimination. The time course of integral of each proton indicated in Scheme 2-8 are plotted in Figure 2-3b. Similarly to the previous experiment, alkylruthenium complex was not observed during the reaction.

**Scheme 2-8.** Stoichiometric reaction of **1** with 1-decene-$d_2$ and monitored protons
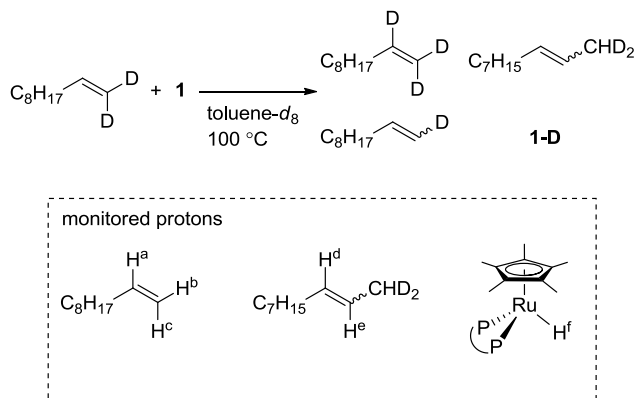
(a)
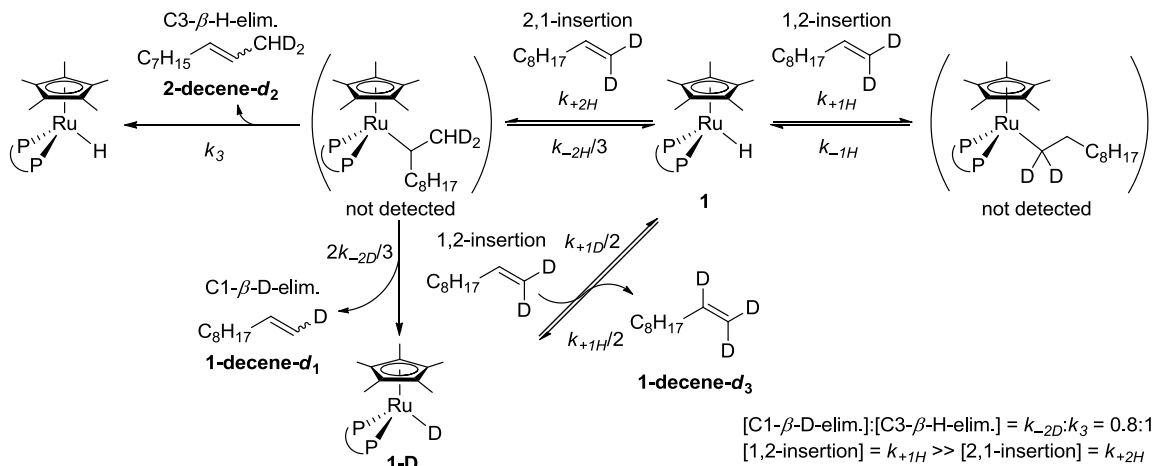


(b)
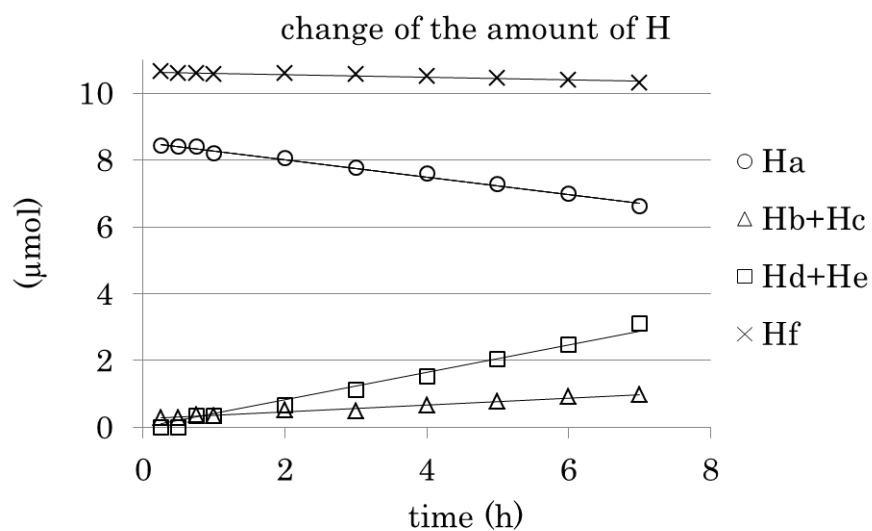


**Figure 2-3.** (a) Possible mechanism for insertion/β-H elimination of 1-decene-$d_2$ and (b) integral ratio of each proton in 1-decene in $^{1}$H NMR spectra during the course of the reaction

Following 2,1-insertion of 1-decene-$d_2$ to **1**, there are two potential $\beta$-elimination pathways (Figure 2-3a, 2-4). One is $\beta$-elimination on C1 to reform 1-decene. The other is $\beta$-elimination on C3 to give 2-decenes. In the initial stage of the reaction, increase of $H^b$ + $H^c$ (0.10 µmol h$^{-1}$) corresponds to the formation of 1-decene-$d_1$ and increase of $H^d$ + $H^e$ (0.41 µmol h$^{-1}$) corresponds to the formation of 2-decene-$d_2$ (incorporation of deuterium on C2 and C3 of 2-decene was confirmed to be negligibly slow. Therefore, the increase of $H^d$ + $H^e$ exactly represents the amount of 2-decenes). The integral ratio of these signals gave the ratio between the rates of the C1-$\beta$-D-elimination and the C3-$\beta$-H-elimination to be $k_{-2D}$:$k_3$ = 0.8:1. Taking into account the reported kinetic isotope effect for $\beta$-H-elimination as 1.0~3.3,[7] $k_{-2H}$:$k_3$ could be corrected as 0.8:1 ~ 2.6:1 showing that the two pathways are comparable to each other.
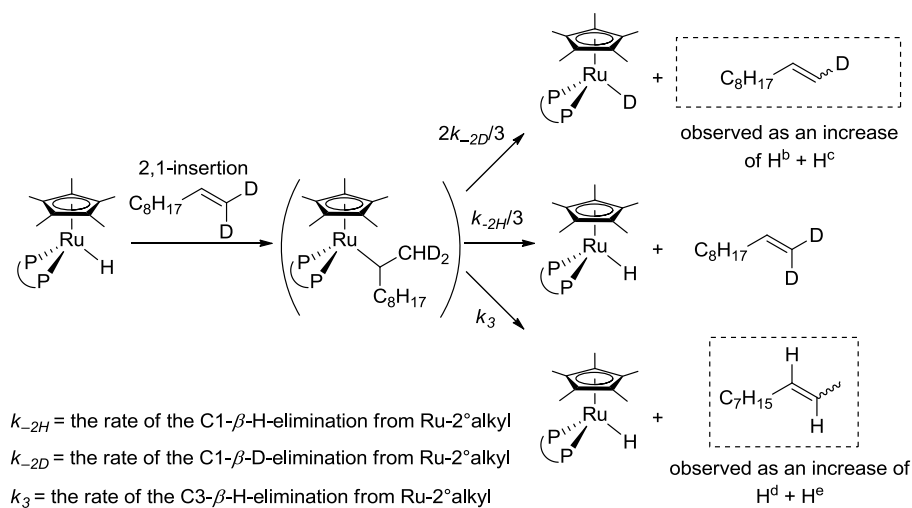


**Figure 2-4.** 2,1-insertion-$\beta$-elimination process.

On the other hand, the ratio of 1-decene-$d_3$ to Cp*Ru(xantphos)**D** (**1-D**) remained constant at 1:1 during the reaction. The decrease of $H^a$ was ascribed to the conversion of 1-decene-$d_2$ to 2-

decene-$d_2$ or 1-decene-$d_3$ assuming that the participation of 1-decene-$d_1$ to this process was negligible at the initial stage of the reaction (Figure 2-5). Thus, the rate of formation of 1-decene-$d_3$ was calculated as 0.04 μmol h$^{-1}$. During the increase of H$^b$, H$^c$, H$^d$, and H$^e$, the ratio of 1-decene-$d_3$ and **1-D** was constant at 0.9:1.0. This implies the much faster 1,2-insertion-$\beta$-H(D)-elimination than the 2,1-insertion-$\beta$-D-elimination so that **1-D** plus 1-decene-$d_2$ and **1** plus 1-decene-$d_3$ are equilibrated. Otherwise the ratio of 1-decene-$d_3$:**1-D** would have increased as the reaction proceeded; namely, the concentration of **1-D** could have first increased, and then 1-decene-$d_3$ could have gradually formed. Therefore, the rate of 1,2-insertion ($k_{+1}$) represents the rate of 1,2-insertion-$\beta$-H-elimination. In the same way, $k_{+2}$ represents the rate of 2,1-insertion-$\beta$-H-elimination. In conclusion, 1,2-insertion estimated to be much faster than 2,1-insertion.
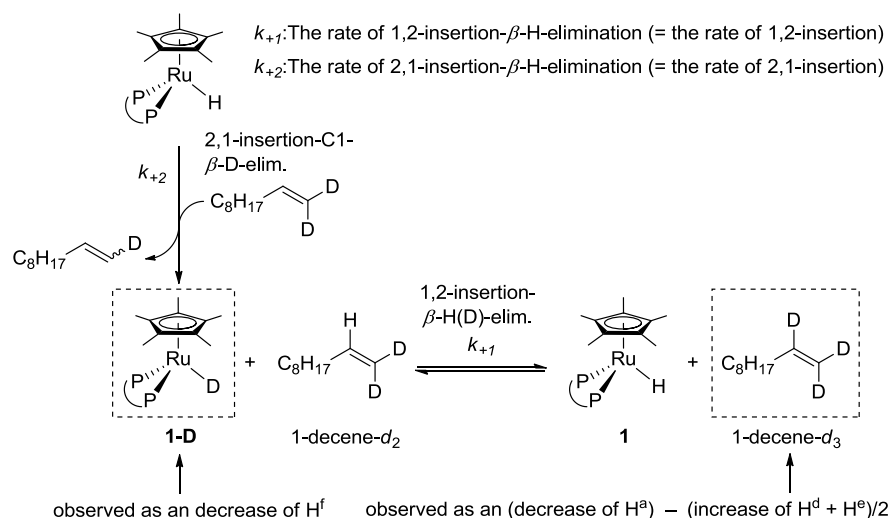


**Figure 2-5.** Figure for the comparison of 1,2-insertion and 2,1-insertion process.

## 2-7-2 Hydroformylation of 1-decene-$d_2$ by 1

Hydroformylation of 1-decene-$d_2$ in the real conditions clarified reversibility of insertion-$\beta$-elimination process. The hydroformylation of 1-decene-$d_2$ catalyzed by **1**/XANTPHOS afforded

49

product $n$-aldehyde-$d_n$, 2-decene-$d_n$, and decane-$d_n$ as well as recovered 1-decene-$d_n$. Deuterium contents of those compounds were determined by the ${}^1$H and ${}^2$H NMR spectra shown in Figures 2-6 and 2-7. By ${}^1$H NMR spectrum, the deuterium contents of $H^a$-$H^e$ were determined as described in Figure 2-6. In the ${}^2$H NMR spectrum, the signals on the spectrum were assigned according to the literature,[4b] and the deuterium contents of $D^a$-$D^j$ were determined as illustrated in Figure 2-7. The contents for $D^a$-$D^e$ were consistent with the value for $H^a$-$H^e$ determined by ${}^1$H NMR. In the recovered 1-decene-$d_n$, the deuterium content was 88% on C1 and 3% on C2. In the obtained $n$-aldehyde-$d_n$, deuterium was incorporated in <1% on C1, 79% on C2, and 5% on C3. The decrease of terminal D content in 1-decene-$d_2$ indicates that 2,1-insertion/C1-$\beta$-D-elimination took place to some extent. Since 1,2-insertion was estimated to be much faster than 2,1-insertion as mentioned in the previous paragraph, *the 1,2- insertion step should occur reversibly at a rate much faster than that of 2,1-insertion.* Therefore in the catalytic cycle drawn in Scheme 2-3, either coordination-insertion of CO or hydrogenolysis is irreversible step.


**Scheme 2-9.** Hydroformylation of 1-decene-$d_2$



50
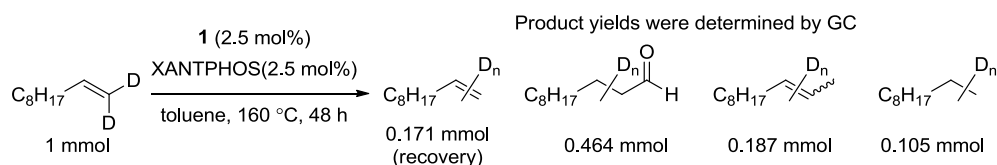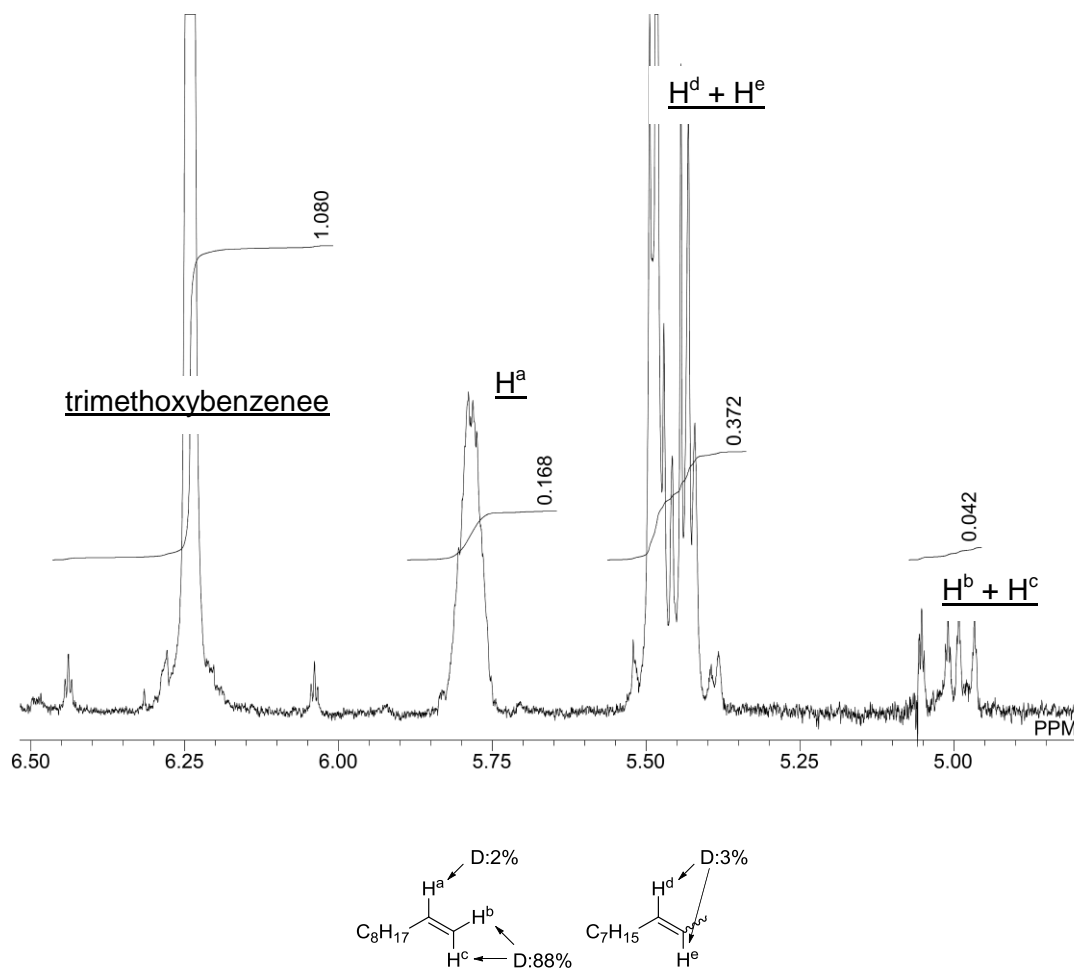
**Figure 2-6.** Vinylic region of ^{1}H NMR spectrum for the crude product obtained from hydroformylation of 1-decene-$d_2$ (1,3,5-trimethoxybenzene 0.360 mmol was used as internal standard) and deuterium contents determined by ^{1}H NMR.
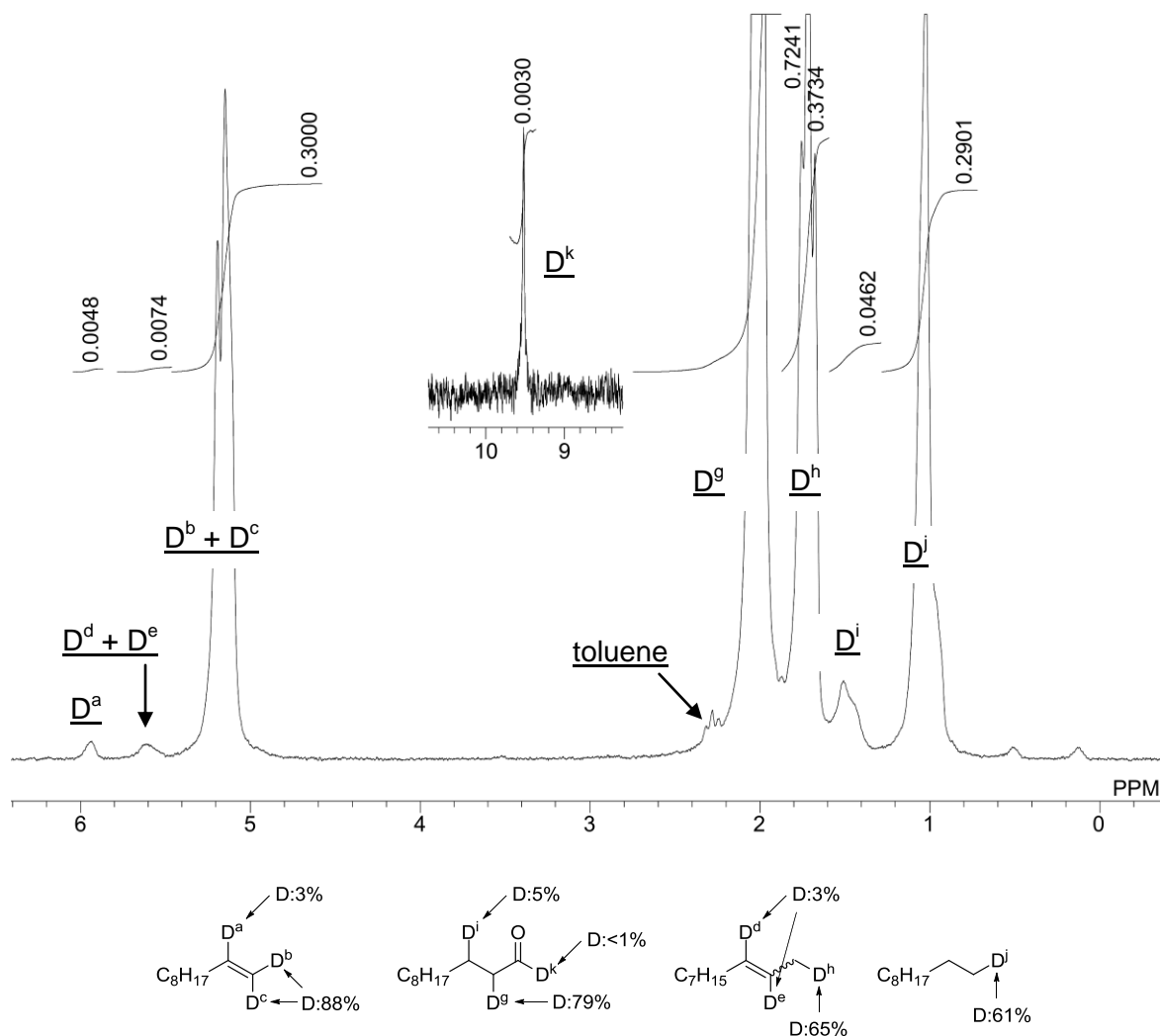
**Figure 2-7.** The partial $^2$H NMR spectrum of the crude product obtained from hydroformylation of 1-decene-$d_2$. (The integration was normalized with setting the deuterium on C1 of 1-decene $D^b+D^c$ as 0.300 mmol (0.171 mmol× 2 (mmol of terminal H+D) − 0.042 mmol (mmol of terminal H)) and deuterium contents determined by $^2$H NMR.

Exchange of deuterium of **1-D** with $H_2$ gas is implied by the fact that total D content of all products was decreased. This process was thought to interfere in the transfer of terminal D onto

internal carbons by releasing deuterium as HD to the gas phase. Possible mechanisms are described in Scheme 2-10.

**Scheme 2-10.** Exchange process of H–H to H–D
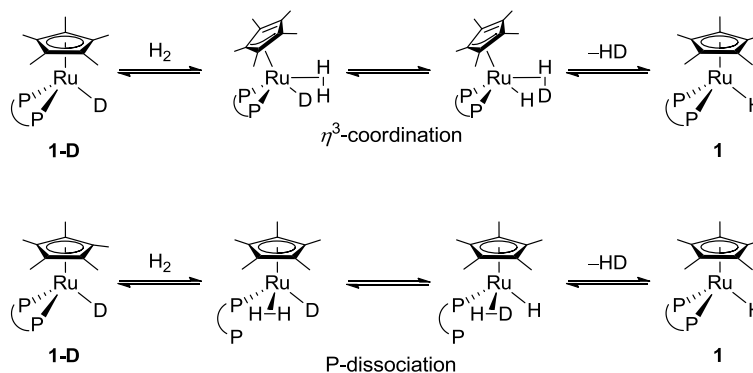


## 2-7-3 Effect of initial concentration of 1-decene on the rate of hydroformylation

Finally, effect of initial 1-decene concentration ($[1\text{-decene}]_0$) on the reaction rate was examined (Figure 2-8). Reaction was performed with various initial concentrations of 1-decene, and average TOFs in initial 24 h were plotted. Linear relationship between TOF and $[1\text{-decene}]_0$ was indicated. Assuming there was no induction period and the amounts of $H_2$ and CO were enough excess, and the reaction rate is first-order with respect to concentration of 1-decene, the rate equasion could be expressed as

$d/dt\,[1\text{-decene}]_t = -\,k[1\text{-decene}]_t$ ($t$: reaction time (h), k: rate constant ($h^{-1}$))

Therefore,

$[1\text{-decene}]_t = [1\text{-decene}]_0(\exp(-\,kt))$

When $t = 24$ h (const.),

$[1\text{-decene}]_{24} = [1\text{-decene}]_0(\exp(-\,24k))$

Therefore, concentration of 1-decene after 24 h should correlate with initial concentration of 1-decene if the reaction is first order on 1-decene concentration. Actually, [1-decene] after 24 h could be linearly plotted against [1-decene]$_0$.
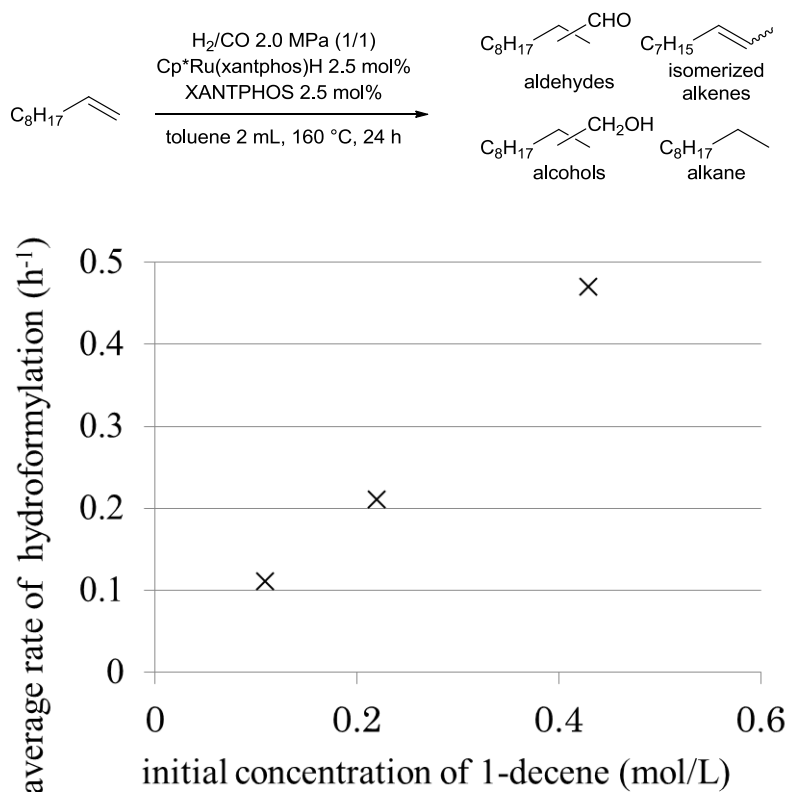


**Figure 2-8.** Dependency of average rate of hydroformylation on the initial concentration of 1-decene

## 2-7-4 Effect of pressure of dihydrogen on the rate of hydroformylation

The hydroformylation of 1-eicosene was examined under various $H_2$ pressure. As a result, average TOF ($h^{-1}$) was positively correlated with the pressure of $H_2$ (Figure 2-9). This fact indicated that in the proposed catalytic cycle (Scheme 2-3), hydrogenolysis of the acylruthenium intermediate is the rate-determining step.
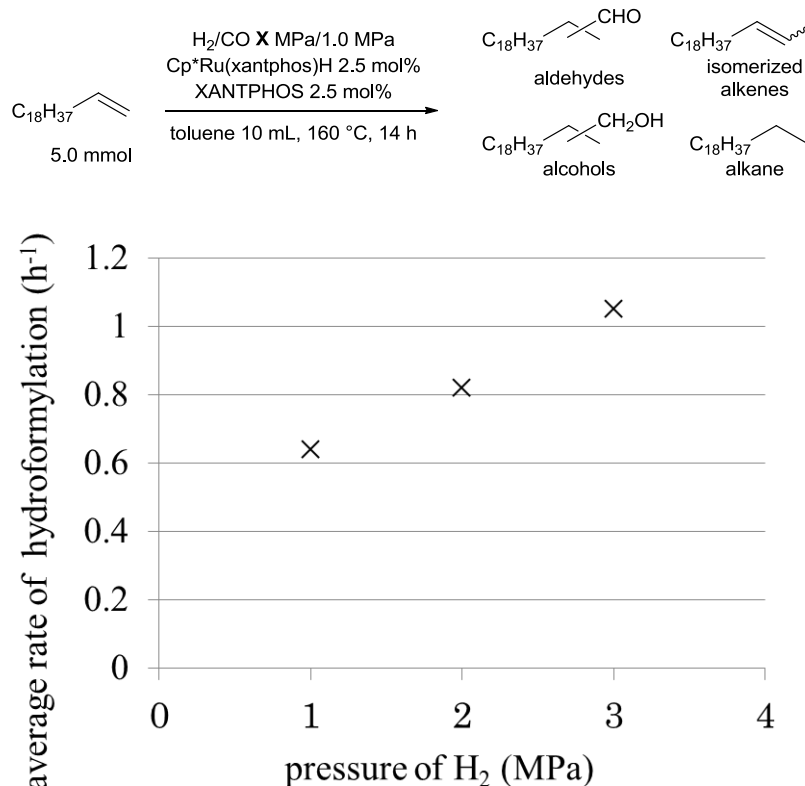
**Figure 2-9.** Dependency of average rate of hydroformylation on the initial pressure of H$_2$

## 2-7-4 Summary of mechanistic investigations

The mechanistic considerations obtained in this section are summarized in Scheme 2-11. First, coordination of an alkene takes place, being accompanied by phosphine dissociation or Cp-ring slippage. Insertion takes place to give Ru(alkyl) intermediate. This coordination-insertion process is reversible (between **D** and **E**). Rate-determining step is supposed to be the hydrogenolysis of the acylruthenium intermediate. Higher concentration of 1-decene increases the amount of intermediate (**E** or **F**) by changing the pre-equilibrium (between **D** and **E** or **D** and **F**), which results in a higher reaction rate. High *n/i* selectivity observed in the presence of bulky bisphosphorus ligands could be attributed to destabilization of *iso*-acylruthenium species or

transition state of hydrogenolysis of acylruthenium intermediate with the larger steric repulsion between ligand of the ruthenium. As for the pathway to give open coordination site for the alkene- or CO-insertion and $H_2$-coordination, higher activity by indenyl derivatives may suggest involvment of $\eta^3$-Cp intermediate. However, dissociation of one of the phosphorus atoms is still possible.

**Scheme 2-11.** Proposed mechanism for hydroformylation of an alkene by CpRu complex



## 2-8 Conclusion

In this chapter, cyclopentadienylruthenium/bisphosphine or bisphosphite systems were developed as *normal*-selective hydroformylation catalysts. The cyclopentadienyl ligand was essential for suppressing side reactions. On the other hand, the bulky bisphosphorus ligand was required for high *n/i* ratio. Mechanistic investigations using an isolated catalytically active complex, Cp*Ru(xantphos)H, revealed the reversible coordination-insertion of an alkene to

Ru–H bond under reaction conditions. The rate-determining step is considered to be the coordination of $H_2$ and hydrogenolysis. Although *normal*-selectivities were comparable to the conventional cobalt and rhodium catalysts, the reaction rates of these catalysts needs improvement. One of the possible ideas to improve catalytic activity was to use indenyl derivatives to lower the barrier to give $\eta 3$-cyclopentadienyl intermediate. It was successfully demonstrated by using indenyl and trimethylindenyl ruthenium complexes, which exhibited 5 and 10 times higher activities respectively compared to pentamethylcyclopentadienyl ruthenium complex.

As for catalytic activity, here is a question. Why is rhodium so active for hydroformylation? Under standard condition, coordination-insertion of alkene to Rh–H is the rate-determining step (Scheme 2-12). On the other hand, in the author's ruthenium system, hydrogenolysis is the rata-determining step. In the hydrogenolysis, dihydrogen needs to coordinate to metal center as a sigma-$H_2$ ligand. However, dihydrogen is a so weak ligand that its coordination is disturbed by carbon monoxide and alkene, which are relatively stronger ligands. Considering the fact that the hydrogenolysis is not the rate-determining step in the rhodium catalysed hydroformylation, the formation of sigma-$H_2$ complex and/or hydrogenolysis of acylrhodium intermediate is relatively preferred. This might be one of the possible reasons why rhodium is so active in the hydroformylation. On the other hand, in our system, hydrogenolysis is the rate-determining step.

**Scheme 2-12.** Consideration of the reason of high catalytic activity of rhodium-based system
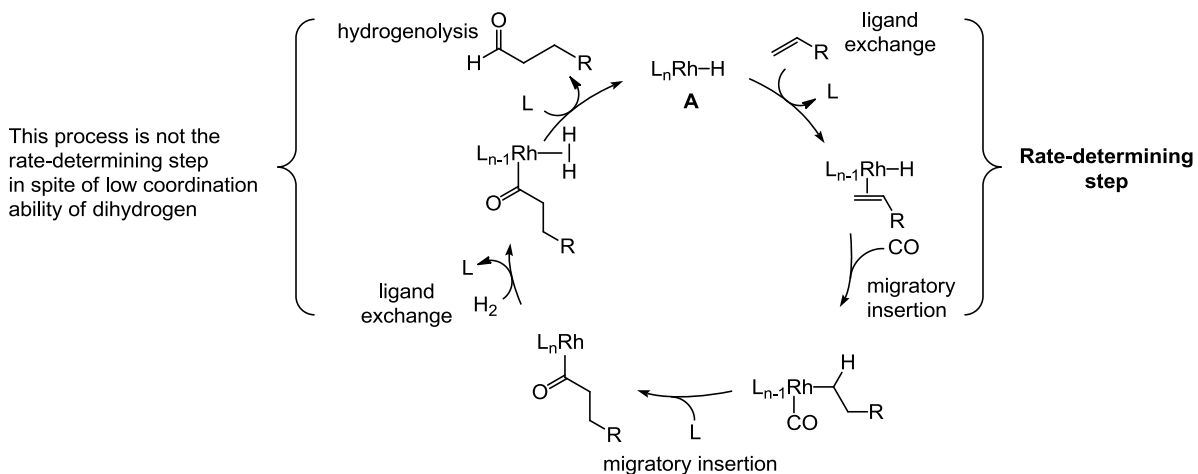


So far our ruthenium system is considered to be potentially more *normal*-selective than rhodium based system if the problem of low activity is overcome. Now the *n/i* ratio of hydroformylation of 1-decene by Cp*Ru/XANTPHOS is around 30 at 160 °C, which is probably much higher than rhodium catalysed hydroformylation performed at the same temperature (in chapter 4, hydroformylation of 1-decene catalysed by Rh(acac)(CO)$_2$/XANTPHOS gave *n/i* of 24 at 120 °C). Therefore, if our ruthenium catalyst system is active enough that the reaction could be performed at low temperature, *n/i* selectivity higher than rhodium system is expected.

## Experimental section

### General

All the manipulations involving the air- and moisture-sensitive compounds were carried out by using standard Schlenk technique or glovebox under argon purified by passig through a hot column packed with BASF catalyst R3-11. $H_2/CO$ mixed gas ($H_2$:CO = 49.1:50.9) and liquid propene were purchased from Suzuki-Shoukan and used without further purification. Commercially available anhydrous methanol, ethanol, and 1,4-dioxane were used without further purification. Commercially available anhydrous toluene was passed through solvent purification columns prior to use. Commercially available 1-decene, dodecane, and 1,2-dimethoxyethane were distilled and degassed by freeze-pump-thaw cycling two times before use. $RuCl_3 \cdot H_2O$ was purchased from Tanaka Kikinzoku. $[Cp*Ru(acac)]_2$,[9] $Ru_3(CO)_{12}$,[10] $[NEt_4][HRu_3(CO)_{11}]$,[11] $[(indenyl)Ru(CO)_2]_2$,[12] $[(1,2,3-trimetyhlindenyl)Ru(CO)_2]_2$,[13] and $[Cp*RuCl_2]_2$[14] were prepared by the literature methods. They were further purified by recrystalization before use of the catalytic reactions. XANTPHOS[3] and BISBI[4] were prepared by the literature methods. A4N3 was provided by Mitsubishi Chem. Co.[15] The mole of ruthenium complexes was based on ruthenium atom. 1-decene-$d_2$[16] (D content 96% on C1-position) and (Z)-2-decene[17] (purity 95%, containing decane 1.6%, (E)-2-decene 2.5%, and other C10 alkenes 0.9%) were prepared by the literature method.

The TOFs or yields of butanals, butanols, decane, isomerized decenes, undecanals, and undecanols were determined by Shimadzu-GC-2014 equipped with InertCap 5MS/Sil capillary column (0.25 ID, 0.25 μm df 30 m) with calibration curve using dodecane as an internal standard. The TOFs of unidentified high boiling products were determined based on the ratio of the area

on GC spectrum compared to *n*-aldehyde. NMR spectra were recorded on a JEOL JIN–ECP500 or JEOL–ECS400 spectrometers. Chemical shifts are reported in ppm relative to the residual protiated solvent for $^1$H, deuterated solvent for $^{13}$C, and external 85% $H_3PO_4$ for $^{31}$P nuclei. $^1$H-decoupled experiments were indicated with {$^1$H}. Data are presented in the following space: chemical shift, multiplicity (s = singlet, d = doublet, t = triplet, m = multiplet, br = broad), coupling constant, and signal area integration in natural numbers. Each signal on $^{13}$C NMR spectra was assigned as $CH_3$, $CH_2$, $CH$ or 4° with $^{13}$C dept experiments. Melting points were determined on a SRS OptiMelt melting point apparatus. High resolution mass spectra are taken with JEOL JMS–T100LP mass spectrometer. IR spectra were recorded on Shimadzu FTIR-8400. X-ray crystallographic analyses were performed on Rigaku Mercury CCD or VariMax Saturn diffractometer.

**General procedure for the hydroformylation of 1-decene or *(Z)*-2-decene**

   To a 50 mL stainless autoclave with a magnetic stir bar, Ru complex and bisphosphine were charged with 2 mL of solvent. To this, a mixture of 1-decene or *(Z)*-2-decene and dodecane (2:1 by molar ratio, 300 µL, ca. 1-decene or *(Z)*-2-decene 1 mmol) was added and then the autoclave was pressurized with appropriate pressure of $H_2$/CO. After completion of the reaction under conditions written on the tables, the autoclave was cooled to 0 °C with water/ice bath. The gas pressure was released and the resulting solution was analyzed by GC. Initial charges of $H_2$ and CO were enough high to neglect the drops of their partial pressures.

**General procedure for the hydroformylation of propene**

To a 50 mL stainless autoclave with a magnetic stir bar, an appropriate amounts of Ru complex and bisphosphine were charged with 2 mL of solvent. The autoclave was pressurized with 0.8 MPa of propene. Immediately it was further pressurized with 2.0 MPa of $H_2$/CO (total pressure was 2.8 MPa at r.t.). After completion of the reaction under conditions written on the tables, the autoclave was cooled to 0 °C with water/ice bath and kept for 30 min. The gas pressure was released and then dodecane (75 mg, 0.44 mmol) was added as an internal standard for GC analysis. Judging from the propene conversion to aldehydes, initial charges of $H_2$ and CO were enough high that the drops of their partial pressures were negligible.

**Reproductive experiment of hydroformylation of propene using [NEt$_4$][HRu$_3$(CO)$_{11}$]**

Reproductive experiment of hydroformylation of propene using [NEt$_4$][HRu$_3$(CO)$_{11}$][1e] was done by decreasing the amount of catalyst and solvent to 1/5 of the original report using a 50 mL stainless autoclave (in the original report, 100 mL).

**Preparation of chloro(1,2,3,4,5-pentamethylcyclopentadienyl)($\kappa^2$-xantphos)ruthenium**



Cp*Ru(xantphos)Cl
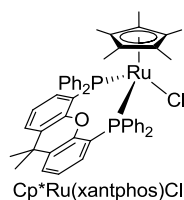
To a 80 mL Schlenk flask, bis(dichloro(pentamethylcyclopentadineyl)ruthenium) (200 mg, 0.651 mmol) and XANTPHOS (452 mg, 0.781 mmol) were charged with ethanol (40 mL) and the mixture was stirred at 50 °C. During the reaction, yellow powder gradually precipitated. After 3 h, the Schlenk was kept at room temperature for 1 h. Filtration of the mixture gave the desired complex (498 mg, 89.9%). For the use of catalytic reaction, it was further purified by

recrystalization from CHCl$_3$/hexane. Single crystals suitable for X-ray analysis was grown by slow diffusion of hexane into THF solution of the title compound. $^1$H NMR (CD$_2$Cl$_2$, 500 MHz) δ 0.88 (s, 15H), 1.52 (s, 3H), 1.91 (s, 3H), 6.56 (t, $J$ = 7 Hz, 4H), 6.68 (t, $J$ = 7 Hz, 3H), 7.08 (brs, 4H), 7.17 (t, $J$ = 8 Hz, 2H), 7.25-7.45 (m, 8H), 7.52 (dd, $J$ = 1, 8 Hz, 2H); $^{13}$C{$^1$H} NMR (CDCl$_3$, 101 MHz) δ 8.97 (s, CH$_3$), 22.8 (s, CH$_3$), 30.9 (s, CH$_3$), 36.8 (s, 4°), 87.9 (s, 4°), 122.9 (s, CH), 125.2 (s, CH), 126.0 (s, 4°), 126.2 (d, $J$ = 4 Hz, 4°), 126.4 (s, 4°), 127.2 (s, CH), 127.4 (t, $J$ = 15 Hz, CH), 129.1 (s, CH), 129.7 (s, CH), 135.2 (s, 4°), 136.3 (t, $J$ = 20 Hz, 4°), 137.2 (t, $J$ = 6 Hz), 138.8 (t, $J$ = 16Hz, 4°); $^{31}$P{$^1$H} NMR (CDCl$_3$, 162 MHz) δ 34.8 (s); mp;261-265 °C (decomp.); IR (KBr, cm$^{-1}$):690, 775, 1232, 1402, 1433; HRMS-ESI(+) (m/z) [M−Cl]+ calcd for C$_{49}$H$_{47}$OP$_2$Ru, 815.21456; found, 815.21550.

**Preparation of hydrido(1,2,3,4,5-pentamethylcyclopentadienyl)($\kappa^2$-xantphos)ruthenium (1)**



Cp*Ru(xantphos)H (**1**)
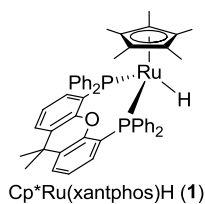
To a 80 mL Schlenk flask, chloro(1,2,3,4,5-pentamethylcyclopentadienyl)($\kappa^2$-xantphos)ruthenium (300 mg, 0.353 mmol) and NaOMe (67.7 mg, 1.25 mmol) were charged with toluene (30 mL) and ethanol (9 mL). The solution was stirred at 50 °C until the $^{31}$P NMR signal of starting material disappeared. After evaporation of the solvent, the resulting yellow powder was dissolved in toluene and cooled at −35 °C. Collection of the precipitated yellow powder and drying under vacuo gave desired product (75.6 mg, yield 26.3%). Single crystals for X-ray analysis was grown by cooling hexane solution of **1** at −35 °C. However disorder of solvent molecule was so significant that the obtained data could not be correctly solved. $^1$H NMR

(THF-$d_8$, 500 MHz) δ −12.1 (t, $J$ = 35 Hz, 1H), 1.11 (s, 15H), 1.71 (s, 3H), 1.94 (s, 3 H), 6.46 (s, 4H), 6.53 (t, $J$ = 5 Hz, 2H), 6.85 (brs, 4H), 7.11 (t, $J$ = 5 Hz, 2H), 7.22 (s, 4H), 7.24 (t, $J$ = 5 Hz, 2H), 7.30 (brs, 2H), 7.51 (d, $J$ = 5 Hz, 2H), 7.91 (s, 4H); $^{13}$C{$^1$H} NMR (THF-$d_8$, 101 MHz) δ 10.09 (s, CH$_3$), 22.09 (s, CH$_3$), 29.93 (s, CH$_3$), 36.92 (s, 4°), 90.60 (s, 4°), 122.04, (s, CH), 124.29 (s, CH), 126.43 (d, $J$ = 10 Hz, CH), 127.79 (s, CH), 127.99 (s, 4°), 128.15 (s, 4°), 128.26 (s, CH), 136.06 (s, 4°), 136.36 (t, $J$ = 6 Hz, CH), 140.71 (m, 4°), 156.10 (s, 4°); $^{31}$P NMR (THF-$d_8$, 202 MHz) δ 65.5 (t, $J_{PH}$ = 34 Hz); mp 266-272 °C (decomp.); IR (KBr, cm$^{-1}$):1863.1 ($\nu_{Ru-H}$); HRMS-ESI(+) (m/z) [M−H]+ calcd for C$_{49}$H$_{47}$OP$_2$Ru, 815.21456; found, 815.21084.

**Details for X-ray crystallography for complex Cp\*Ru(xantphos)Cl, and 1**

Details of the crystalographic data, and the intensity data collection parameters for Cp\*Ru(xantphos)Cl and **1** are listed in Table S1. In each case a suitable crystal was mounted with a mineral oil to a glass fiber and transferred to the goniometer of a Rigaku Mercury CCD or VariMax Saturn CCD diffractometer with graphite-monochromated Mo Kα radiation (λ = 0.71070 Å). The structures were solved by direct methods (SIR-97)[18] and refined by full-matrix least-squares techniques against $F^2$ (SHELEXL-97).[19,20] The intensities were corrected for Lorentz and polarization effects or NUMABS program (Rigaku 2005). The non-hydrogen atoms were refined anisotropically. Hydrogen atoms were placed using AFIX instructions. Structural optimization of **1** could not be completed due to disordering of a co-crystallized hexane molecule. ORTEP drawings of Cp\*Ru(xantphos)Cl and **1** are shown below in Figure 2-10.

**Table 2-3.** Crystallographic data and structure refinement details for Cp*Ru(xantphos)Cl and **1**

| | Cp*Ru(xantphos)Cl | **1** (preliminary) |
|---|---|---|
| formula | $C_{49}H_{47}ClOP_2Ru$ | $C_{49}H_{48}OP_2Ru$ |
| fw | 850.37 | 815.92 |
| $T$ (K) | 103(2) | 93 |
| $\lambda$ (Å) | 0.71070 | 0.71070 |
| cryst syst | monoclinic | monoclinic |
| space group | P21/c | C2/c |
| $a$, (Å) | 20.173(12) | 41.60(2) |
| $b$, (Å) | 11.033(7) | 17.746(9) |
| $c$, (Å) | 23.394(14) | 12.812(6) |
| $\alpha$, (°) | 90 | 90 |
| $\beta$, (°) | 94.187(3) | 102.235(7) |
| $\gamma$, (°) | 90 | 90 |
| $V$, ($Å^3$) | 5193(5) | 9244(8) |
| $Z$ | 4 | 8 |
| $D_{calc}$, (g / $cm^3$) | 1.364 | 1.296 |
| $\mu$ ($mm^{-1}$) | 0.463 | 0.447 |
| F(000) | 2240.0 | 3792 |
| cryst size (mm) | $0.60 \times 0.45 \times 0.20$ | $0.60 \times 0.45 \times 0.20$ |
| $2\theta$ range, (deg) | 3.17-25.00 | 3.05-25.00 |
| reflns collected | 29445 | 38201 |
| indep reflns/$R_{int}$ | 8952/0.0882 | 8115/0.1079 |
| params | 629 | 654 |
| GOF on $F^2$ | 1.302 | 1.287 |
| $R_1$, w$R_2$ [I>2$\sigma$(I)] | 0.1081, 0.1912 | 0.0957, 0.1500 |
| $R_1$, w$R_2$ (all data) | 0.1265, 0.2002 | 0.1071, 0.1547 |
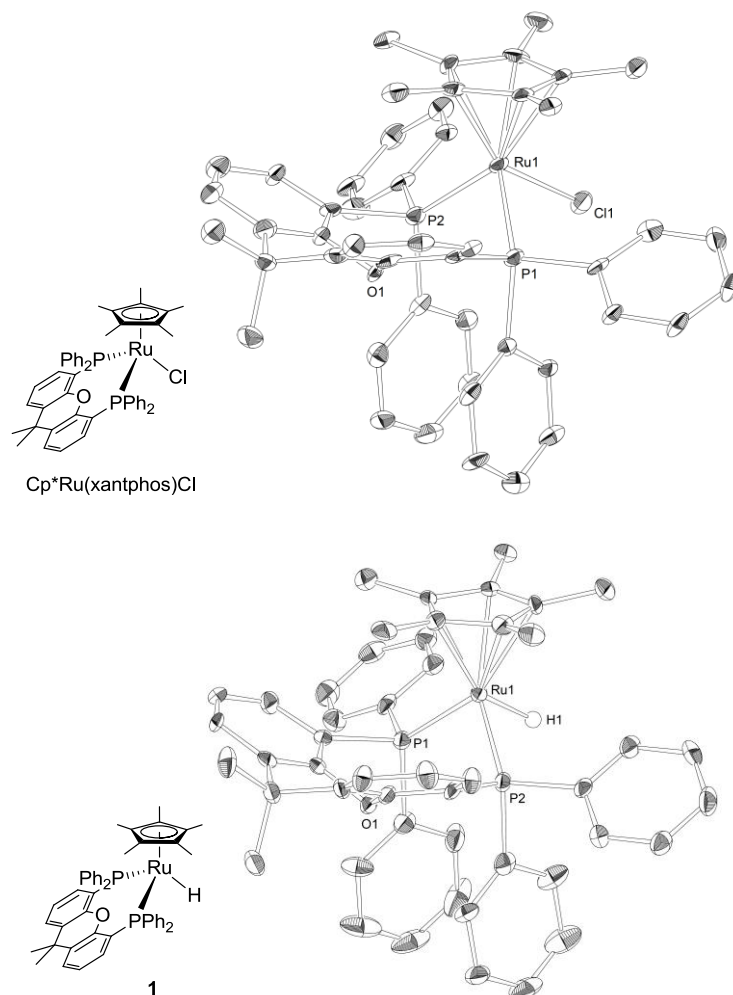
**Figure 2-10.** Ortep drawing of Cp*Ru(xantphos)Cl, and **1** (50% thermal ellipsoid, hydrogen atoms except for that bonded to Ru in **1** were omitted for clarity).

**Stoichiometric reaction of Cp\*Ru(xantphos)H and 1-decene**
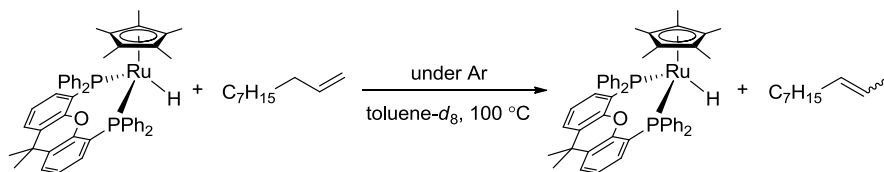


To a toluene-$d_8$ (0.5 mL) solution of Cp\*Ru(xantphos)H (8.1 mg, 10 μmol) in an NMR sample tube, a 2:1 (molar ratio) mixture of 1-decene/dodecane (3.0 μL (ca. 1-decene 10 μmol)) was added and heated at 100 °C. After 19, 22, 26 and 39 hours, the mixture was analyzed by $^1$H and $^{31}$P NMR spectroscopy and after 6 days, it was analyzed by GC using dodecane as an internal standard. During the reaction, almost no change was detected for Cp\*Ru(xantphos)H. Meanwhile, 1-decene was gradually consumed and (*E*)- and (*Z*)-2-decene were accumulated (Figure 2-11).
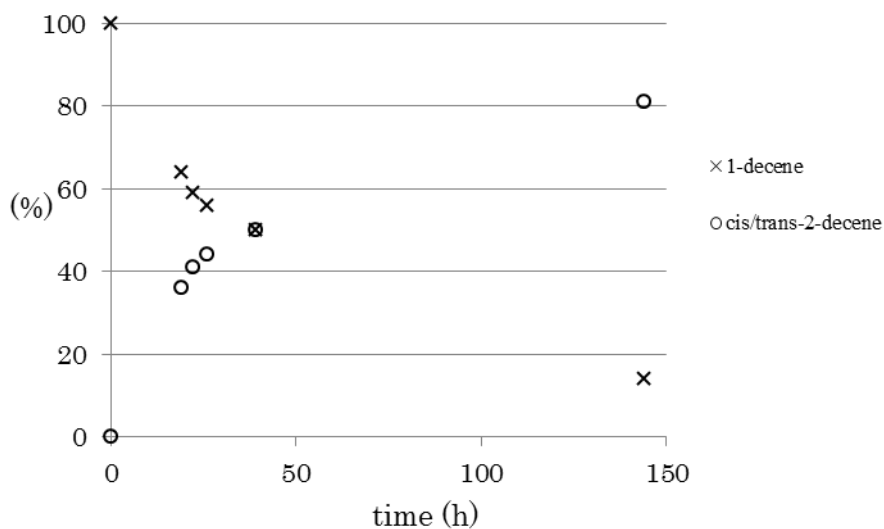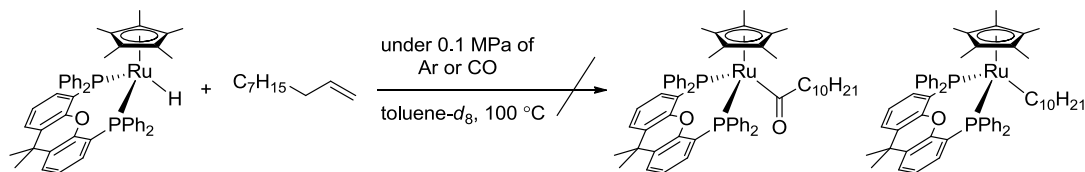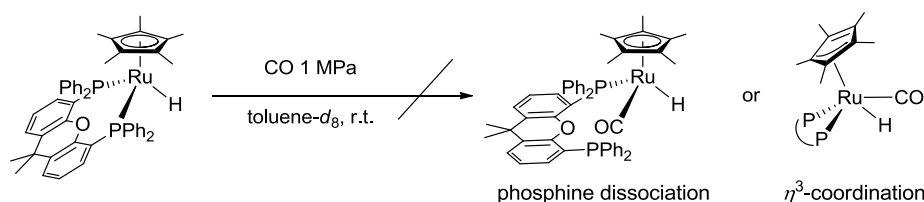


**Figure 2-11.** Stoichiometric reaction of Cp\*Ru(xantphos)H and 1-decene.

## Attempted reaction of Cp*Ru(xantphos)H and 1-decene under Ar or CO atmosphere



To a toluene-$d_8$ (0.5 mL) solution of Cp*Ru(xantphos)H (8.1 mg, 10 μmol) in an NMR sample tube, a 2:1 (molar ratio) mixture of 1-decene/dodecane 3 μL (1-decene ca. 10 μmol) was added and heated at 100 °C under CO atmosphere. After 24 and 48 hours, the sample was analyzed by $^1$H and $^{31}$P NMR spectroscopy. Only Cp*Ru(xantphos)H and dissociated XANTPHOS were observed in the $^{31}$P NMR spectrum. No evidence for the formation of the acylruthenium complex was found in the $^1$H NMR spectrum (no signal was detected for the triplet at alpha to the carbonyl, Ru-C(=O)-C$\underline{H}_2$-CH$_2$-).

## Attempted reaction of Cp*Ru(xantphos)H and CO



Toluene-$d_8$ solution of Cp*Ru(xantphos)H was treated with CO (0.1 MPa) at 100 °C or at room temperature. Ruthenium complexes coordinated by carbon monoxide were not detected.

**Stoichiometric reaction of 1-decene-*d*₂ and 1**

To a toluene-$d_8$ (0.5 mL) solution of **1** (8.1 mg, 10 μmol) and 1,3,5-trimethoxybenzene (1.5 mg, 8.9 μmol, added as an internal standard and inactive under the reaction condition) in an NMR sample tube, 1-decene-$d_2$ 2.1 μL (96% D on C1, ca. 10 μmol) was added and heated at 100 °C. The sample was analyzed by $^1$H NMR spectroscopy with 60 seconds of relaxation delay.
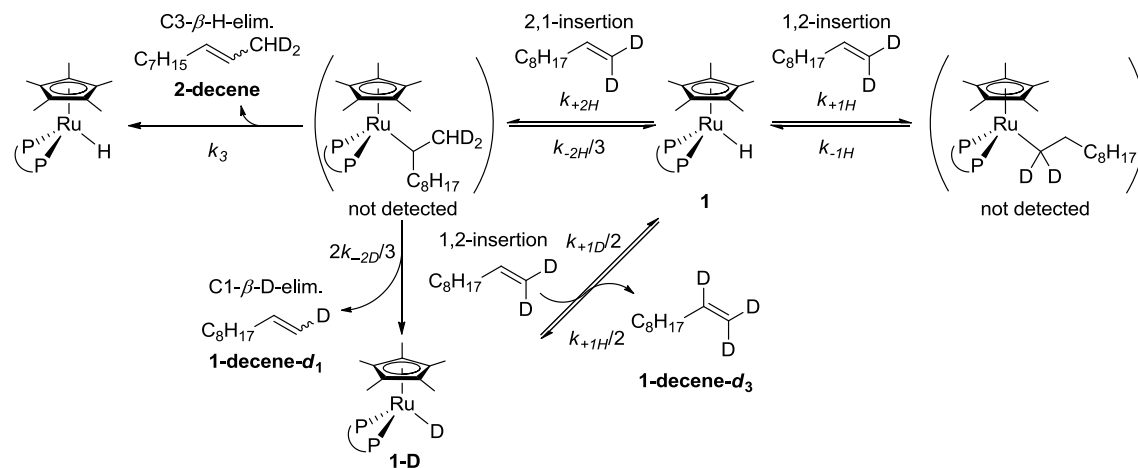


Representative spectrum is shown below. The isotopomers were not distinguishable. (For example, H on C2 of $C_8H_{17}C\underline{H}=CD_2$ and $C_8H_{17}C\underline{H}=CHD$ were integrated as one signal).
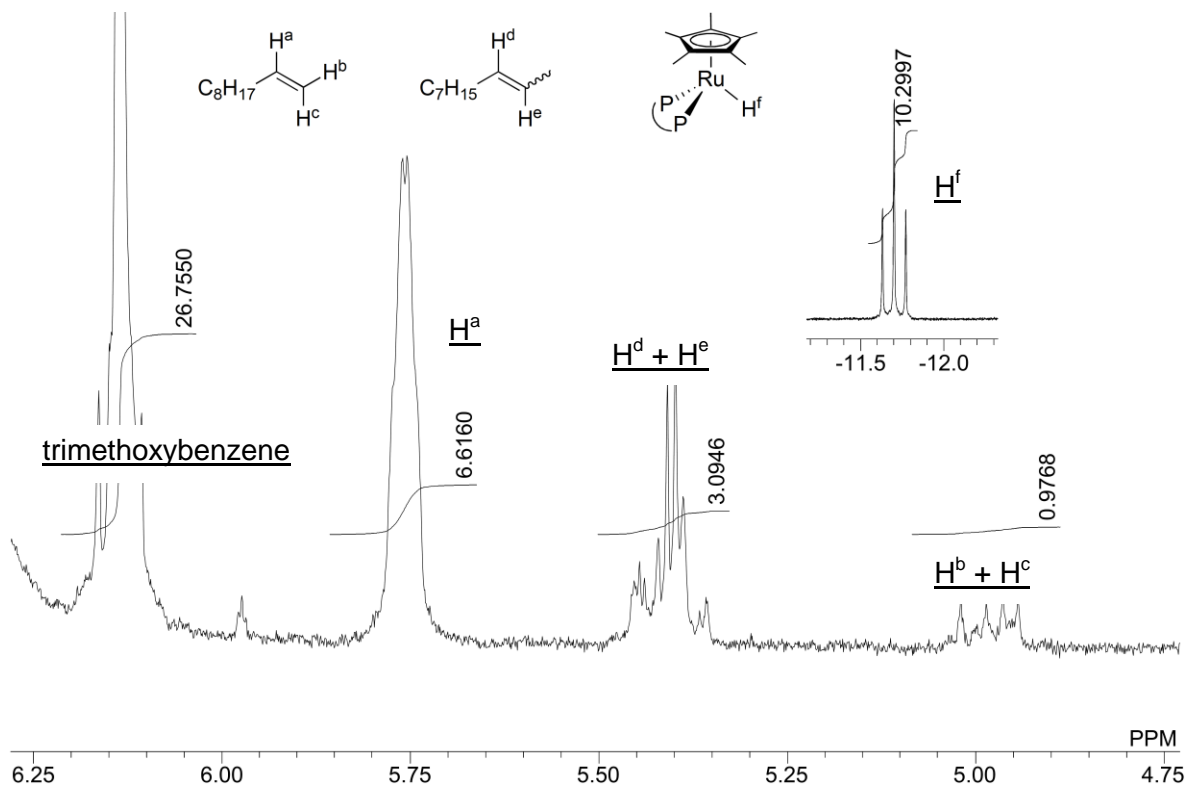
**Figure 2-12.** Vinylic region of $^1$H NMR spectrum after 7 hours.
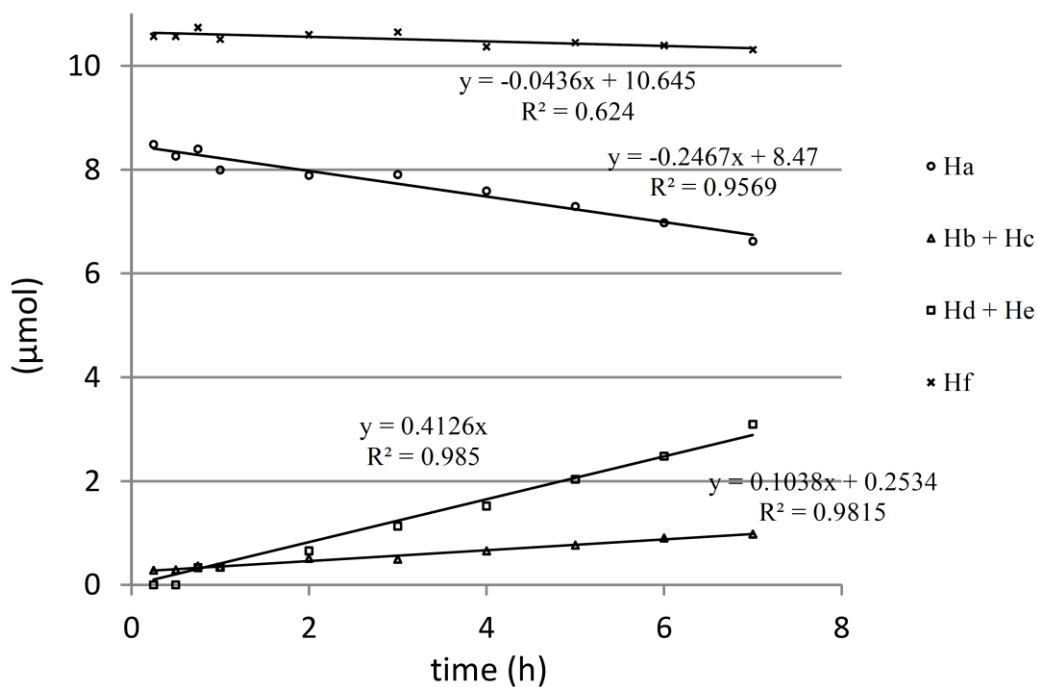


**Figure 2-13.** Time course for the integral ratio of vinylic protons in the stoichiometric reaction of 1-decene-$d_2$ and **1**.
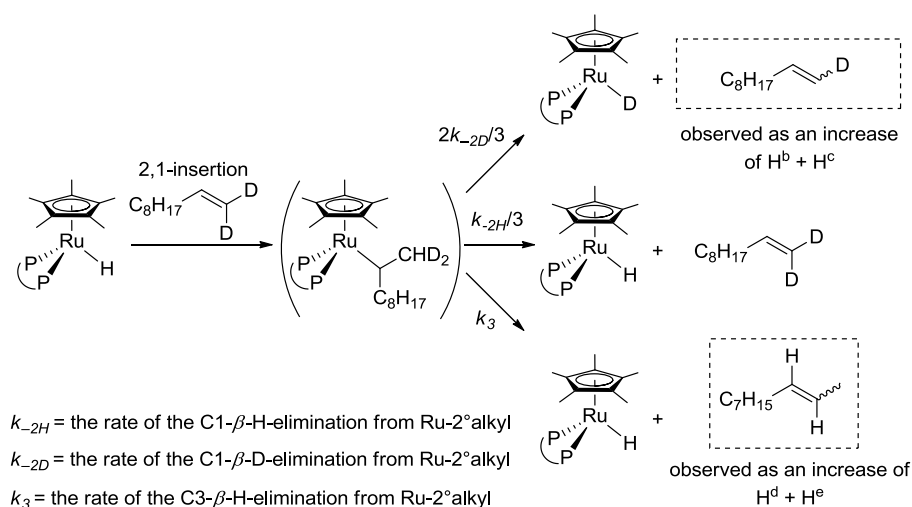
**Figure 2-14.** 2,1-insertion-$\beta$-elimination process.

In the initial stage of the reaction, increase of $H^b + H^c$ (0.10 µmol h$^{-1}$) corresponds to the formation of 1-decene-$d_1$ and increase of $H^d + H^e$ (0.41 µmol h$^{-1}$) corresponds to the formation of 2-decene-$d_2$ (incorporation of deuterium on C2 and C3 of 2-decene was confirmed to be negligibly slow by $^2$H NMR). The integral ratio of these signals gave the ratio between the rates of the C1-$\beta$-D-elimination and the C3-$\beta$-H-elimination to be $k_{-2D}$:$k_3$ = 0.8:1 (0.1038 × 3/2:0.4126/2 = 0.7547:1). Considering the reported kinetic isotope effect for $\beta$-H-elimination 1.0 ~ 3.3, $k_{-2H}$:$k_3$ could be estimated to be 0.8:1 ~ 2.6:1 showing that they are comparable to each other.
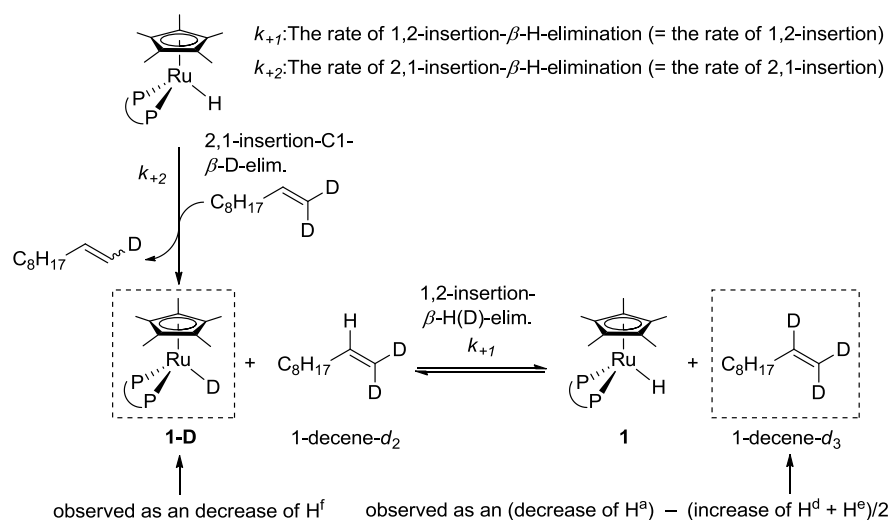
**Figure 2-15.** Scheme for comparison of 1,2-insertion and 2,1-insertion process.

The decrease of $H_a$ was ascribed to the conversion of 1-decene-$d_2$ to 2-decene-$d_2$ or 1-decene-$d_3$ assuming that the participation of 1-decene-$d_1$ to this process was negligible at the initial stage of the reaction,. Thus, the rate of formation of 1-decene-$d_3$ was calculated as 0.04 µmol h$^{-1}$ (0.2467 – 0.4126/2 = 0.0404). During the increase of $H^b$, $H^c$, $H^d$, and $H^e$, the ratio of 1-decene-$d_3$ and **1-D** was constant at 0.9:1.0 (0.0404:0.0436 = 0.926:1.000). This implies the much faster 1,2-insertion-$\beta$-H(D)-elimination than the 2,1-insertion-$\beta$-D-elimination so that there existed rapid equilibrium between **1-D** plus 1-decene-$d_2$ and **1** plus 1-decene-$d_3$. Otherwise the ratio of 1-decene-$d_3$:**1-D** would have increased as the reaction proceeded; namely, the concentration of **1-D** could have first increased, and then 1-decene-$d_3$ could have gradually formed. Since any Ru-alkyl species was not observed in the above experiment, any insertion steps of 1-decene to Ru–H was considered to be much slower than $\beta$-elimination. Therefore, the rate of 1,2-insertion ($k_{+1}$) represents the rate of 1,2-insertion-$\beta$-H-elimination. In the same way, $k_{+2}$ represents the rate of 2,1-insertion-$\beta$-H-elimination. In conclusion, 1,2-insertion estimated to be much faster than 2,1-insertion.

**Hydroformylation of 1-decene-$d_2$**

To a 50 mL stainless autoclave with magnetic stirring bar, **1** (20.4 mg, 0.025 mmol) and XANTPHOS (14.5 mg, 0.025 mmol) were charged with 2 mL of toluene. To the mixture, 1-decene-$d_2$ (96% D on C1, 143 mg, 1.00 mmol) was added and then the autoclave was pressurized with $H_2/CO$ (2 MPa). At 160 °C, after 48 h, the autoclave was cooled to 0 °C with water/ice bath. The gas pressure was released and to the resulting solution was added dodecane (82.1 mg, 0.482 mmol, internal standard for GC) and 1,3,5-trimethoxybenzene (60.5 mg, 0.360 mmol, internal standard for $^1H$ NMR). The resulting solution was diluted with $C_6D_6$ and the sample was analyzed by $^2H$ and $^1H$ NMR spectroscopy. The product solution was diluted by toluene and was analyzed by GC.

**Hydroformylation of 1-decene by 1/XANTPHOS under various initial concentration of 1-decene**

To a stainless autoclave (50 mL) charged with Ru complex (25.0 µmol), XANTPHOS (14.5 mg, 25.0 µmol) and magnetic stir bar under Ar, toluene (2.0 mL) and 2:1 mole ratio mixture of 1-decene and dodecane (total 300 µL, 150µL , or 75µL, 1-decene 1.0 mmol, 0.5 mmol, or 0.25 mmol) were added via syringe. The autoclave was pressurized with 2.0 MPa of $H_2/CO$ and stirred at 160 ºC, at 800 rpm, for 24 hours. Then the autoclave was cooled with water/ice bath for 30 minutes, the pressure was released. Then the solution was analyzed by GC.

# References

1) (a) Evans, D.; Osborn, J. A.; Jardine, F. H.; Wilkinson, G. *Nature* **1965**, *208*, 1203. (b) (c) Fusi, A.; Cesarotti, E.; Ugo, R. *J. Mol. Cat.* **1981**, *10*, 213. (d) Bianchi, M.; Menchi, G.; Frediani, P.; Matteoli, U.; Piacenti, F. *J. Organomet. Chem.* **1983**, *247*, 89. (e) Sussfink, G.; Schmidt, G. F. *J. Mol. Cat.* **1987**, *42*, 361. (f) Hayashi, T.; Gu, Z. H.; Sakakura, T.; Tanaka, M. *J. Organomet. Chem.* **1988**, *352*, 373. (g) Khan, M. M. T.; Halligudi, S. B.; Abdi, S. H. R. *J. Mol. Cat.* **1988**, *45*, 215. (h) Knifton, J. F. *J. Mol. Cat.* **1988**, 47, 99. (i) Mitsudo, T.; Suzuki, N.; Kondo, T.; Watanabe, Y. J. Mo, *J. Mol. Cat. A* **1996**, *109*, 219. 1j) Multiple species are possibly formed under $H_2/CO$. There is a report isolating $H_4Ru_4(CO)_{12}$ by treating $Ru_3(CO)_{12}$ under high $H_2/CO$ pressure: Piacenti, F.; Bianchi, M.; Frediani, P.; Benedetti, E. *Inorg. Chem.* **1971**, *10*, 2759.

2) Omatsu, T.; Tokihiko, Y.; Yoshimura, N. EP0303060, 1989.

3) Kranenburg, M.; van der Burgt, Y. E. M.; Kamer, P. C. J.; van Leeuwen, P. W. N. M.; Goubitz, K.; Fraanje, J. *Organometallics* **1995,** *14*, 3081.

4) (a) Devon, T. J. P., G. W.; Puckette, T. A.; Stavinoha, J. L.; Vanderbilt, J. J. US4694109, 1987. (b) Casey, C. P.; Petrovich, L. M. *J. Am. Chem. Soc.* **1995**, *117,* 6007.

5) (a) Davis, A. J. H.; Mawby, R. J. *J. Am. Chem. Soc. A.* **1969**, 2403. (b) Casey, C. P.; O'Connor, J. M. *Organometallics* **1985**, *4*, 384. (c) Davis, A. J.; White, C.; Mawby, R. J. *Inorg. Chim. Act.* **1970**, *4*, 441. (d) Ligand Substitution Ractions. *Organotransition Metal Chemistry: From Bonding to Catalysis*, Hartwig, J. F. Eds.; University Science Books: Sausalito, 2010, 250.

6) van Leeuwen, P. W. N. M.; Claver, C., *Rhodium Catalyzed Hydroformylation*. Springer - Verlag: 2000.

7) Among the reported values, $k_H/k_D = 2.28 \pm 0.20$ for the thermolysis of $[Ir(CO)(^noctyl)(PPh_3)_2]$ better represents the KIE of $\beta$-hydride elimination. In this case, $k_{-2H}/k_3$=1.8:1. See: Evans, J.; Schwartz, J.; Urquhart, P. W. *J. Organomet. Chem.* **1974**, *81*, C37. Other reports are Cobalt: Ikariya, T.; Yamamoto, A. *J. Organomet. Chem.* **1976**, *120*, 257. Platinum: Bryndza, H. *J. Chem. Soc. Chem. Commun.* **1985**, 1696. and review: Sierra, M.; Gallego, G. *Chem. Rev.* **2011**, *111*, 4857.

8) (a) Blum, Y.; Shvo, Y. *Inorg. Chim. Acta* **1985**, *97*, L25. (b) Shvo, Y.; Czarkie, D. *J. Organomet. Chem.* **1986**, *315*, C25. (c) Shvo, Y.; Czarkie, D.; Rahamim, Y.; Chodosh, D. F. *J. Am. Chem. Soc.* **1986**, *108*, 7400. (d) Aleix, C. V.; Gregori, U.; Agusti, L. *Organometallics* **2008**, *27*, 4854.

9) Kölle, U.; Kossakowski, J.; Raabe, G. *Angew. Chem. Int. Ed.* **1990**, *29*, 773.

10) Eady, C. R.; Jackson, P. F.; Johnson, B. F. G.; Lewis, J.; Malatesta, M. C.; McPartlin, M.; Nelson, W. J. H. *J. Chem. Soc., Dalton Trans.* **1980**, 383.

11) Johnson, B. F. G.; Lewis, J.; Raithby, P. R.; Suss, G. *J. Chem. Soc., Dalton Trans.* **1979**, 1356.

12) Sridevi, V. S.; Leong, W. K. *J. Organomet. Chem.* **2007**, *692,* 4909.

13) Ghosh, P.; Fagan, P. J.; Marshall, W. J.; Hauptman, E.; Bullock, R. M. *Inorg. Chem.* **2009**, *48*, 6490.

14) Oshima, N.; Suzuki, H.; Moro-oka, Y. *Chem. Lett.* **1984**, 1161.

15) M. Takai, I. Nakajima, T. Tsukahara, Y. Tanaka, H. Urata, A. Nakanishi, US2002049355, 2002.

16) Lloyd-Jones, G. C.; Robinson, A. J.; Lefort, L.; Vries, J. G. *Chem. Eur. J.* **2010**, *16*, 9449.

17) Belger, C.; Neisius, N. M.; Plietker, B. *Chem. Eur. J.* **2010**, *16,* 12214.

18) Altomare, A.; Burla, M. C.; Camalli, M.; Cascarano, G. L.; Giacovazzo, C.; Guagliardi, A.; Moliterni, A. G. G.; Polidori, G.; Spagna, R., *J. Appl. Crystallogr.* **1999,** *32*, 115.

19) Sheldrick, G. M. SHELXL-97, Program for the Refinement of Crystal Structures, University of Göttingen: Göttingen, Germany, 1997.

20) Sheldrick, G. M.; Schneider, T. R., SHELXL: High-resolution refinement. In *Macromolecular Crystallography, Pt B*, Academic Press Inc: San Diego, 1997; Vol. 277, pp 319.

# Chapter 3
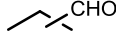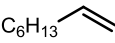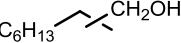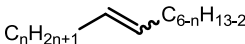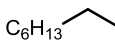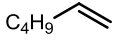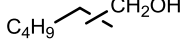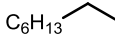
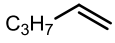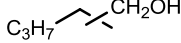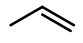# Hydroformylation/Hydrogenation of Terminal Alkenes Catalyzed by Ru-Based Catalyst Systems
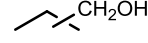
# 3 Hydroformylation/hydrogenation of Terminal Alkenes Catalyzed by Ru-Based Catalyst Systems

## 3-1 Background

There has been relatively small number of reports about ruthenium-based hydroformylation/hydrogenation catalyst (Table 3-1). Some of them has already introduced in chapter 2. In general, strong electron donar ligands enables catalysts to mediate hydrogenation under $H_2$/CO, which is also the case for rhodium and cobalt systems (detail explanation is in chapter 4). For example, ruthenium modified by tri-*normal*-butylphosphine catalyze this tandem reaction under relatively harsh conditions with low $n/i$ ratio.[1] $Ru_3(CO)_{12}$/2,2'-bipyridyl/$P^nBu_4Br$ melt catalyst system gives alcohols with higher $n/i$ selectivity up to 6.1 from 1-octene.[2] Polymeric carbonylruthenium catalyst is intrresting system, which can affords alcohol without assistance of phosphorus ligand.[3] Recently, Beller *et al*. reported ruthenium modified by 2-imidazolylphosphin ligand to facilitate this reaction with relatively high activity and $n/i$ selectivity as a ruthenium-based catalyst.[4] So far the problem of these sys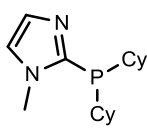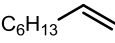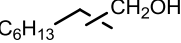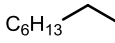tems is their low catalytic activities and $n/i$ selectivities compared to rhodium and cobalt systems. In most cases the activity for hydrogenation is derived from high nucleophilicity of hydride ligand on the ruthenium increased by the strong electron donation from ligands. Also, such species can potentially react with alkene to give alkane, which is a problematic side reaction in this tandem reaction. Therefore, new design of catalyst that enables ruthenium center to proceed hydrogenation of aldehyde under $H_2$/CO selectivly in the presence of alkene is desired.

**Table 3-1.** Previous examples of ruthenium-based tandem hydroformylation/hydrogenation

| complex (mmol) additive (mmol) | condition | substrate | product (yield, *n/i*) | byproduct (yield) | ref |
|---|---|---|---|---|---|
| RuCl$_3$/$^n$Bu$_3$P/NaOAc[x)] (0.07 M, 0.14 M, 0.35 M) | H$_2$/CO = 2/1 MPa, octane, 195 °C | C$_3$H$_7$ ⟍⟍ (2.3 M) Conv. 93.6% | C$_3$H$_7$ ⟍⟍CH$_2$OH *n/i* = 2 | | 1 |
| Ru$_3$(CO)$_{12}$ (6.0 mmol)[x)] 2,2'-bipyridyl (6.0 mmol) Bu$_4$PBr (29 mmol) | H$_2$/CO = 5.6/2.8 MPa, neat, 160 °C, 4 h | ⟍⟍ (0.4 mol) | ⟍⟍CH$_2$OH (89.5% of liquid) | ⟍⟍CHO (6.4%) | 2 |
| Ru$_3$(CO)$_{12}$ (6.0 mmol)[x)] 2,2'-bipyridyl (6.0 mmol) Bu$_4$PBr (29 mmol) | H$_2$/CO = 5.6/2.8 MPa, neat, 180 °C, 4 h | C$_6$H$_{13}$ ⟍⟍ (0.2 mol) | C$_6$H$_{13}$ ⟍⟍CH$_2$OH (79.6%, 6.1) | C$_n$H$_{2n+1}$⟍⟍⟍C$_{6-n}$H$_{13-2n}$ (9.0%) ; C$_6$H$_{13}$⟍⟍ (9.0%) | 2 |
| [Ru(CO)$_4$]$_n$ (0.26 mmol)[x)] | H$_2$/CO = 2.5/2.5 MPa, toluene, 150 °C, 17 h | C$_4$H$_9$ ⟍⟍ (0.5 mL) | C$_4$H$_9$ ⟍⟍CH$_2$OH (92%, 1.7) | C$_6$H$_{13}$⟍⟍ (4%) | 3 |
| Ru$_3$(CO)$_{12}$ (0.04 mmol)[x)] LiCl (5.00 mmol mmol) [imidazolyl–P(Cy)(Cy)] (0.132 mmol) | H$_2$/CO = 3.0/3.0 MPa, H2O (56 mmol), NMP, 130 °C, 20 h | C$_6$H$_{13}$ ⟍⟍ (20.0 mmol) | C$_6$H$_{13}$ ⟍⟍CH$_2$OH (90%, 7.3) | C$_6$H$_{13}$⟍⟍ (3%) | 4 |

## 3-2 Tandem *normal*-selective hydroformylation/hydrogenation of 1-decene

In the previous chapter, cyclopentadienylruthenium/bisphosphine system was developed as *normal*-selective hydroformylation catalyst (**A**, in Figure 3-1). On the other hand, hydroxycyclopentadienylruthenium was known to be a hydrogenation catalyst, which preferably reacts with aldehydes over alkenes (**B**, in Figure 3-1, for detail, see chapter 1).[5] This type of catalyst reacts with substrates in a concerted mechanism. In this mechanism, polar double bonds such as C=O bond are more rapidly hydrogenated than less polar double bond such as C=C

bond.[1d] Then, it was assumed that (hydroxyCp)Ru(bisphosphine)H (**C**) is supposed to have feature of both of catalyst **A** and **B**, and capable of catalyzing tandem *normal*-selective hydroformylation/hydrogenation. In this work, ruthenium complexes **1**-**4** (Figure 3-2), which are known to generate hydroxycyclopentadienylruthenium under $H_2$, were studied.
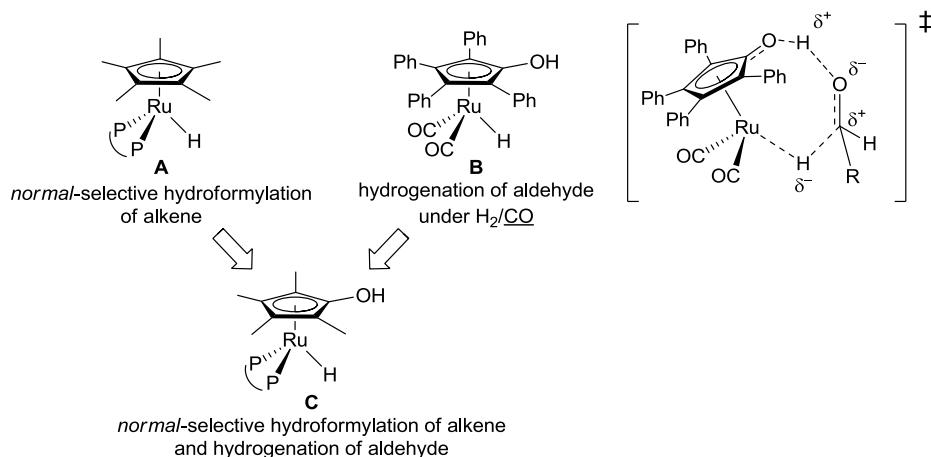


**Figure 3-1.** Design of ruthenium-based hydroformylation/hydrogenation catalyst
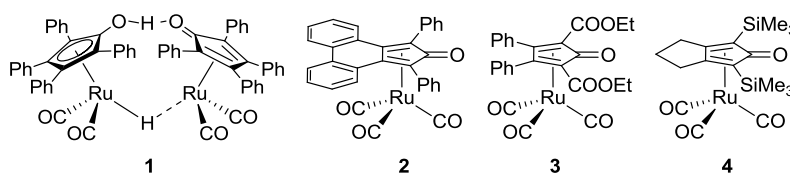


**Figure 3-2.** Ruthenium complexes investigated in this work

When 1-decene was treated with a catalytic amounts of **1** and XANTPHOS,[6] *normal*-undecanol was obtained in moderate yield and with high *n*/*i* selectivity (58%, *n*/*i* = 35, run 1, Table 3-2). The major side product was isomerized alkenes. When **2** possessing phenanthrene fused cyclopentadienone was used, the *n*-alcohol was obtained in a yield similar to **1** (run 2). On the other hand, a ruthenium complex with ethoxycarbonyl substituted cyclopentadienone (**3**)

exhibited high activity towards isomerization of the alkene and was not effective either in hydroformylation or hydrogenation (run 3). The highest yield of alcohol was obtained with **4** up to 70% yield and $n/i$ ratio of 29 (run 4). This value of $n/i$ ratio is highest reported for ruthenium based tandem hydroformylation/hydrogenation and highest level if it is compared to those of cobal and rhodium systems. The difference of activity among complex **1–4** could be explained by the stability of these catalysts. Under high carbon monoxide pressure and temperature, cyclopentadienone can be replaced by carbon monoxide to generate ineffective carbonylruthenium multinuclear complex. In the case of **3**, ethoxycarbonyl substituted cyclopentadienone is relatively electron poor diene. Therefore, the coordination to ruthenium is supposed to be weaker. On the other hand, trimethylsilyl substituted cyclopentadienone is relatively electron rich ligand. So the coordination to ruthenium is stronger. Actually, when the IR absorption frequencies of the stretch of C–O bond is compared, they are 2002, 2029, and 2100 cm$^{-1}$ for **3** and 2006 and 2070 cm$^{-1}$ for **4** respectively. These values indicate the stronger electron donation from the cyclopentadienone makes ruthenium center of **4** more electron rich, that resulted in stronger backdonation to carbon monoxide, and weaker bond between C–O. Use of BISBI[7] resulted in lower rate of hydroformylation and hydrogenation (run 5). This is probably due to relatively stronger electron donating property of BISBI compared to XANTPHOS (benzyldiaryl phosphine versus triaryl phosphiine). Stronger donation from BISBI to ruthenium center resulted in stronger backdonation to and coordination of carbon monoxide, and this disturbs the coordination of other substrate. On the other hand, isomerization of the alkene was predominant when A4N3[8] was used (run 6). One of the possibilities is that A4N3 is so a weak electron donor that makes coordination of carbon monoxide relatively weak. That slows down the rate of insertion of carbon monoxide relatively slower than $\beta$-hydride elimination, which

resulted in rapid isomerization of C=C bond of alkenes. In summary, cyclopentadienone needs to be basic to maintain its coordination to ruthenium center. On the other hand, phosphorus ligands can't be a too strong or weak base because of the balance of lability of carbon monoxide on ruthenium center and susceptibility to the isomerization of alkenes.

**Table 3-2.** Tandem hydroformylation/hydrogenation catalyzed by ruthenium-based systems.[a]



| run | catalyst | conv. (%) | aldehydes | | alccohols | | internal alkenes (%) | alkane (%) |
|-----|----------|-----------|-----------|-----|-----------|-----|----------|--------|
| | | | yield (%) | n/i | yield (%) | n/i | | |
| 1 | **1**/XANTPHOS | 95 | 12 | 6.9 | 58 | 35 | 8 | 2.9 |
| 2 | **2**/XANTPHOS | 100 | 17 | 29 | 50 | 26 | 24 | 3.0 |
| 3 | **3**/XANTPHOS | 60 | 7.0 | 32 | 0.5 | - | 50 | nd[b] |
| 4 | **4**/XANTPHOS | 98 | 1.2 | - | 70 | 29 | 12 | 2.3 |
| 5 | **4**/BISBI | 87 | 43 | 24 | 18 | 19 | 14 | 1.9 |
| 6 | **4**/A4N3 | 96 | 0.5 | 2.3 | 10 | 26 | 77 | nd[b] |

[a]Reaction condition: 1-decene 1.0 mmol, Ru complex 25 µmol (based on Ru atom), phosphorus ligand 50 µmol, toluene 2.0 mL, $H_2$ 1.0 MPa, CO 1.0 MPa, 160 °C, 24 h. The yields in the table were determined by gas chromatography using dodecane as internal standard. $n/i$ = (mol of $n$-product)/(mol of $i$-products). [b]Not determined due to peak overlapping of isomerized alkenes and alkane on GC spectrum.

For the next stage, hydroformylation/hydrogenation of 1-eicosene was monitored by in-situ infrared spectroscopy (Figure 3-3). As a result, aldehyde was not observed as intermediate of this tandem reaction. This fact indicated that the rate of hydrogenation of aldehyde is much faster than the rate of hydroformylation of 1-eicosene. Alternatively, it could be interpreted that aldehyde is not an intermediate of this tandem reaction. Although it is not a direct evidence, hydrogenation of aldehyde under $H_2$/CO was confirmed to be catalyzed by **4**, which supports that aldehyde is produced as an intermediate. Another important fact is that the rate of

hydroformylation is zero-order to 1-decene concentration because the time course of 1-eicosene was linearly plotted versus time. This will be revisited in the discussion of the reaction mechanism.
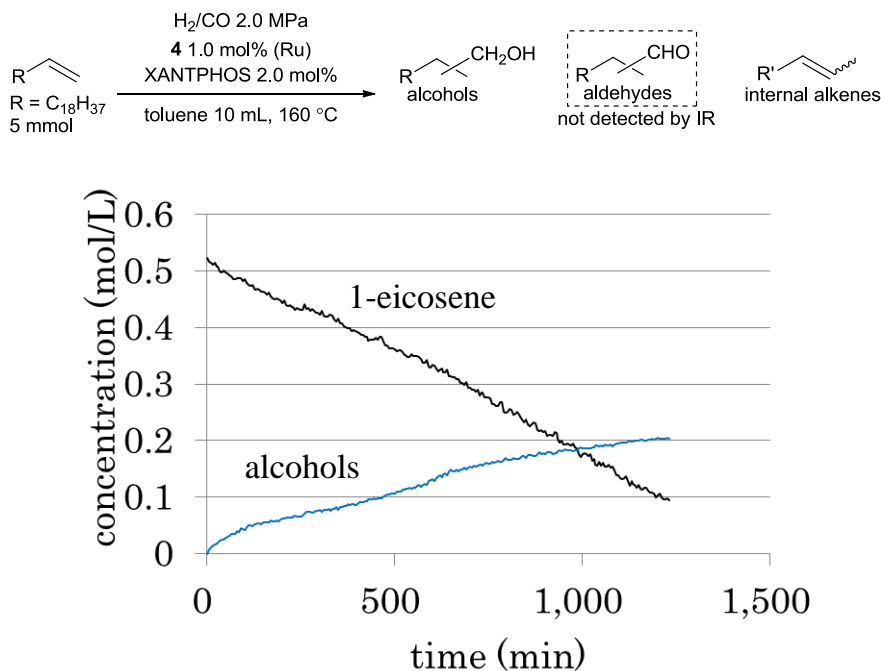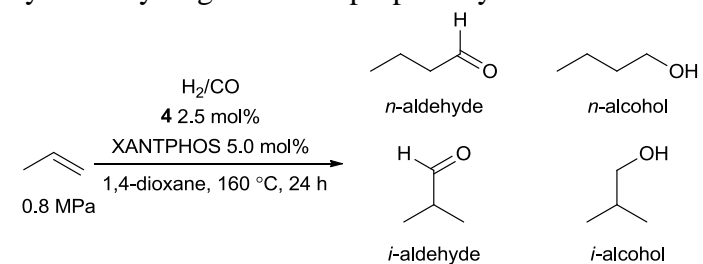


**Figure 3-3.** Time courses of 1-decene and alcohol in the hydroformylation/hydrogenation of 1-eicosene

## 3-3 Tandem *normal*-selective hydroformylation/hydrogenation of propene

Finally, this system was applied to hydroformylation/hydrogenation of propene (Table 3-3). In the case of 1-decene, isomerization to internal alkenes was a problematic side reaction, which is not the case for propene. Aldehydes remained under 1.0 MPa of $H_2$ and 1.0 MPa of CO. Hydrogenation was accelerated by lowering CO pressure down to 0.5 MPa. With this change, alcohols were obtained as major product with *n/i* ratio of 11. Catalytic activity and *n/i* ratios were similar to those of [Cp*Ru(acac)]$_2$/XANTPHOS system.

**Table 3-3.** Hydroformylation/hydrogenation of propene by **4**/XANTPHOS [a]



| run | H$_2$/CO (MPa) | aldehyde | | alcohol | |
|---|---|---|---|---|---|
| | | TOF for aldehydes (h$^{-1}$) | n/i | TOF for alcohols (h$^{-1}$) | n/i |
| 1 | 1.0/1.0 | 1.9 | 14 | 1.1 | 7.7 |
| 2 | 1.0/0.5 | 0.05 | - | 3.1 | 11 |

[a]1,4-dioxane 2.0 mL, TOFs were determined by GC using dodecane as an internal standard.

## 3-4 Proposed reaction mechanism

The reaction mechanism is proposed as illustrated in Scheme 3-1. Under H$_2$/CO, (cyclopentadienone)ruthenium(0) complex is equilibrated with hydrido(hydroxycyclopentadienyl)ruthenium. Similarly to the Cp*Ru system, insertion of an alkene to the Ru–H takes place to give an alkylruthenium complex. Sequential insertion of carbon monoxide and hydrogenolysis release aldehyde and regenerate hydrido(hydroxycyclopentadienyl)ruthenium. The aldehyde is successively hydrogenated via a concerted mechanism to affords alcohol accompanied by coordination of CO to form (cyclopentadienone)ruthenium(0).

**Scheme 3-1.** Proposed catalytic cycle for the tandem hydroformylation/hydrogenation catalysed by cyclopentadienoneruthenium



L = phosphorus ligand or CO
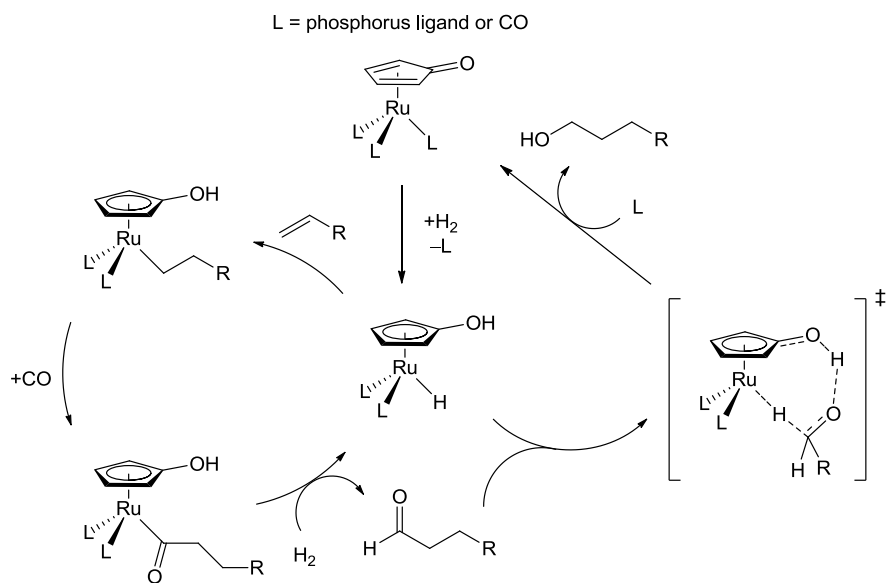
Although it is not clear which step is the selectivity determining step, bulky bisphosphorus ligands supposed to make any of the intermediates or transition states for the *normal*-alkyl complexes more preferable than the *iso* counterparts with steric repulsion with their alkyl chain. The result of real-time IR monitoring indicated that the reaction rate is zero order on alkene concentration. One possible interpretation is that the rate-determining step is the generation of hydridoruthenium from (cyclopentadienone)ruthenium(0), which is independent of the concentration of alkene. The preferential hydrogenation compared to hydroformylation could be explained by the relatively lower barrier of hydrogenation of aldehyde than insertion of alkene to Ru–H. Lledós *et al*. reported DFT calculation for these processes (Figure 3-4).[9] They proposed that the insertion of alkene proceeded via $\eta^2$-Cp complex and the transition state barrier is 32.1 kcal/mol in the case of the model complex (Ph of Shvo's catalyst is replace by H) and ethylene. Therefore, the barrier to release aldehyde is at least the same or higher than 32.1 kcal/mol. On

the other hand, the highest barrier for the transfer of hydrogen atoms to formaldehyde via concerted mechanism to release methanol is 11.0 kcal/mol. This result supports the author's explanation for the reason why hydrogenation takes place preferably to hydroformylation.
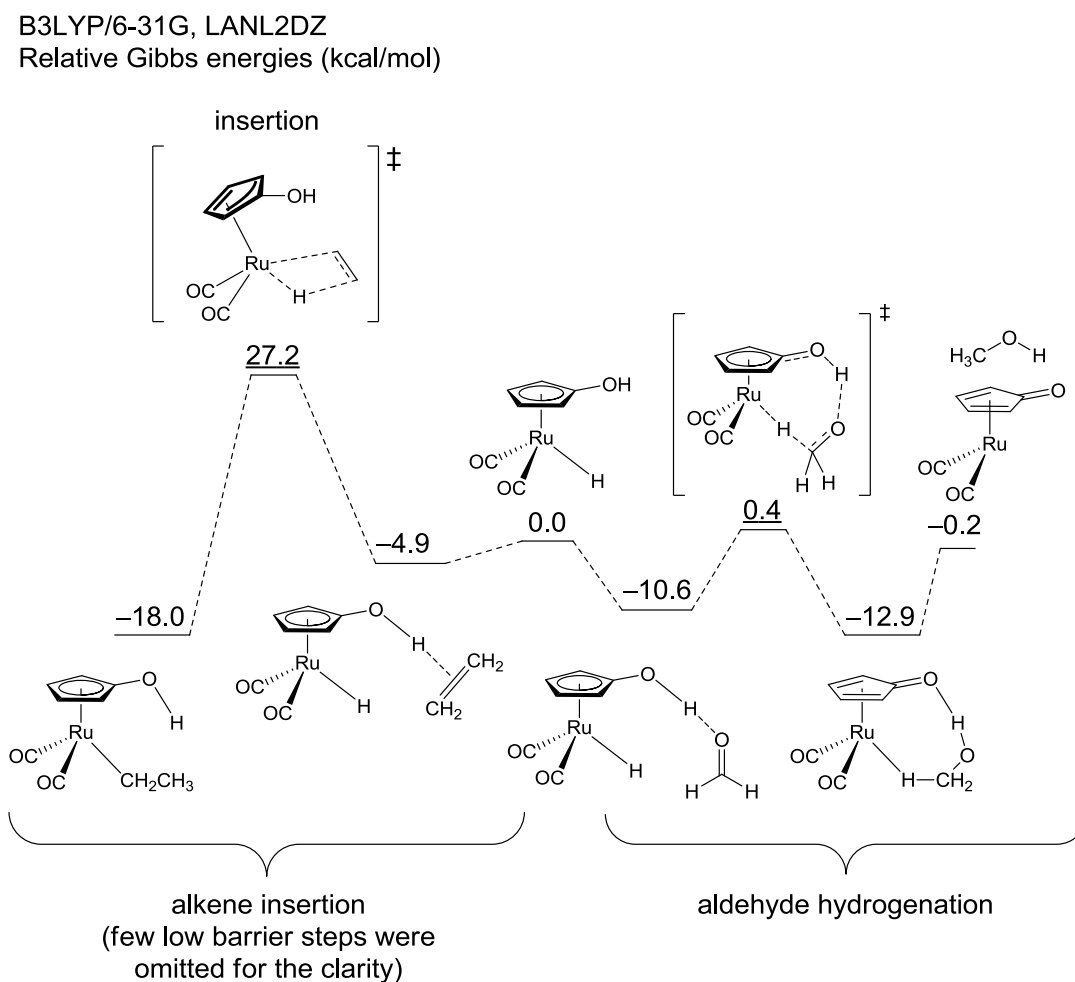


**Figure 3-4.** Comparison of the computationally calculated barrier of alkene insertion and aldehyde hydrogenation by model complex of Shvo's catalyst

## 3-5 Conclusion

In this chapter, based on the speculation that hydroxycyclopentadienylruthenium/ bisphosphine system would be a tandem *normal*-selective hydroformylation/hydrogenation catalyst,

cyclopentadienoneruthenium/bisphosphine system was investigated and found to catalyze the reaction in one-pot in moderate yield and reaction rate but with highest level of $n/i$ ratio as a tandem hydroformylation/hydrogenation catalyst. If the rate-determining step is the generation of hydridoruthenium from (cyclopentadienone)ruthenium(0), the reaction rate should be increased by introducing electron withdrawing ligand, which facilitates dissociation of CO. However, as demonstrated with bisphosphite ligand in Table 3-2, that will result in rapid isomerization of terminal alkene to internal alkenes.

## Experimental Section

### General

General experimental details are common with those in Chapter 2.

### Hydroformylation/hydrogenation of 1-decene by Ru singular catalyst

To a stainless autoclave (50 mL) charged with Ru complex (25.0 µmol), XANTPHOS (28.9 mg, 50.0 µmol) and magnetic stir bar under Ar, toluene (2.0 mL) and 2:1 mole ratio mixture of 1-decene and dodecane (total 300 µL, 1-decene 1.0 mmol, dodecane 0.5 mmol) were added via syringe. The autoclave was pressurized with 2.0 MPa of $H_2$/CO and stirred at 160 ºC, at 800 rpm, for 24 hours. Then the autoclave was cooled with water/ice bath for 30 minutes, the pressure was released. Then the solution was analyzed by GC.

### Hydroformylation/hydrogenation of propene by Ru singular catalyst

To a stainless autoclave (50 mL) charged with Ru complex (25.0 µmol), XANTPHOS (28.9 mg, 50.0 µmol) and magnetic stir bar under Ar, toluene (2.0 mL) was added via syringe. The autoclave was pressurized with 0.8 MPa of propene and desired pressure of $H_2$/CO, and stirred at 160 ºC, at 800 rpm, for 24 hours. Then the autoclave was cooled with water/ice bath for 30 minutes, the pressure was released. Then the solution was analyzed by GC.

### Real-time IR monitoring of hydroformylation/hydrogenation of 1-eicosene by Rh(acac)(CO)$_2$/XANTPHOS/1

An autoclave (100 mL) equipped with IR probe was charged with **4** (22.5 mg, 50 μmol), XANTPHOS (57.8 mg, 100 μmol) and magnetic stir bar was flushed with Ar. It was added toluene (10.0 mL) and 1-eicosene (1.75 mL, c.a. 5.0 mmol), and heated at 160 °C. The integration of the characteristic peaks for 1-decene (912 cm$^{-1}$, terminal C=C), undecanal (1726 cm$^{-1}$, C=O), and undecanol (1058 cm$^{-1}$, C-O) were monitored during the reaction time. After appropriate reaction time, the autoclave was cooled with water/ice bath for 30 minutes and the pressure was released. 1,3,5-Trimethoxybenzene 100.0 mg, 0.595 mmol) was added to the crude solution. Then the solution was analyzed by $^1$H NMR with longer relaxation delay (15 s).

The actual amount of substrate injected into the autoclave was estimated as sum of the observed product with GC analysis. The actual liquid volume was estimated with the following equation

Data treatment of IR was as follows. Background was measured before experiment under air. During the reaction, the peak area for 1-decene (912 cm$^{-1}$, terminal C=C) and alcohols (1058 cm$^{-1}$, C-O) were plotted versus time (*t*) in every 5 minutes (256 scans were integrated). Aldehydes (1726 cm$^{-1}$, C=O) were not observed.

Catalytic species could not be characterized by in-situ infrared spectroscopy because of low intensity of those signals.


**Preparation of tricarbonyl(2,5-bis(ethoxycarbonyl)3,4-diphenylcycopentadienone)ruthenium (3)**

To a 50 mL double necked round-bottomed flask containing Ru$_3$(CO)$_{12}$ (507 mg, 2.38 mmol(mol Ru)) and 2,5-bis(methoxycarbonyl)-3,4-diphenylcyclopentadienone (879 mg, 2.34 mmol), Toluene (17 mL) was added and refluxed until starting materials were consumed as

confirmed by TLC. After cooled the reaction mixture to room temperature, solvent was evaporated. Recrystallization from CHCl$_3$/hexane gave the title compound as yellow crystals (766 mg, yield 58.5%). $^1$H NMR (CD$_2$Cl$_2$, 500 MHz) δ 0.97 (t, *J* = 7 Hz, 6H) 4.03 (dq, *J* = 16, 7 Hz, 2H), 4.05 (dq, *J* = 16, 7 Hz, 2H), 7.21-7.33 (m, 10H); $^{13}$C NMR (CDCl$_3$, 101 MHz) δ 13.4 (CH$_3$), 61.3 (CH$_2$), 70.8 (4°), 109.5 (4°), 128.0 (CH), 129.1 (CH), 131.1 (CH), 164.7 (4°), 170.8 (4°), 192.1 (4°); mp 165-169 °C (decomp.); IR (KBr, cm$^{-1}$):1653 (s), 1709 (s), 1722 (s), 2002 (s), 2029 (s), 2100 (s); Anal. Calced for C$_{26}$H$_{20}$O$_8$Ru: C, 55.61; H, 3.59. Found: C, 55.38; H, 3.61.

**Preparation of tricarbonyl(2,4-bis(trimethylsilyl)bicycle[3,3,0]octa-1,4-dien-3-one)ruthenium (4)**

To a 50 mL stainless autoclave, 1,7-bis(trimethylsilyl)-hepta-1,6-diyne (970 μL, 3.3 mmol) and triruthenium dodecacarbonyl (700 mg, 1.10 mmol) were charged with acetonitrile (50 mL). Then the autoclave was pressurized with CO 0.5 MPa and the resulting mixture was stirred at 120 °C for 12 h. After evaporation of the solvent, the residue was dissolved in CH$_2$Cl$_2$, and passed through short silica-gel column. The volatiles of the filtrate was evaporated and then the residue was recrystallized from toluene at −35 °C (to afford **4** as 1.011 g, yield 68.0%). $^1$H NMR (CDCl$_3$, 500 MHz) δ 0.26 (s, 18H) 1.75-1.89 (m, 1H), 2.33 (m, 1H), 2.50-2.67 (m, 4H); $^{13}$C NMR (CDCl$_3$, 101 MHz) δ 0.07 (CH$_3$), 25.8 (CH$_2$), 27.8 (CH$_2$), 67.6 (4°), 118.8 (4°), 186.9 (4°), 195.0 (4°); mp;146-147 °C (decomp.), IR (KBr, cm$^{-1}$):1609, 2006, 2070; Anal. Calced for C$_{17}$H$_{24}$O$_4$RuSi$_2$: C, 45.41; H, 5.38. Found: C, 45.25; H, 5.34.

**Details for X-ray crystallography for complexes 3 and 4**

Details of the crystal graphical data, and a summary of the intensity data collection parameters for **3** and **4** are listed in Table 3-4. In each case a suitable crystal was mounted with a mineral oil to glass fiber and transferred to the goniometer of a Rigaku Mercury CCD diffractometer with graphite-monochromated Mo Kα radiation (λ = 0.71070 Å) or . The structures were solved by direct methods with (SIR-97)[10] and refined by full-matrix least-squares techniques against $F^2$ (SHELEXL-97).[11,12] The intensities were corrected for Lorentz and polarization effects or NUMABS program (Rigaku 2005). The non-hydrogen atoms were refined anisotropically. Hydrogen atoms were placed using AFIX instructions. ORTEP drawings of **3** and **4** are shown in Figure 3-5 (thermal ellipsoids set at 50% probability; hydrogen atoms except bonded to Ru are omitted for clarity.).

**Table 3-4.** Crystallographic data and structure refinement details for **3** and **4**

|  | **3** | **4** |
|---|---|---|
| formula | $C_{26}H_{20}O_8Ru$ | $C_{17}H_{24}O_4RuSi_2$ |
| fw | 561.49 | 449.61 |
| $T$ (K) | 103(2) | 103(2) |
| $\lambda$ (Å) | 0.71070 | 0.71070 |
| cryst syst | monoclinic | orthorhombic |
| space group | $P2_1$ | $P2_12_12_1$ |
| $a$, (Å) | 9.810 (4) | 7.705(3) |
| $b$, (Å) | 10.483(3) | 13.954(5) |
| $c$, (Å) | 11.670(5) | 19.299(7) |
| $\alpha$, (°) | 90 | 90 |
| $\beta$, (°) | 102.2858(16) | 90 |
| $\gamma$, (°) | 90 | 90 |
| $V$, (Å$^3$) | 1172.7(7) | 2075.1(13) |
| $Z$ | 2 | 4 |
| $D_{calc}$, (g / cm$^3$) | 1.590 | 1.439 |
| $\mu$ (mm$^{-1}$) | 0.718 | 0.887 |
| F(000) | 568 | 920 |
| cryst size (mm) | $0.70 \times 0.70 \times 0.10$ | $0.25 \times 0.20 \times 0.10$ |
| $2\theta$ range, (deg) | 3.05-25.00 | 3.02-25.00 |
| reflns collected | 7590 | 13582 |
| indep reflns/$R_{int}$ | 3931/0.0192 | 3652/0.0406 |
| params | 345 | 223 |
| GOF on $F^2$ | 1.162 | 1.092 |
| $R_1$, w$R_2$ [I>2$\sigma$(I)] | 0.0257, 0.0585 | 0.0370, 0.0804 |
| $R_1$, w$R_2$ (all data) | 0.0275, 0.0610 | 0.0409, 0.0840 |
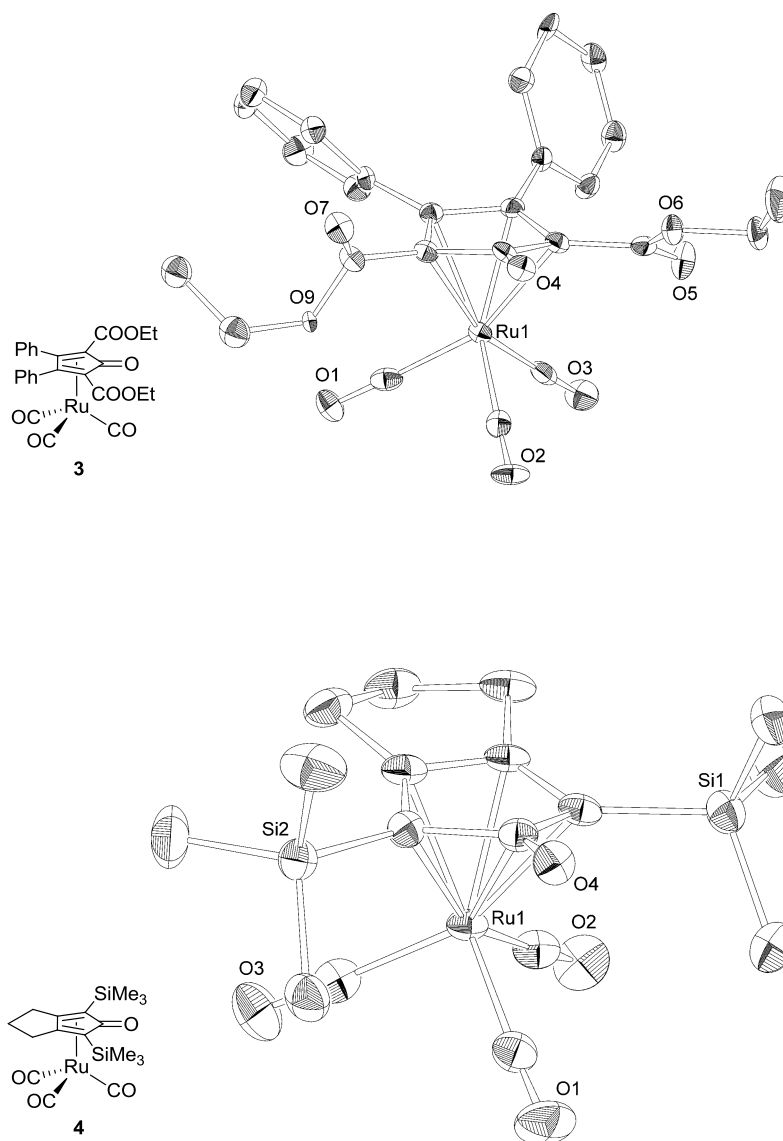
**Figure 3-5.** Ortep drawing of **3** and **4** (50% thermal ellipsoid, hydrogen atoms were omitted for clarity).

## References

1)

2) Knifton, J. F. *J. Mol. Cat.* **1988**, 47, 99.

3) Oresmaa, L.; Moreno, M. A.; Jakonen, M.; Suvanto, S.; Haukka, M. **2009**, *353*, 113-116.

4) (a) Fleischer, I.; Dyballa, K. M.; Jennerjahn, R.; Jackstell, R.; Franke, R.; Spannenberg, A.; Beller, M. *Angew. Chem. Int. Ed.* **2012**,*52*, 2949. (b) Wu, L.; Fleischer, I.; Jackstell, R.; Profir, I.; Franke, R.; Beller, M. *J. Am. Chem. Soc.* **2013**, *135*, 14306.

5) (a) Blum, Y.; Shvo, Y. *Inorg. Chim. Acta* **1985**, *97*, L25. (b) Shvo, Y.; Czarkie, D. *J. Organomet. Chem.* **1986**, *315*, C25. (c) Shvo, Y.; Czarkie, D.; Rahamim, Y.; Chodosh, D. F. *J. Am. Chem. Soc.* **1986**, *108*, 7400. (d) Aleix, C. V.; Gregori, U.; Agusti, L. *Organometallics* **2008**, *27*, 4854.

6) Kranenburg, M.; van der Burgt, Y. E. M.; Kamer, P. C. J.; van Leeuwen, P. W. N. M.; Goubitz, K.; Fraanje, J. *Organometallics* **1995,** *14*, 3081.

7) (a) Devon, T. J. P., G. W.; Puckette, T. A.; Stavinoha, J. L.; Vanderbilt, J. J. US4694109, 1987. (b) Casey, C. P.; Petrovich, L. M. *J. Am. Chem. Soc.* **1995**, *117,* 6007.

8) Omatsu, T.; Tokihiko, Y.; Yoshimura, N. EP0303060, 1989.

9) Comas-Vives, A.; Ujaque, G.; Lledós, A. *Organometallics* **2008**, *27*, 4854.

10) Altomare, A.; Burla, M. C.; Camalli, M.; Cascarano, G. L.; Giacovazzo, C.; Guagliardi, A.; Moliterni, A. G. G.; Polidori, G.; Spagna, R. *J. Appl. Crystallogr.* **1999**, *32*, 115.

11) Sheldrick, G. M. SHELXL-97, Program for the Refinement of Crystal Structures, University of Göttingen: Göttingen, Germany, 1997.

12) Sheldrick, G. M.; Schneider, T. R., SHELXL: High-resolution refinement. In *Macromolecular Crystallography, Pt B*, Academic Press Inc: San Diego, 1997; Vol. 277, pp 319.

# Chapter 4

# Tandem Hydroformylation/Hydrogenation of

# Terminal Alkenes to *Normal*-Alcohols Using a

# Rh/Ru Dual Catalyst System

## 4 Tandem Hydroformylation/Hydrogenation of Terminal Alkenes to *Normal-Alcohols Using a Rh/Ru Dual Catalyst System*

### 4-1 Background

As mentioned in the chapter 1, one-pot conversion of an alkene to a *nomal*-alcohol (tandem *normal*-selective hydroformylation/hydrogenation) would be an advantageous process by reducing the numbers of reactors and distillation steps for hydrogenation and the separation of dihydrogen from synthesis gas. Although this process was already commercialized with cobalt system, it is suffering from required harsh conditions (150−200 °C, >10 MPa of $H_2$/CO) and low selectivity of desired *normal*-alcohol (~70%). Therefore, the tandem reaction is still being well investigated. Representative examples are summarized in the Table 4-1. Most of the early examples are alkylphosphine modified systems. For example, Co-monodentate trialkylphosphine system was first patented in 1960's (*n/i* ratio up to 5). Shell modified this system further to find bulky bidentate trialkylphosphine ligand is more efficient.[1] With this modification, *normal*-selectivity was improved (*n*-alcohol yield 77%, *n/i* = 8.1). For the modification of cobalt by trialkylphosphine, there are several advantages and disadvantages. One of the advantages is that trialkylphosphines enhance activity for hydrogenation probably by increasing nucleophilicity of cobalt hydride. Also, steric bulk of trialkylphosphine suppresses the deactivation of cobalt species by dimerization to inactive species. As a result, reaction could be performed under relatively lower CO pressure compared to unmodified systems. Third advantage is that the *n/i* ratio is improved compared to the unmodified system due to the steric bulk of trialkylphosphine. On the other hand, one of the disadvantages is that the rate is decreased by the stronger coordination of carbon monoxide due to enhanced electron density of the cobalt center. Another
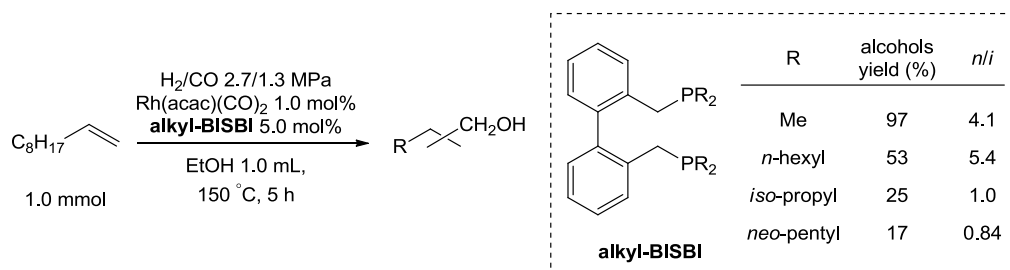
drawback is that trialkylphosphines are pyrophoric. As for catalytic activity and selectivity, similar tendencies to cobalt system were known for other metal based systems. For example, Cole-Hamilton *et al.* reported tris(triethylphosphine)hydridorhodium (RhH(PEt$_3$)$_3$) gives alcohols selectively in EtOH. Yield of alcohols was excellent, but low *n/i* ratio remained as problem (93% alcohols yield, *n/i* = 4.3).[2] They examined the reaction mechanism and proposed that the reaction was proceeded not via aldehyde as an intermediate. When the hydroformylation/hydrogenation of 1-hexene was performed by employing D$_2$/CO in EtOH, deuterium distribution of the obtained heptanol was C$_4$H$_9$<u>CHD</u>CH$_2$<u>CD$_2$</u>OH. On the other hand, hydrogenation of heptanal using the same catalyst under D$_2$/CO afforded heptanol with deuterium content of C$_4$H$_9$<u>CH$_2$</u>CH$_2$<u>CHX</u>OH [X = H (60%), D (40%)]. These results mean in the hydrogenation/hydroformylation of 1-heptene, deuterium appears on the C1 of the resulting heptanol, while in the hydrogenation of heptanal, both hydrogen and deuterium was found on C1 (one of the hydrogens was derived from formyl proton of heptanal). Therefore, they concluded that heptanal was not released as an intermediate in the tandem reaction. The proposed mechanism to explain such results is described in Figure 4-1. The key is the formation of a carbene complex from an acylrhodium species assisted by the protonation by methanol, and the sequential oxidative addition of D$_2$ and the migration of one of the deuterium followed by reductive elimination affords alcohol.

**Scheme 4-1.** Proposed mechanism of one-pot conversion of alkene to alcohol catalyzed by RhH(PEt₃)₃
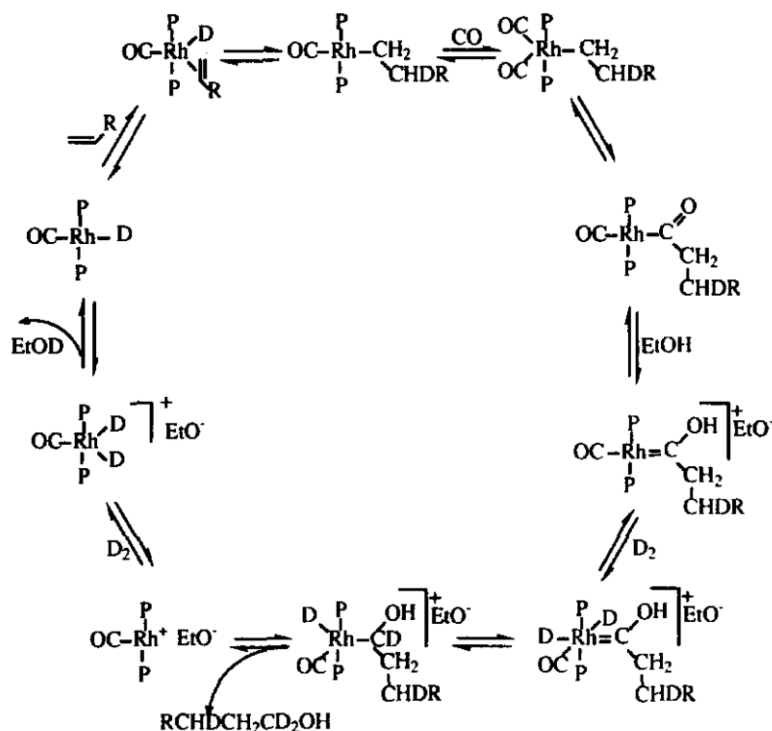


Nozaki *et al.* synthesized BISBI-type ligand possessing alkyl substituent on the phosphorus atoms (Scheme 4-2). As alkyl substituents, methyl, *n*-hexyl, *i*-propyl, and *neo*-pentyl were investigated. The observed *n/i* ratios were 4.1, 5.4, 1.0 and 0.84 respectively.[3] One interpretation of such results is that the coordination abilities of phosphorus atoms is weaker in the presence of bulkier substituents on them, and that resulted in smaller effect on the *n/i* selectivity. However, analysis of the catalyst solution by ^{31}P NMR spectroscopy did not give clear evidence of coordination of Me-BISBI whereas coordination of [i]Pr-BISBI was evident.

**Scheme 4-2.** Tandem hydroformylation/hydrogenation catalyzed by bisdialkylphosphinomethylbiphenyl



| R | alcohols yield (%) | *n/i* |
|---|---|---|
| Me | 97 | 4.1 |
| *n*-hexyl | 53 | 5.4 |
| *iso*-propyl | 25 | 1.0 |
| *neo*-pentyl | 17 | 0.84 |

As other trialkylphosphine modified systems, ruthenium[4] and palladium[5] based systems were also developed. Palladium based system reported by Drent *et al*. can afford *normal*-alcohol not only from terminal alkenes but also internal alkenes via isomerization to terminal alkene, *normal*-selective hydroformylation, and hydrogenation due to the relatively high activity of the palladium based system for isomerization of alkenes. The important aspect of the system is that the reaction rate and the *n/i* selectivity are improved in the presence of catalytic amount of halide. In the comparative experiment, the order of the extent of acceleration was Cl (7 times) ≳ Br (7 times) > I (4 times), and that of enhancement of *n/i* was Cl (2.6) < Br (3.5) < I (4.6) compared to 1.9 in the absence of halide. However, the mechanisms of such effects were not well understood. The best result using **L1** is described in Scheme 4-3.

**Scheme 4-3.** Isomerization/hydroformylation/hydrogenation of a mixture of internal alkenes by a palladium alkylphosphine catalyst
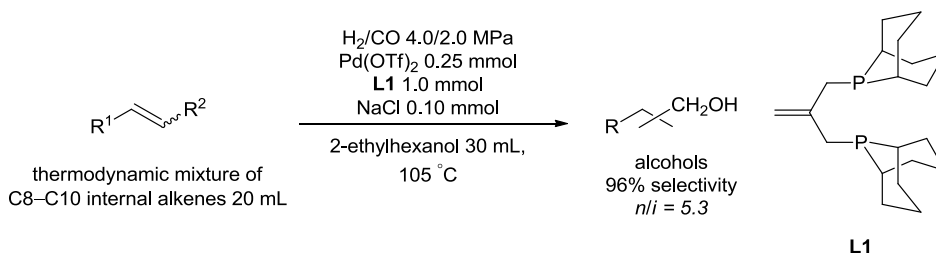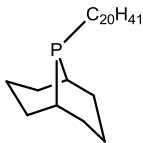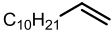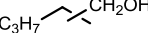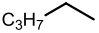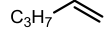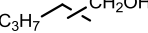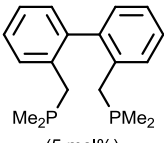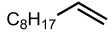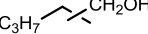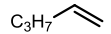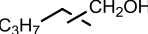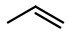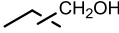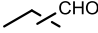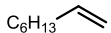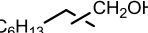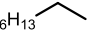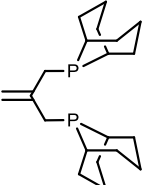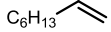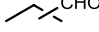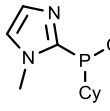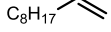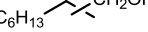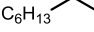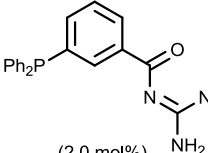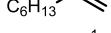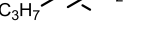


As explained, previous examples of alkylphosphine modified systems exhibit only low *n/i* ratios. Of course, there have been numerous examples of alkylphosphine ligands however none of them has ever reported to exhibit high *n/i* selectivity. This is probably due to flexibility of alkylphosphine ligands. Most of the examples of highly *normal*-selective hydroformylation catalysts are employing bisphosphorus ligands having rigid back bone and wide bite angle. From this fact, these properties are considered to be the requirement for high *n/i* ratio and are difficult to achieve by alkyl group, which is more flexible compared to aryl group in general. One intriguing example, which does not contain electron donating ligand is reported by Breit *et al*.[6] They developed guinidine tethered phosphine ligands, which interact with carbonyl of aldehyde with hydrogen bonding (Scheme 4-4). With this interaction, hydrogenation of aldehyde was accelerated while hydroformylation proceeded with relatively high *n/i* ratio probably due to its steric bulkiness of the ligand.
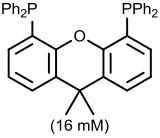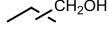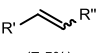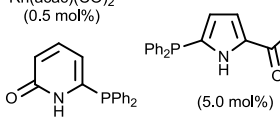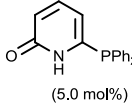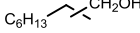
**Scheme 4-4.** Proposed mechanism of hydrogenation of aldehyde by guanidine tethered phosphine ligand
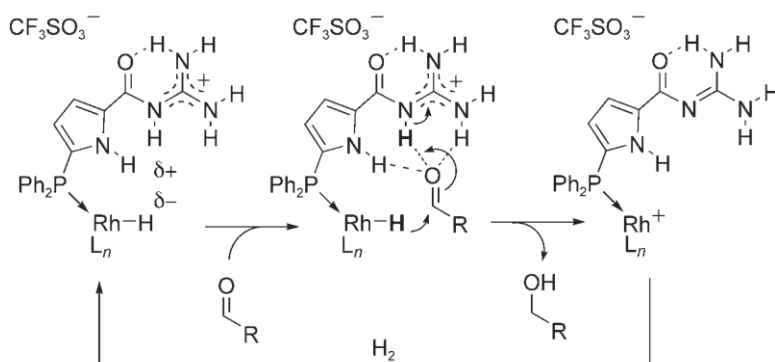


Another idea to achieve highly *normal*-selective hydroformylation/hydrogenation is utilizing single metal/dual ligand systems. This type of system consists of a mixture of rhodium source and two phosphorus ligands, one mediates *normal*-selective hydroformylation, and the other is for hydrogenation under $H_2/CO$ is employed. Rhodium species coordinated by these two ligands are in equilibrium in the reaction mixture and they play respective role in the tandem reaction. For example, in Cole-Hamilton's report,[7] XANTPHOS was used with $RhH(PEt_3)_3$ (by only $RhH(PEt_3)_3$, $n/i = 4.3$) as catalyst precursors, to give alcohols with $n/i$ ratio up to 32 (Table 4-1). In this system, rhodium complexes coordinated by XANTPHOS or triethylphosphine are in equilibrium. The former species catalyzes *normal*-selective hydroformylation, and the latter catalyzes hydrogenation of resulting aldehyde. Similarly, Breit used a pyridone-tethered phosphine ligand for *n*-selective hydroformylation and a guanidine-tethered phosphine ligand for hydrogenation in one-pot (Table 4-1).[8] Observed $n/i$ ratio was as high as 32 with 95% yield of alcohols. So far, this is the highest yield of *normal*-alcohol ever reported for tandem hydroformylation/hydrogenation.

**Table 4-1.** Representative examples of tandem hydroformylation/hydrogenation

| metal precursor | complex additive | condition | substrate (mmol) | alcohols (yield, $n/i$) | byproduct (yield) | ref |
|---|---|---|---|---|---|---|
| $Co_2(CO)_8$ 0.2 wt% |  2 equiv. to Co | $H_2/CO$ 4.7/2.2 MPa, 180 °C | $C_{10}H_{21}$ | $C_3H_7$—CH$_2$OH (86.7%, 8.1) | $C_3H_7$ 11.8% | 1 |
| $RhH(PEt_3)_3$ (8 mM) | | $H_2/CO$ 2/2 MPa, EtOH 4 mL, 125 °C | $C_3H_7$ (1 mL) | $C_3H_7$—CH$_2$OH (93.0%, 4.3) | | 2 |
| $Rh(acac)(CO)_2$ (1 mol%) |  (5 mol%) | $H_2/CO$ 2.7/1.3 MPa, EtOH 1 mL, 170 °C, 5 h | $C_8H_{17}$ (1.0 mmol) | $C_3H_7$—CH$_2$OH (97%, 4.1) | | 3 |
| $RuCl_3/^nBu_3P/NaOAc$[1b)] (0.07 M, 0.14 M, 0.35 M) | | $H_2/CO$ 2/1 MPa, octane, 195 °C | $C_3H_7$ (2.3 M) Conv. 93.6% | $C_3H_7$—CH$_2$OH $n/i$ = 2 | | 4a |
| $Ru_3(CO)_{12}$ (6.0 mmol)[1h)] 2,2'-bipyridyl (6.0 mmol) $Bu_4PBr$ (29 mmol) | | $H_2/CO$ 5.6/2.8 MPa, neat, 160 °C, 4 h | (0.4 mol) | —CH$_2$OH (89.5% of liquid, >99) | —CHO (6.4%) | 4b |
| $Ru_3(CO)_{12}$ (6.0 mmol)[1h)] 2,2'-bipyridyl (6.0 mmol) $Bu_4PBr$ (29 mmol) | | $H_2/CO$ 5.6/2.8 MPa, neat, 180 °C, 4 h | $C_6H_{13}$ (0.2 mol) | $C_6H_{13}$—CH$_2$OH (79.6%, 6.1) | R—R' (9.0%); $C_6H_{13}$ (9.0%) | 4b |
| $Pd(OAc)_2$ (0.25 mmol) TfOH (0.50 mmol) NaCl (0.10 mmol) |  (0.35 mmol) | $H_2/CO$ 2/1 MPa, 2-ethylhexanol 20 mL, 105 °C | $C_6H_{13}$ 20 mL | —CHO (96%, 5.3) | | 5 |
| $Ru_3(CO)_{12}$ (0.2 mol%) LiCl (25 mol%) $H_2O$ (280 mol%) |  0.66 mol% | $H_2/CO$ 3.0/3.0 MPa, NMP 3 mL, 130 °C, 20 h | $C_8H_{17}$ (20 mol) | $C_6H_{13}$—CH$_2$OH (90%, 7.3) | $C_6H_{13}$ (3.0%) | 4c |
| $Rh(acac)(CO)_2$ (0.2 mol%) |  (2.0 mol%) | $H_2/CO$ 2.0/2.0 MPa, $CH_2Cl_2$ 6 mL, 40 °C, 24 h | $C_6H_{13}$ (0.2 molL$^{-1}$) | $C_3H_7$—CH$_2$OH (87%, 11.5) | | 6 |

102

| metal precursor | complex additive | condition | substrate (mmol) | alcohols (yield, *n/i*) | byproduct (yield) | ref |
|---|---|---|---|---|---|---|
| RhH(PEt$_3$)$_3$ (8 mM) | Ph$_2$P / PPh$_2$ xanthene (16 mM); PEt$_3$ (4 mM) | H$_2$/CO 2.0/2.0 MPa, EtOH 4 mL, 120 °C, 2 h | C$_8$H$_{17}$ (11.8 mmol) | CH$_2$OH (89.0%, 31.8) | R' R" (7.5%) | 7 |
| Rh(acac)(CO)$_2$ (0.5 mol%); (5.0 mol%) | Ph$_2$P pyrrole guanidine (5.0 mol%) | H$_2$/CO 1.0/1.0 MPa, toluene 80 °C, 24 h | C$_6$H$_{13}$ (1 molL$^{-1}$) | C$_6$H$_{13}$ CH$_2$OH (95%, 32) | | 8 |

In summary, tandem hydroformylation/hydrogenation reaction has been well investigated but still attracting attention. Selectivity to *normal*-alcohol has been improved by the intensive studies, but they are not sufficiently effective for industrial application probably due to the low activities or the costs of the catalyst preparations.

## 4-2 Design of the dual catalyst system of this work

In this work, a dual catalyst system for one-pot *n*-selective hydroformylation/hydrogenation was developed by employing rhodium-based hydroformylation catalyst and ruthenium-based hydrogenation catalyst (Scheme 4-2). In this system, rhodium-based *normal*-selective hydroformylation catalyst is expected to convert an alkene to *normal*-aldehyde and subsequent hydrogenation of the aldehyde by ruthenium-based hydrogenation catalyst gives *normal*-alcohol. For that purpose, acetylacetonatodicarbonylrhodium (Rh(acac)(CO)$_2$) and XANTPHOS[9] (See Chapter 1) was employed as *normal*-selective hydroformylation catalyst because of its high *normal*-selectivity and robustness against alcohol. On the other hand, selective hydrogenation of aldehyde over alkenes is required for ruthenium-based hydrogenation catalyst. Metal–ligand bifunctional hydrogenation catalyst is suitable for the requirement (Figure 4-1).[10] This type of

103

hydrogenation catalyst hydrogenates unsaturated double bond via concerted transfer of hydridic hydrogen on the metal center and protic hydrogen on the ligand. The barrier of the transfer of hydrogen atoms is lower with polar double bond such as C=O than C=C.[11] Therefore, this type of catalyst preferably hydrogenates aldehyde and is relatively inert to alkenes. Although cyclopentadienyl ruthenium complex has activity in hydroformylation as investigated in the previous chapters, it is negligibly slow compared to Rh/XANTPHOS system.

**Scheme 4-2.** Rh/Ru dual catalyst system for the one-pot conversion of alkenes to *normal*-alcohol
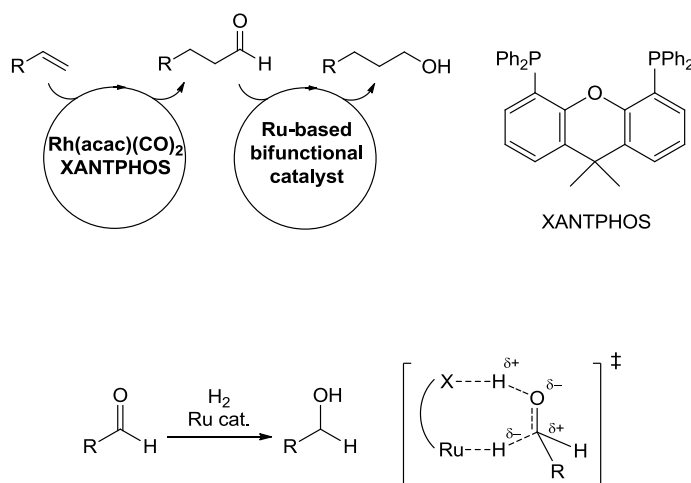


**Figure 4-1.** Ru-based metal–ligand bifunctional hydrogenation catalyst

## 4-3 Screening of hydrogenation catalysts

Based on the speculation, literature reported ruthenium-based metal–ligand bifunctional hydrogenation catalysts were screened. Screened catalyst systems **1-6**[12-16] and their proposed transition state in hydrogen transfer step are described in Figure 4-2. As a proton source on ligand, active species produced from complex **1**[12] reacts with substrates O-H group on the ligand and **2**,[13] **3/4**,[14] **5**,[15] or **6**[16] react with substrates with the N-H group on the ligand. For **2-6**, one

equivalent of $^t$BuOK to ruthenium catalyst was used to generate hydridoruthenium under $H_2$ by losing potassium chloride. Under 2.0 MPa of $H_2$/CO (1:1), 1-decene was treated with a catalytic amount of Rh(acac)(CO)$_2$, XANTPHOS, and hydrogenation catalyst at 160 °C for 1 hour. Results are summarized in Table 4-2. Among the catalysts, **1** gave the highest selectivity to *n*-undecanol. When **2-6** were used as the catalyst, low rate of hydrogenation was problematic. Formations of high boiling products such as acetals or aldol products were also problematic for **2-6**. Relatively slow rate of hydrogenation by **2-6** resulted in higher concentration of aldehyde during the reaction, which supposed to facilitate those side reactions.



**Figure 4-2.** Screened hydrogenation catalyst and their proposed transition state in hydrogenation.

**Table 4-2.** Tandem hydroformylation/hydrogenation by Rh/XANTPHOS and various Ru-based bifunctional catalyst$^a$



105

| run | Cat. | alcohols | | n/i | aldehyde | | n/i | alkane (%) | others (%) |
|---|---|---|---|---|---|---|---|---|---|
| | | n(%) | i(%)[b] | | n(%) | i(%)[b] | | | |
| 1 | **1** | 85 | 5.0 | 17 | 0.9 | 0.5 | 2 | 1.3 | internal alkenes $(1.7)^c$ formate (1.2) |
| 2 | **2**+$^t$BuOK | 64 | 2.8 | 23 | 14 | 1.6 | 9 | 2.7 | internal alkenes $(2.5)^c$ formate (3.3) |
| 3 | **3**+**4**+$^t$BuOK | 37 | 1.9 | 19 | 41 | 4.1 | 10 | 2.2 | internal alkenes $(2.7)^c$ formate (2.0) high boiling products $(4.3)^d$ |
| 4 | **5**+$^t$BuOK | 5.4 | trace | >100 | 64 | 4.9 | 13 | 2.0 | internal alkenes $(26)^c$ high boiling products $(2.4)^d$ |
| 5 | **6**+$^t$BuOK | 59 | 1.6 | 37 | 7.2 | 0.6 | 12 | 2.4 | internal alkenes $(11)^c$ high boiling products $(3.9)^d$ |

[a]Yields were determined by gas chromatography by using dodecane as internal standard otherwise mentioned. [b]Yields were estimated by using calibration curve for *normal*-isomer. [c]Yields were estimated by using calibration curve for 1-decene. [d]Yields were estimated by using calibration curve for *normal*-aldehyde.

## 4-4 Optimization of reaction conditions

Reaction conditions were optimized employing **1** as hydrogenation catalyst. Results are summarized in Table 4-3.

**Table 4-3.** Optimization of reaction condition$^a$
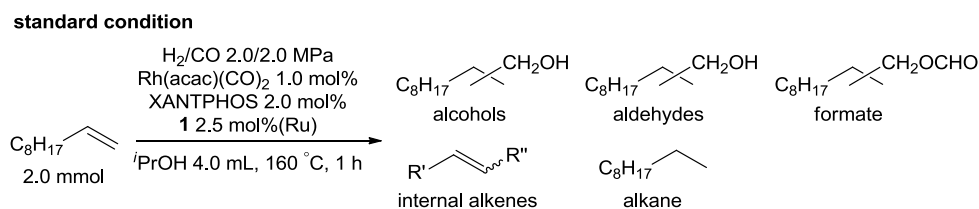
| run | deviation from standard condition | alcohols | | n/i | aldehyde | | n/i | alkane (%) | internal alkenes (%)[c] | formate (%) |
|---|---|---|---|---|---|---|---|---|---|---|
| | | n(%) | i(%)[b] | | n(%) | i(%)[b] | | | | |
| 1 | - | 85 | 5.0 | 17 | 0.9 | 0.5 | 2 | 1.3 | 1.6 | 1.1 |
| 2 | H$_2$ 3.0 MPa | 83 | 4.6 | 18 | 0.9 | 0.3 | 3 | 5.3 | 1.9 | 0.4 |
| 3 | CO 3.0 MPa | 88 | 4.6 | 19 | 0.4 | 0.6 | 0.7 | 1.2 | 4.4 | 1.4 |
| 4 | H$_2$ 3.0 MPa, CO 3.0 MPa | 85 | 4.3 | 20 | 0.6 | 0.5 | 1.3 | 3.3 | 3.1 | 1.2 |
| 5 | XANTPHOS 5.0 mol% | 83 | 4.9 | 17 | trace | trace | - | 2.7 | 1.1 | 2.9 |
| 6 | **1** 1.25 mol% | 81 | 4.8 | 17 | trace | trace | - | 2.7 | 1.1 | trace |
| 7 | **1** 0.63 mol% | 70 | 4.7 | 15 | 7.4 | trace | - | 2.7 | 1.1 | 5.7 |
| 8 | in toluene | 79 | 4.2 | 19 | 0.9 | 0.6 | 1.4 | 2.7 | 2.8 | 8.6 |
| 9 | in THF | 61 | 5.0 | 14 | 4.2 | 0.6 | 7.0 | 3.8 | 8.6 | 15 |
| 10 | in DMF | 83 | 3.3 | 21 | 0.6 | 0.4 | 1.5 | 2.5 | 4.8 | 4.5 |
| 11 | in DMA | 87 | 3.9 | 22 | 1.0 | 0.4 | 2.7 | 2.4 | 4.9 | 1.4 |
| 12 | in DMA, 120 °C, 12.5 h | 90 | 4.2 | 22 | 1.0 | 0.9 | 1.1 | 1.3 | 2.0 | 1.7 |

[a]Yields were determined by gas chromatography by using dodecane as internal standard otherwise mentioned. [b]Yields were estimated by using calibration curve for *normal*-isomer. [c]Yields were estimated by using calibration curve for 1-decene.

Deviation of pressures of H$_2$ and/or CO (runs 2-4) or increase of the amount of XANTPHOS (run 5), or decrease of **1** (run 6, 7) resulted in little change or decrease of the yield of *n*-alcohol. These effects of pressures of H$_2$ and CO, and concentrations of ruthenium and XANTPHOS on the rate of hydrogenation will be discussed later. Solvent effect was also examined (runs 8-11). DMA gave the best yield. In relatively less polar solvent such as toluene or THF, formation of undecyl formate via carbonylation of undecanol was significant. Finally, the yield was enhanced up to 90% at 120 °C with elongated reaction time.

## 4-5 Substrate scope and limitation

Substrate scope and limitation are summarized in Table 4-4. Allyl alcohol is important target of this reaction because of the significance of corresponding homologated *n*-alcohol, 1,4-butandiol (produced more than 1 million t/year mainly by hydrogenation of maleic anhydride). However, the yield was as low as 35%, because of the formation of propanol and γ-butyrolactone (run 2). Reaction mechanisms giving them are proposed in Scheme 4-3. Complex **1** catalyzes the isomerization of allyl alcohol to propanal,[17] which is susceptible to hydrogenation by **1**. Also, corresponding homologated *n*-aldehyde produced from allyl alcohol rapidly forms cyclic acetal, which is dehydrogenated to give γ-butyrolactone.

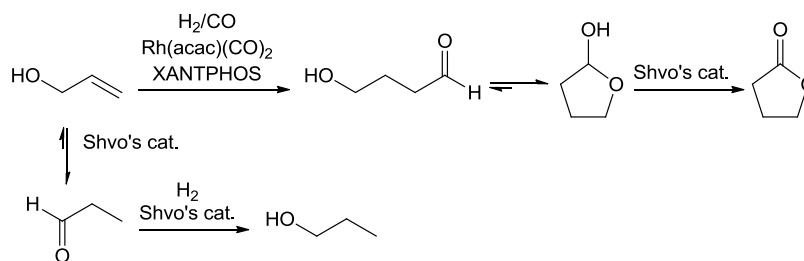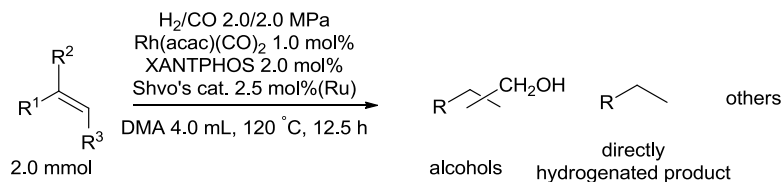**Scheme 4-3.** Pathway to form propanol and γ-butyrolactone



**Table 4-4.** Substrate scope and limitation[a]

| run | $R^1, R^2, R^3$ | alcohols | | $n/i$ | direct hydrogenation (%) | others[c] (%) |
|---|---|---|---|---|---|---|
| | | $n(\%)$ | $i(\%)^b$ | | | |
| 1 | $C_8H_{17}$, H, H | 90 | 4.1 | 22 | 1.4 | internal alkenes (1.9) |
| 2 | $HOCH_2$, H, H | 31 | 3.5 | 8.9 | $20^d$ | $\gamma$-butyrolactone $(10)^d$ high boiling products $(4)^{d,e}$ |
| 3 | $AcOCH_2$, H, H | 78 | trace | >100 | 1.9 | butanol (9) isobutanol $(10)^b$ |
| 4 | $HO(CH_2)_2$, H, H | 75 | 2.4 | 32 | 4.5 | cyclic acetals $(3)^f$ $\delta$-valerolactone $(11)^f$ |
| 5 | $AcO(CH_2)_2$, H, H | 87 | 5.6 | 16 | 4.5 | nd |
| 6 | $HO(CH_2)_3$, H, H | 95 | 2.9 | 33 | 4.0 | none |
| 7 | $THPO(CH_2)_4{}^g$, H, H | $80^f$ | $5.0^f$ | 16 | nd | $n$-aldehyde $(4)^f$ internal alkenes $(2)^f$ |
| 8 | $PhCH_2O(CH_2)_4$, H, H | $81^f$ | $4.1^d$ | 20 | nd | internal alkenes (2) formates $(6)^f$ |
| 9 | $TBSO(CH_2)_4{}^h$, H, H | $80^f$ | $3.7^f$ | 22 | nd | formate $(4)^f$ |
| 10 | $(1,3\text{-dioxolan-2-yl})(CH_2)_8$, H, H | $79^f$ | $4.2^f$ | 19 | nd | formate $(3)^f$ |
| 11 | $PhNHCO_2(CH_2)_4$, H, H | $75^f$ | $4.9^f$ | 15 | nd | nd |
| 12 | cyclohexyl, H, H | $87^f$ | $4.9^f$ | 18 | nd | nd |
| 13 | $C_7H_{15}$, $CH_3$, H, | 62 | trace | >50 | nd | starting material (15) internal alkenes (8) |
| 14 | $C_7H_{15}$, H, $CH_3$ | $22^i$ | 34 | 0.6 | nd | internal alkenes (34) aldehydes (4.2) |
| 15 | Ph, H, H | 60 | 39 | 1.5 | 0 | none |

[a]The yields in the table were determined by gas chromatography analysis with dodecane or tridecane as internal standard otherwise mentioned. $n/i$ = (mol of $n$-alcohol)/(mol of $i$-alcohols). The yields of aldehydes were trace otherwise mentioned. nd = not determined [b]The yields were estimated by using calibration curve for $n$-alcohol. [c]The number in the parentheses are the yield of the products. [d]The yields were estimated by using calibration curve for $n$-alcohol and corrected based on the number of carbon. [e]Probably acetals or aldol products. [f]The yield was determined by ^{1}H NMR with 1,3,5-trimethoxybenzene as internal standard. [g]THP = 2-tetrahydropyranyl. [h]TBS = $tert$-butyldimethylsilyl [i]Yield of $n$-undecanol.

On the other hand, allyl acetate was converted to the corresponding *n*-alcohol in better yield (78%, run 3). Hydrogenation of C=C was suppressed because isomerization to aldehyde did not take place. Also, cyclization was not occurred because intermolecular acetalization was suppressed. Similar to allyl alcohol and allyl acetate, homoallyl alcohol was susceptible to formation of lactone (11%) and homoallyl acetate was not (*n*-alcohol 75% and 87% in runs 4 and 5). 4-Penten-1-ol gave 1,6-hexanediol in 95% yield with no lactone as side product (run 6). As for other functional group, tetrahydropyranyloxy (80%, run 7), benzyloxy (81%, run 8), *tert*-butyldimethylsilyloxy (80%, run 9), 1,3-dioxolane-2-yl (79%, run 10), phenylcarbamate (75%, run 11), and cyclohexyl (87%, run 12) were applicable to this reaction. A trace amount of *i*-alcohol was formed from 2-methyl-1-nonene, and yield of *n*-alcohol was 62% (run 13). Volatility of substrate was problematic that the total yield of recovered product was 85%. (*Z*)-2-decene was converted to *n*-undecanol (22%, run 14) via isomerization to 1-decene and successive hydroformylation/hydrogenation. However, formation of *i*-alcohol was predominant. Styrene was quantitatively converted to alcohols but *n/i* ratio was as low as 1.5 because styrene is intrinsically *iso*-selective in hydroformylation (run 15).[9]

## 4-6 Investigation of the independency of Rh/XANTPHOS and 1

High yield of *n*-alcohol could be attributed to the independency of two catalyst systems, Rh/XANTPHOS and **1**. Control experiments were performed to prove it.

## 4-6-1 Observation of catalyst species

Catalyst solution independently prepared in NMR sample tube was analyzed by $^{31}$P NMR spectroscopy. Obtained spectrum is shown in Figure 4-3.
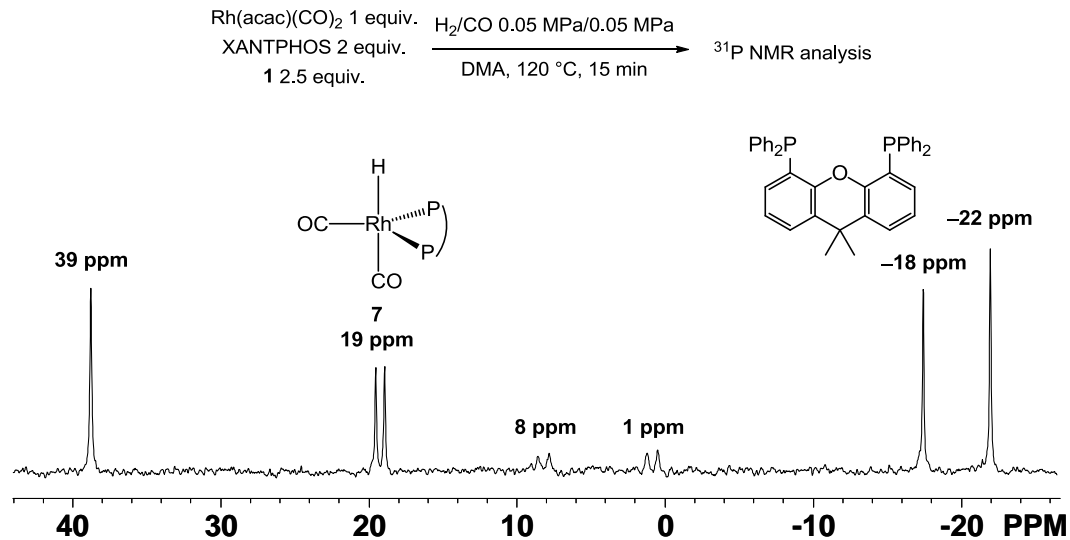
**Figure 4-3.** $^{31}$P NMR spectrum of catalyst solution for tandem reaction under 1 atm of H$_2$/CO

Doublet at 19 ppm ($J$ = 122 Hz) is assigned as dicarbonylhydrido(xantphos)rhodium (**7**),[9] which is known as an active species for *n*-selective hydroformylation. Singlet at −18 ppm is ascribed to free XANTPHOS.[9] Other signals were assigned by additional control experiments. When XANTPHOS and **1** were heated under Ar, two singlets at 39 ppm and −22 ppm appeared with 1:1 ratio (Figure 4-4). They could be assigned as (tetraphenylcyclopentadienone)($\kappa^1$-xantphos)dicarbonylruthenium (**8**). $^{31}$P NMR chemical shift of 39 ppm is similar to that of (tetraphenylcyclopentadienone)(triphenylphosphine)dicarbonylruthenium (**9**)[18] (33 ppm) and −22 ppm is similar to free XANTPHOS. Since **9** was reported to be formed by a reaction of 1 with triphenylphosphine (Scheme 4-4), **8** is supposed to be similarly formed.
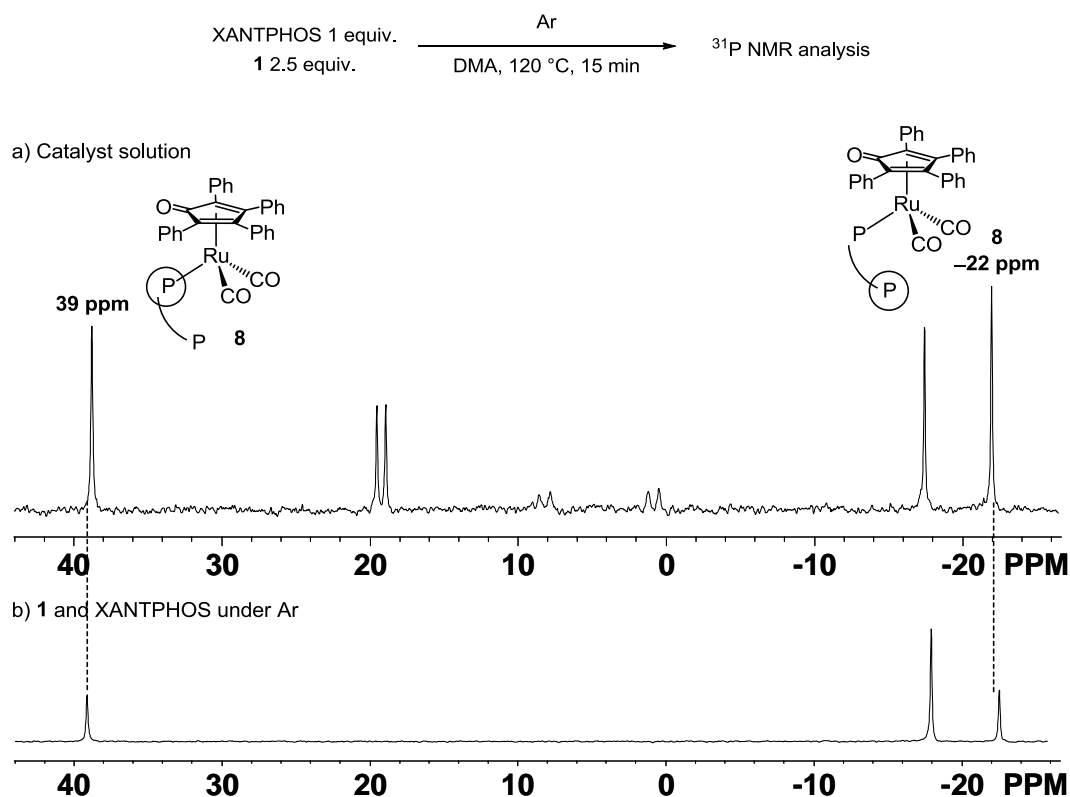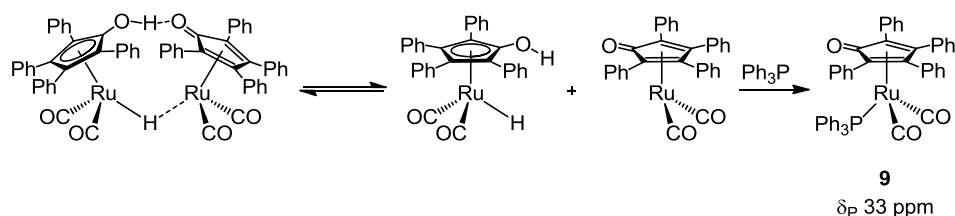
**Figure 4-4.** Comparison of $^{31}$P NMR spectrum of (a) catalyst solution for tandem reaction with (b) a solution mixture of **1** and XANTPHOS under Ar

**Scheme 4-4.** Reaction mechanism to form phosphine coordinated Ru(0) species[18]



In order to assign doublets at 8 ($J$ = 135 Hz) and 1 ppm ($J$ = 148 Hz), first, (acetylacetonato)(carbonyl)(xantphos)rhodium (Rh(acac)(CO)(xantphos), $\delta_P$ 14 ppm, $J$ = 38) was isolated (See experimental section). Only one broad signal was observed by $^{31}$P NMR spectroscopy for a DMA solution of Rh(acac)(CO)(xantphos). This is probably due to rapid

exchange of two phosphorus atoms, one is coordinated to rhodium and the other is not. When it was treated under CO, those two doublets were appeared (Figure 4-5). Since the integral of those two signals were 1:1 in all the case, they were assigned as two non-equivalent phosphorus atoms of single species. One of the possible structures, $Rh(acac)(CO)_2(xantphos)$ is described in Figure 4-5. Another possibility is carbonyl-bridged dimer. In both case, under high pressure of $H_2$ and CO, rapid hydrogenolysis of Rh(acac) to give Rh–H and acetylacetone, and/or coordination by CO is supposed to generate **7**.

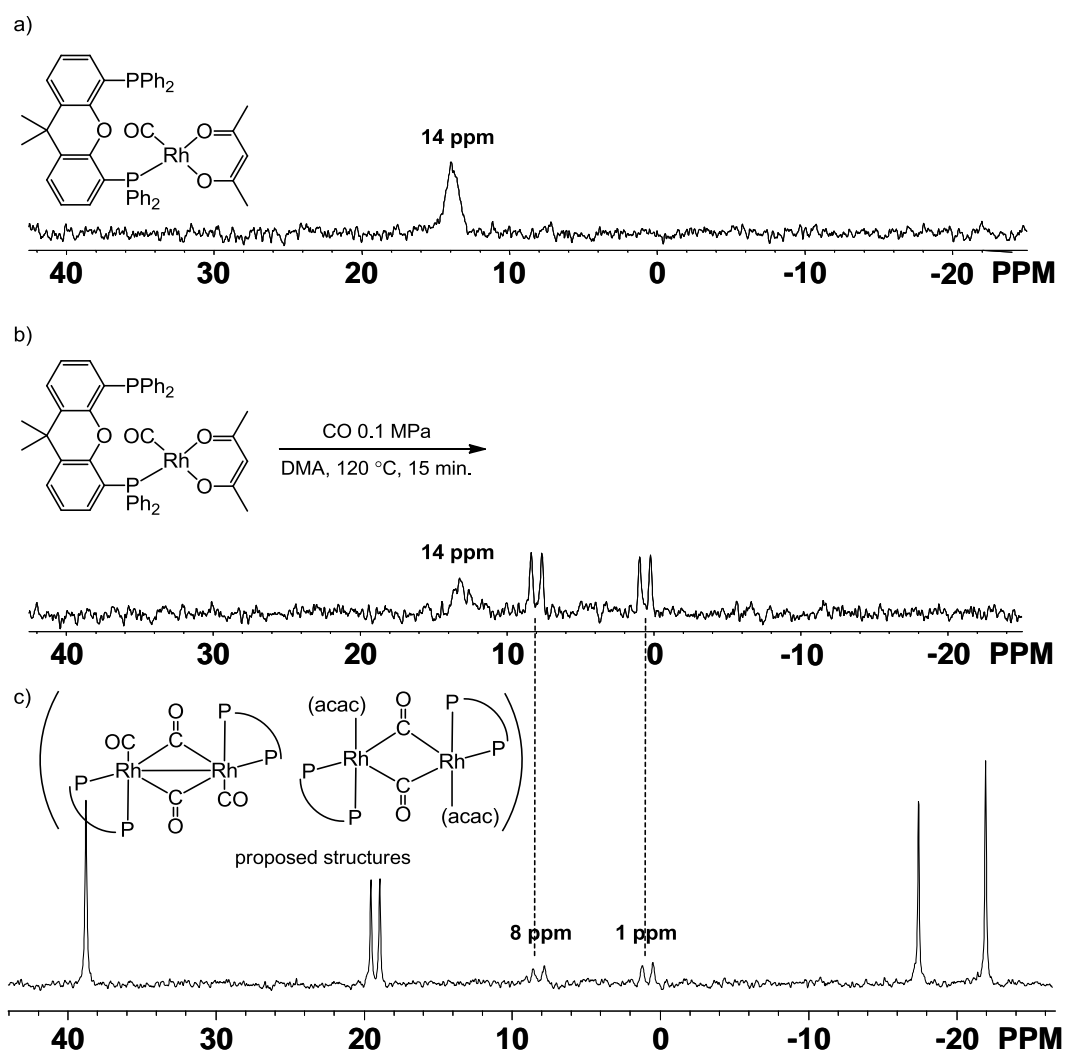**Figure 4-5.** $^{31}$P NMR spectra of control experiments to assign doublets at 8 and 1 ppm. a) Rh(acac)(CO)($\kappa^1$-xantphos) in DMA. b) DMA solution of Rh(acac)(CO)($\kappa^1$-xantphos) treated under CO. c) Catalyst solution.

Stoichiometry of the reaction estimated by $^{31}$P NMR spectrum was shown in Scheme 4-5. Although the values of the integration of the signals were not accurate because of relatively low S/N and difference of relaxation time of phosphorus nuclear with different chemical environment, not all rhodium and ruthenium were coordinated by XANTPHOS. As discussed above, all signals were assigned and there was no sign of Rh-Ru dimeric species bridged by XANTPHOS. In order to know the state of ruthenium species without phosphine ligand under H$_2$/CO pressure, **1** was treated under H$_2$/CO pressure. Evaporation of the solvent afforded carbonyl(tetraphenylcyclopentadienone)ruthenium (**10**) as a sole product in a quantitative yield (Scheme 4-6). Therefore, ruthenium species except for **9** supposed to exist as **10** under H$_2$/CO pressure.

**Scheme 4-5.** Stoichiometry of generated species in the control experiment



114
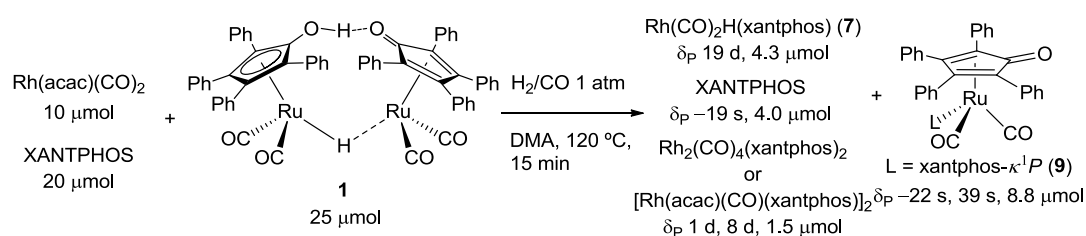
**Scheme 4-6.** Isolation of the resting species formed from **1** under H$_2$/CO in the absence of phosphorus ligand
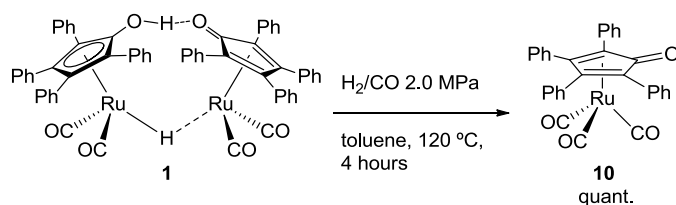


In summary, no XANTPHOS bridged Rh-Ru complex was found at least by NMR experiments. Coordination of XANTPHOS to ruthenium was observed. It might decrease the rate of hydrogenation.

## 4-6-2 Kinetic analysis by *in-situ* infrared spectroscopy

Next, kinetic investigation by *in-situ* infrared spectroscopy was performed to estimate independency of Rh/XANTPHOS and **1**. The reactions of 1-decene, undecanals, and undecanols were monitored in hydroformylation/hydrogenation of 1-decene by Rh(acac)(CO)$_2$/XANTPHOS/**1** (Reaction **a**, Figure 4-6a), hydroformylation of 1-decene by Rh(acac)(CO)$_2$/XANTPHOS (Reaction **b**, Figure 4-6b), isomerization of 1-decene by **1** (Reaction **c**, Figure 4-6c), and hydrogenation of undecanal with **1** (Reaction **d**, Figure 4-6d) respectively. The results and calculated rate equations are summarized in Scheme 4-7.

The rate of hydroformylation was not affected by the presence of **1**. The observed rate equations of hydroformylation in the presence and absence of **1** were $(6.4 \pm 0.8) \times 10^{-3}$ [1-decene] (Figure 4-6a) and $(6.6 \pm 0.8) \times 10^{-3}$ [1-decene] (Figure 4-6b), respectively. However, increase of the amount of *iso*-product was observed as decrease of $n/i$ ratio ($n/i$ = 16 and 24 respectively). It can be ascribed to the isomerization of 1-decene by **1** to internal alkenes and

successive direct hydroformylation by Rh/XANTPHOS. When the isomerization of 1-decene by

**1** was independently monitored, it was first order on the concentration of 1-decene during initial

50% conversion (Figure 4-6c). The observed rate equation was $(3.6 \pm 0.4) \times 10^{-4}$ [1-decene].

This rate constant was 6% of the observed rate constant of hydroformylation of 1-decene by

Rh/XANTPHOS. Formations of decane and alcohols by **1** were confirmed to be slow by low

yield of decane (3.9%) and alcohols (6.2%).

On the other hand, the rate of hydrogenation of aldehyde by **1** was quite similar in the

presence or absence of Rh/XANTPHOS. The observed rate equations were $(8.4 \pm 0.8) \times 10^{-5}$

$[\text{undecanal}]^0$ (Figure 4-6a) and $(9.1 \pm 0.9) \times 10^{-5}$ $[\text{undecanal}]^0$, respectively (Figure 4-6d). The

difference between the reaction rates was within the margin of error. Selectivity to alcohol was

>95% in both cases.

**Scheme 4-7.** Summary of observed rate constants as a function of substrate concentration for

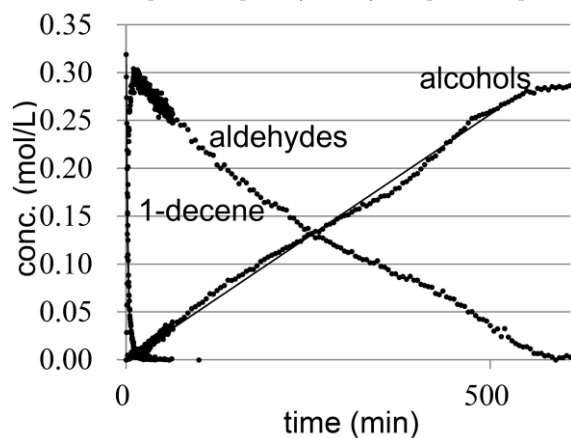each step. [S]: concentration of substrate in each reaction.
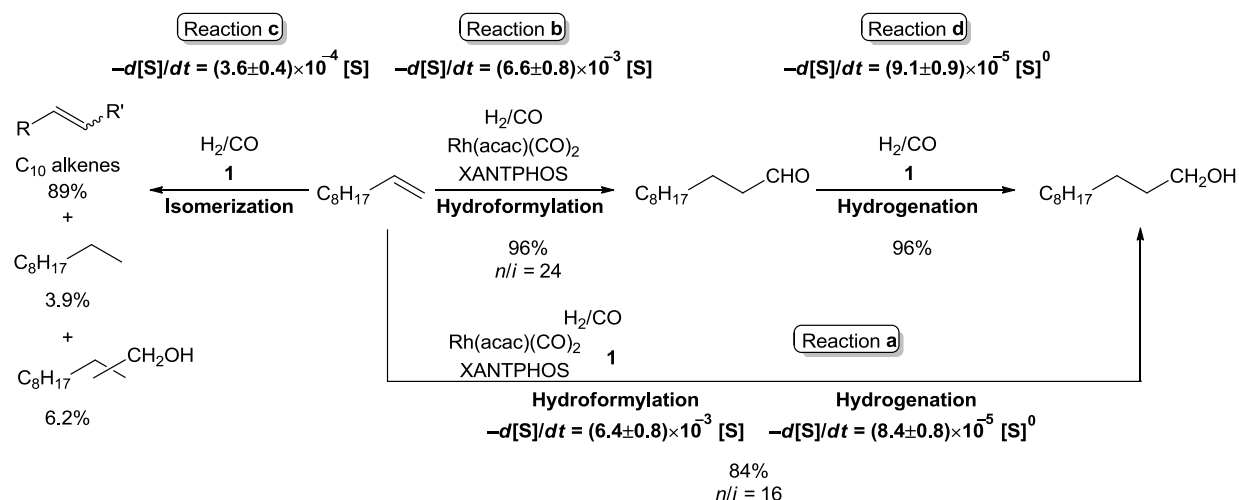
(a) Reaction **a**: Hydroformylation/hydrogenation of 1-decene by Rh/XANTPHOS/**1**
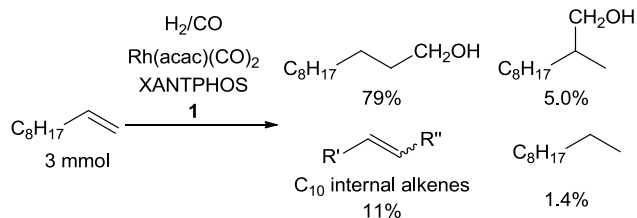


Hydroformylation: $-d[\text{1-decene}]/dt = (6.4\pm0.8)\times10^{-3}$ [1-decene]

Hydrogenation: $-d[\text{undecanal}]/dt = (8.4\pm0.8)\times10^{-5}$ [undecanal]$^{0}$

Isomerization: $-d[\text{1-decene}]/dt = (8.3\pm0.8)\times10^{-4}$ [1-decene]

(b) Reaction **b**: Hydroformylation of 1-decene by Rh/XANTPHOS.
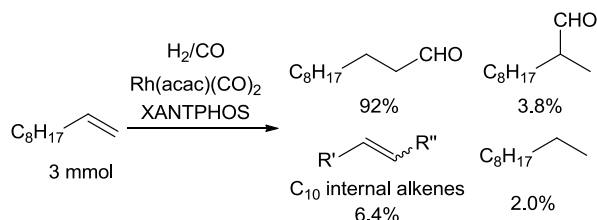


Hydroformylation: $-d[\text{1-decene}]/dt = (6.6\pm0.8)\times10^{-3}$ [1-decene]

Isomerization: $-d[\text{1-decene}]/dt = (4.4\pm0.5)\times10^{-4}$ [1-decene]

117

(c) Reaction **c**: Isomerizaion of 1-decene by **1** under $H_2/CO$ atmosphere.



Isomerization: $-d[\text{1-decene}]/dt = (3.6\pm0.4)\times10^{-4}\,[\text{1-decene}]$



(d) Reaction **d**: Hydrogenation of undecanal by **1** under $H_2/CO$ atmosphere.



Hydrogenation: $-d[\text{undecanal}]/dt = (9.1\pm0.9)\times10^{-5}\,[\text{undecanal}]^{0}$
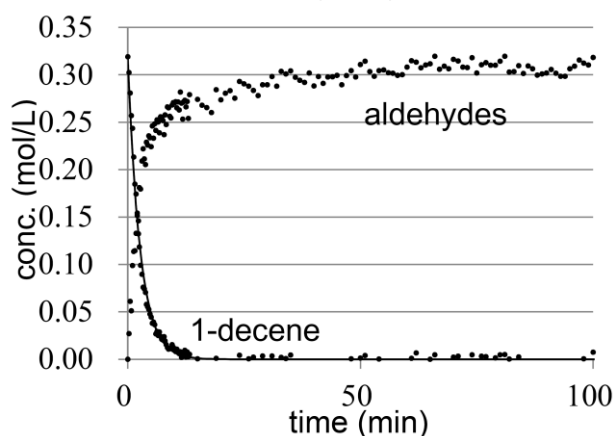


**Figure 4-6.** Time courses of substrate and products concentration in the reaction of 1-decene catalyzed by Rh/XANTPHOS in the presence of **1** (a) and in the absence (b), in the presence of **1**

(c), and time courses of undecanal and undecanol concentration in the presence of **1** (d) monitored by real-time IR spectrpscopy. Decay of 1-decene until 95% conversion was fitted with first-order equation in (a) and (b). Formation of alcohols was fitted with zero-order reaction in (a) and (d). Decay of 1-decene until 50% conversion was fitted with first-order equation in (c). Black line shows the fitted functions. Common conditions: DMA, 9 mL; $H_2$, 1.0 MPa; CO, 1.0 MPa. (a) 1-decene, 3 mmol; Rh(acac)(CO)$_2$, 50 μmol; XANTPHOS, 100 μmol; **1** 125 μmol (based on mol of Ru atom). (b) 1-decene, 3 mmol; Rh(acac)(CO)2, 50 μmol; XANTPHOS, 100 μmol. was fitted with zero-order reaction. Common conditions: DMA, 9 mL; H2, 1.0 MPa; CO, 1.0 MPa. (c) 1-decene, 3 mmol; **1**, 125 μmol (based on mol of Ru atom). The rate constant was determined from the initial 50% conversion. (d) Undecanal, 3 mmol; **1**, 125 μmol (based on mol of Ru atom).

In the context, it could be concluded that the presence of **1** did not affect the rate of hydroformylation by Rh/XANTPHOS but slightly decreased the selectivity. On the other hand, the presence of Rh/XANTPHOS also did not change the rate of hydrogenation of aldehyde.

### 4-6-3 One-pot two step reaction

Independency between two catalyst systems of Rh/XANTPHOS and **1** was also demonstrated by comparison of one-pot reaction with one-pot two step reaction (Scheme 4-8)

**Scheme 4-8.** One-pot two step hydroformylation/hydrogenation
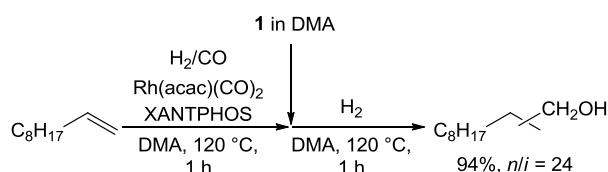


First, hydroformylation was performed by Rh/XANTPHOS under $H_2$/CO for 1 h. Then **1** was added to the mixture, $H_2$/CO was purged by $H_2$, and the solution was heated for 1 h. The yield and *n/i* ratio of undecanol was almost the same as one-pot reaction (94%, *n/i* = 22). It indicates that presence of **1** did not affect the yield of hydroformylation by Rh/XANTPHOS at all. On the other hand, hydrogenation of undecanal under $H_2$ was much faster than that under $H_2$/CO (less

than 1 h versus 10 h). Since Rh/XANTPHOS doesn't affect the rate of hydrogenation by **1**, therefore, the deceleration was ascribed to the presence of carbon monoxide. It should be noted that one-pot two-step reaction affords *n*-alcohol with higher TOF (>38 compared to 3.8 in one-pot reaction (based on the mole of ruthenium)), but there is drawback that it requires purification of $H_2$ from $H_2/CO$ by membrane separation.

## 4-7 Reaction mechanism of hydrogenation under $H_2/CO$

Significant deceleration of hydrogenation under CO was suggested in the previous section. It is a drawback to the system from a viewpoint of industrial application. Therefore, investigation of the mechanism of hydrogenation under $H_2/CO$ may provide a clue to design a new catalyst which is more active under $H_2/CO$ pressure.

### 4-7-1 Kinetics of hydrogenation

First, the effects of pressures of $H_2$ and CO, and concentrations of ruthenium and XANTPHOS on the reaction rate were determined by real-time IR monitoring (Figure 4-7). Based on the obtained data, the rate equation in the absence of XANTPHOS was expressed as

$-d[\text{aldehyde}]/dt = k[\text{aldehyde}]^0 P_{\text{H2}} P_{\text{CO}}^{-1}[\text{Ru}]$

As the amount of XANTPHOS was increased, the rate of hydrogenation was linearly decreased until the stoichiometry of XANTPHOS to Ru reached to one equivalent. Further increase of the amount of XANTPHOS did not change the rate. The rate equation is different from that of under $H_2$ pressure (not simply described but at least the rate depends on aldehyde

concentration, reported in the ref 19). Accordingly, the change of reaction mechanism by CO was suggested.
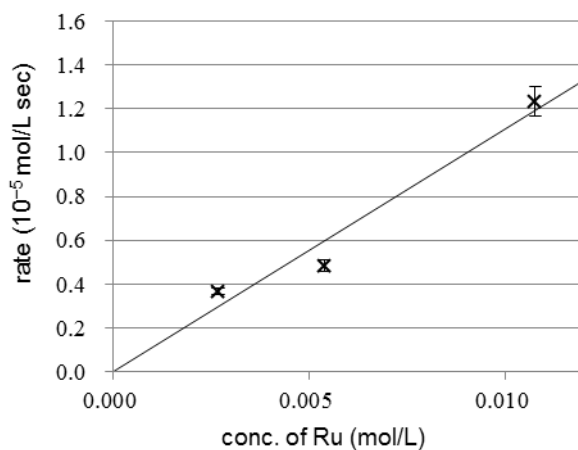
(a) Effect of CO pressure
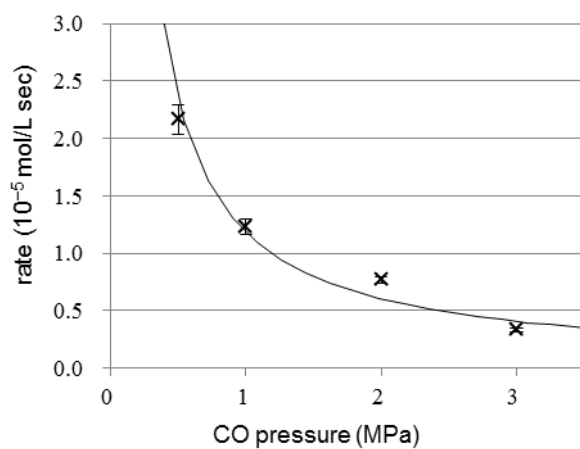


(b) Effect of H$_2$ pressure
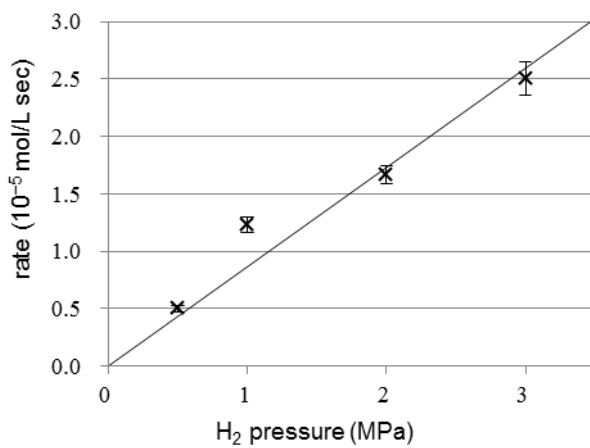
(c) Effect of Ru concentration
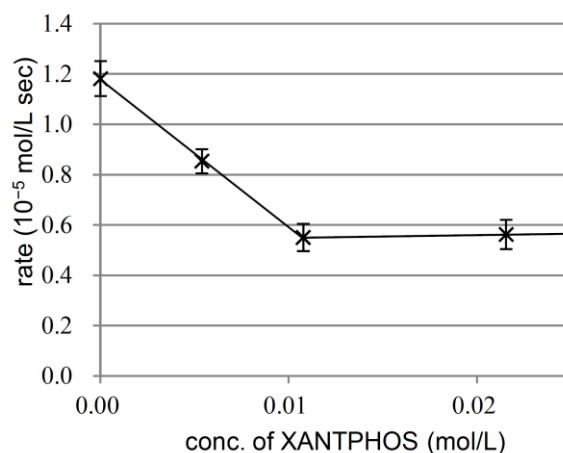


(d) Effect of XANTPHOS



**Figure 4-7.** Rate of hydrogenation of undecanal catalyzed by **1** using $H_2$/CO under varying CO pressure (a), $H_2$ pressure (b), Ru concentration (c), and XANTPHOS concentration (d). Standard condition: DMA 10 mL, $H_2$ 1.0 MPa, CO 1.0 MPa, undecanal 5 mmol, dodecane 2.5 mmol (total 11.6 mL), **1** 0.125 mmol (based on the mol of Ru atom). a) under various CO pressure b) under various $H_2$ pressure c) with various Ru concentration d) with various XANTPHOS concentration in initial 500 minutes. Selectivity from undecanal to undecanol is >95% in all cases. Rate constants were determined from time course of alcohols in initial 200 minutes by fitting with zero-order reaction. Obtained rate constants in each Figure were fitted with inverse proportion to CO pressure in a), direct proportion to $H_2$ pressure in b), direct proportion to Ru concentration in c), direct proportion to XANTPHOS concentration in d). In 3d), two different lines are drawn for XANTPHOS concentration of 0 to $1.1 \times 10^{-2}$ M and $1.1 \times 10^{-2}$ to $2.2 \times 10^{-2}$ M respectively.

## 4-7-2 Proposed mechanism

122

Proposed mechanism is described in Scheme 4-9. As confirmed by the control experiment above, ruthenium mostly existed as **10** under high $H_2$/CO pressure. Considering the fact that the reaction was first-order in ruthenium concentration, equilibrium to dimer is not involved in the reaction mechanism. Since the rate obeys inverse first order kinetics in the pressure of CO and first order kinetics in the pressure of $H_2$, loss of CO to form **11** and successive oxidative addition of $H_2$ to form **12** is the rate determining step. Rapid transfer of two hydrogen atom in concerted manner and coordination by CO regenerated **10**. In the presence of XANTPHOS, **11** could be coordinated by XANTPHOS to form **9**. **9** less favorably lose CO to form **13** and **14** because Ru-CO bond is stronger due to stronger π-back donation from more-electron rich ruthenium center by coordination of XANTPHOS. That resulted in decrease of rate of hydrogenation. As the stoichiometry of XANTPHOS increased from 0 to 1 equivalent to ruthenium, the rate of hydrogenation decreased (Figure 4-7d). More than 1 equivalent, all the ruthenium was coordinated by XANTPHOS then no further decrease took place. Coordination of two XANTPHOS to one ruthenium center is prohibited by steric bukiness. It should be noted that in actual tandem reaction with Rh:XANTPHOS:Ru = 1:2:2.5, XANTPHOS preferably coordinated to Rh and decrease of the rate of hydrogenation was relatively minor.

**Scheme 4-9.** Proposed mechanism of hydrogenation of aldehyde by **1** under $H_2/CO$ in the presence or absence of XANTPHOS.
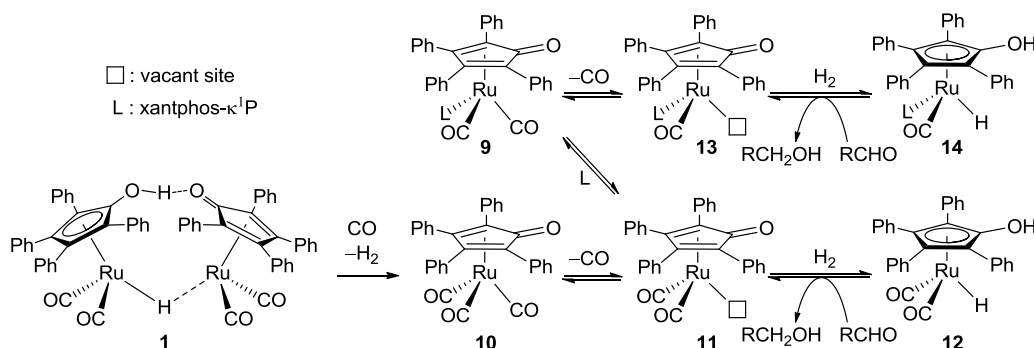


## 4-8 Comparison of hydrogenation activity with other ruthenium-based catalysts

The hydrogenation rate of *normal*-undecanal by **1** was compared with those of other conventional hydrogenation catalysts under $H_2/CO$. $Ru_3(CO)_{12}$, $Ru(CO)H_2(PPh_3)_3$, and $Cp*Ru(cod)Cl(\mathbf{3})/Ph_2PCH_2CH_2NH_2(\mathbf{4})/{}^tBuOK$ were tested here (Table 4-5). However, none of them was active as **1**. Comparison with $\mathbf{3}/\mathbf{4}/{}^tBuOK$ was also done with ${}^iPrOH$ as solvent (runs 5 and 6), which was reported as the best solvent for $\mathbf{3}/\mathbf{4}/{}^tBuOK$, but still **1** was more active and more selective.
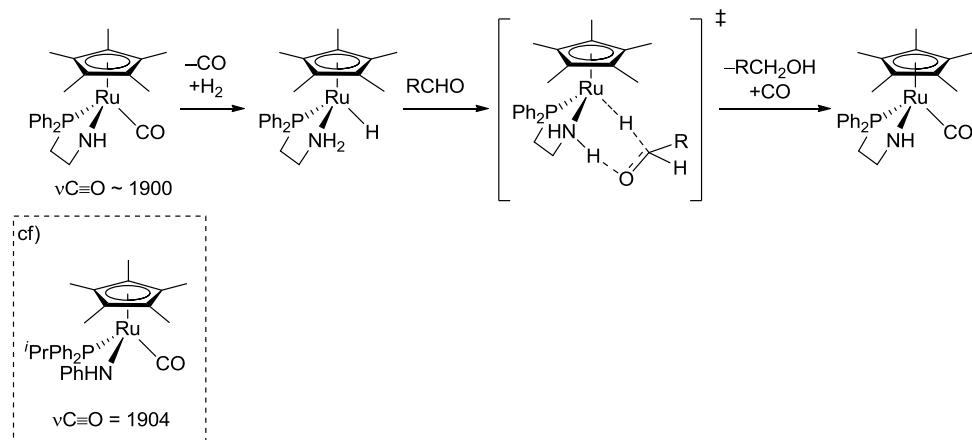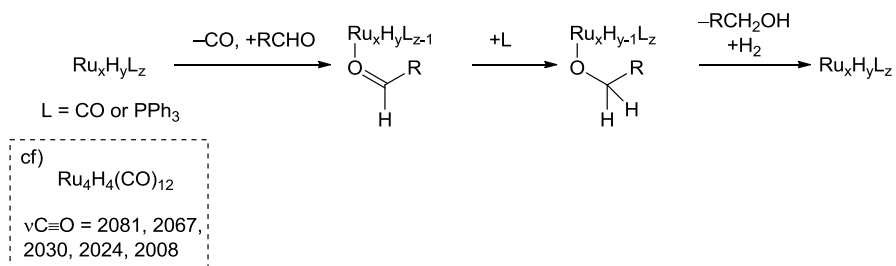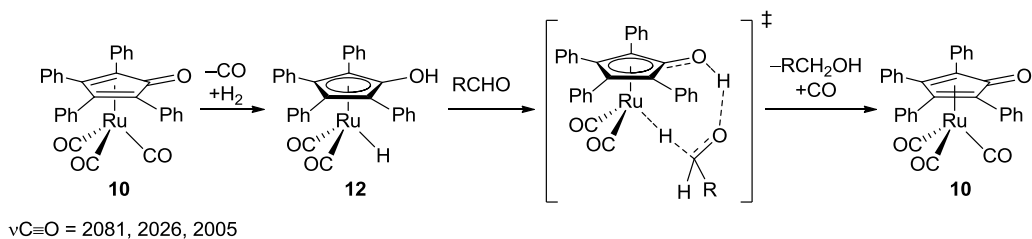
**Table 4-5** Hydrogenation of undecanal under $H_2/CO$ with various catalysts[a]

| run | Cat. | Time (h) | Conv. (%) | Alcohol (%) |
|-----|------|----------|-----------|-------------|
| 1 | **1** | 11 | 99 | 99 |
| 2 | $Ru_3(CO)_{12}$ | 12 | <1 | 0 |
| 3 | $Ru(CO)H_2(PPh_3)_3$ | 23 | 4.7 | 4.4 |
| 4[b] | $Cp*Ru(cod)Cl(\mathbf{3})/Ph_2PCH_2CH_2NH_2(\mathbf{4})/{}^tBuOK$ | 12 | 21 | <1[c] |
| 5[d] | **1** | 13 | 99 | 98 |
| 6[d] | $Cp*Ru(cod)Cl(\mathbf{3})/Ph_2PCH_2CH_2NH_2(\mathbf{4})/{}^tBuOK$ | 10 | 85 | 16[c] |

These results were interpreted as follows (Scheme 4-10). Under $H_2$/CO, **1** is transformed to **10** as discussed above, and $Ru_3(CO)_{12}$ and $Ru(CO)H_2(PPh_3)_3$ were thought to be converted to $Ru_xH_yL_z$ (L = CO or $PPh_3$).[20] Judging from IR absorption band of $\nu_{C\equiv O}$ for **10** (2081, 2026, 2005 $cm^{-1}$) and $Ru_4H_4(CO)_{12}$ (2081, 2067, 2030, 2008 $cm^{-1}$) the extent of $\pi$-backdonation from ruthenium center to carbonyl is similar in those complexes. Therefore the strength of Ru-CO bond is similar and rate of loss of CO should be comparable. The difference should be attributed to the difference in successive steps. **1** hydrogenates substrate in concerted manner. On the other hand, $Ru_xH_yL_z$ is supposed to do via coordination-insertion mechanism. The difference between **1** and **3**/**4**/$^tBuOK$ thought to be derived from the rate of losing CO. Under CO pressure, **3**/**4**/$^tBuOK$ though to form Cp*Ru(CO)($Ph_2PCH_2CH_2NH$). Generation of active species requires dissociation of CO and successive addition of $H_2$. Comparing $\nu_{C\equiv O}$ for **10** (2081, 2026, 2005 $cm^{-1}$) with Cp*Ru(NHPh)($P^iPrPh_2$) (1904 $cm^{-1}$) as a referential compound, generation of active species should be faster in the case of **10**.

**Scheme 4-10.** Proposed mechanisms of hydrogenation with various Ru catalysts



$\nu C{\equiv}O$ = 2081, 2026, 2005

L = CO or PPh$_3$

cf)
Ru$_4$H$_4$(CO)$_{12}$

$\nu C{\equiv}O$ = 2081, 2067, 2030, 2024, 2008

$\nu C{\equiv}O$ ~ 1900

cf)

$\nu C{\equiv}O$ = 1904

## 4-9 Conclusion

In summary, the author developed high-yielding tandem *normal*-selective hydroformylation/hydrogenation for one-pot conversion of terminal alkenes to *normal*-alcohols using dual catalyst system composed of Rh(acac)(CO)$_2$/XANTPHOS/Shvo's catalyst (**1**). This method would be advantageous by simplifying process operation. Mechanistic investigations revealed that Rh/XANTPHOS and **1** independently catalyzed hydroformylation and hydrogenation with minor interference. Poisoning of **1** by carbon monoxide retards the hydrogenation. Reaction mechanism of hydrogenation of aldehyde catalyzed by **1** under H$_2$/CO was revealed by the kinetic esperiments. Further improvement of the rate of hydrogenation would provide a simplified method for industrial *normal*-alcohol synthesis.

**Experimental section**

**General**

Commercially available anhydrous *N,N*-dimethylacetamide, methanol, and 2-propanol were distilled and degassed by freeze-pump-thaw before use. 1-decene, dodecane, tridecane, allyl alcohol, allyl acetate, 3-butenyl alcohol, 3-butenyl acetate, and 4-pentenyl alcohol were purchased from TCI and distilled and degassed by freeze-pump-thaw before use. Undecanal styrene, vinylcyclohexane, 2-methyl-1-nonene, and (*Z*)-2-decene, were purchased from TCI and degassed by freeze-pump-thaw before use. $Ru(CO)H_2(PPh_3)_3$ was purchased from TCI. Compounds **2**, **3**, **4**, **5**, and **6** were purchased from Strem. $Rh(acac)(CO)_2$ was purchased from Aldrich. Shvo's catalyst(**1**) was prepared according to literature method from $Ru_3(CO)_{12}$ and tetraphenylcyclopentadienone and purified by recrystallization from toluene/hexane. 2-(5-hexen-1-yloxy)-tetrahydropyran,[21] (5-hexen-1-yloxy)methylbenzene,[22] (5-hexen-1-yloxy)-*tert*-butyldimethylsilane,[23] 2-(9-decen-1-yl)-1,3-dioxolan,[24] (5-hexen-1-yl)-*N*-phenylcarbamate,[25] XANTPHOS[9] were prepared by the literature method. Product yields were determined by Shimadzu GC-2014 equipped with InertCap 5MS/Sil capillary column (0.25 ID, 0.25 μm df, 30 m) using calibration curve made with dodecane or tridecane as an internal standard. Real-time IR measurement was performed by using METTLER TOLEDO ReactIR™ 45 and analyzed by icIR. NMR yields were determined by ^{1}H experiment with 15 s relaxation delay using 1,3,5-trimethoxybenzene as internal standard.

**General procedure for hydroformylation/hydrogenation of alkene**

To a stainless autoclave (50 mL) charged with $Rh(acac)(CO)_2$ (5.2 mg, 20 μmol), XANTPHOS (23.1 mg, 40.0 μmol) and magnetic stir bar under Ar, appropriate solvent (1.0 mL) was added and the resulting mixture was stirred for 5 minutes at room temperature. Ru catalyst catalyst (50.0 μmol (Ru)) was weighed and dissolved in solvent (2.0 mL) under Ar, which was transferred to the autoclave by cannulation. 2:1 mole ratio mixture of an alkene (2.0 mmol) and internal standard (1.0 mmol) was added via syringe. The autoclave was pressurized with 2.0 MPa of $H_2/CO$ and stirred at 120 ºC, at 800 rpm for 12.5 hours. Then the autoclave was cooled with water/ice bath for 30 minutes, the pressure was released. 1,3,5-trimethoxybenzene (100 mg, 0.590 μmol) was added to the crude solution. Then the solution was analyzed by GC and $^1$H NMR. NMR yield of $n$- or $i$-aldehydes were determined from the integration of corresponding formyl proton (δ 9.8, t, $-CH_2C\underline{H}O$, and δ 9.6, d, $-CHRC\underline{H}O$, respectively). NMR yield of $n$- or $i$-alcohols were determined from the alpha-proton of hydroxyl group (δ 3.6, t, $-CH_2C\underline{H}_2OH$, and δ 3.4-3.5, m, $-CHRC\underline{H}_2OH$). NMR yield of formats were determined by the integration of corresponding formyl proton (δ 8.0, s, $CH_2OC\underline{H}O$). The yields determined by $^1$H NMR were consistent with those determined by GC.

**Preparation of the solution ruthenium catalyst and $^t$BuOK**

To two 20 mL Schlenk flasks, ruthenium complex (**2**, **5**, or **6**, 50 μmol), and $^t$BuOK (5.6 mg, 50 μmol) were separately charged under argon atomosphere. To the Schlenk flask containing ruthenium complex, $^i$PrOH (1.0 mL) was added, and the resulting solution was transferred to the other Schlenk flaks containing $^t$BuOK followed by washing Schlenk with 1.0 mL of $^i$PrOH.

**Preparation of Cp\*Ru(Ph$_2$PCH$_2$CH$_2$NH$_2$)Cl/$^t$BuOK solution**

To three 20 mL Schlenk flasks, Cp*Ru(cod)Cl (**3**, 19 mg, 50 μmol), $Ph_2PCH_2CH_2NH_2$ (**4**, 11.4 mg, 50.0 μmol), and $^tBuOK$ (5.6 mg, 50 μmol) were separately charged under argon atomosphere. To the both Schlenk flasks containing **3** and **4**, $^iPrOH$ (1.0 mL) was added, and they were combined and were stirred for a few minutes. The resulting mixture was transferred to the third Schlenk flaks containing $^tBuOK$. Each Schlenk flask was washed with $^iPrOH$ (1.0 mL) and combined.

## NMR experiments

### Rh/XANTPHOS/Ru = 1/2/2.5 in DMA under $H_2$/CO

To a 20 mL Schlenk flask containing $Rh(acac)(CO)_2$ (2.6 mg, 10 μmol) and XANTPHOS (11.5 mg, 19.9 μmol), DMA (300 μL) was added under $H_2$/CO atmosphere. After stirring the resulting mixture at room temperature for 5 min, a solution of **1** (12.5 mg 11.2 μmol) in DMA (500 μL) was transferred into the Schlenk flask. The mixture was stirred at 120 °C for 15 min, and was cooled down to room temperature. The resulting solution was transferred to a screw-capped NMR tube by a syringe under $H_2$/CO atmosphere to take $^{31}P$ NMR spectrum.

### XANTPHOS/Ru = 1/2 in DMA under $H_2$/CO

To a screw-capped NMR tube containing XANTPHOS (11.1 mg, 19.2 mmol) and **1** (10.9 mg, 10.0 mmol), DMA (600 μL) was added under $H_2$/CO atmosphere. After heating at 120 °C for 15 min, it was cooled down to room temperature to take $^{31}P$ NMR spectrum.

### Rh/XANTPHOS = 1/1 in DMA under $H_2$/CO

To a 20 mL Schlenk flask containing Rh(acac)(CO)$_2$ (2.6 mg, 10 μmol) and XANTPHOS (5.8 mg, 10 μmol), DMA (700 μL) was added under H$_2$/CO atmosphere. The mixture was heated at 120 °C for 15 min, and cooled down to room temperature. The resulting solution was transferred to a screw-capped NMR tube by a syringe under H$_2$/CO atmosphere to take $^{31}$P NMR spectrum.

**Rh/XANTPHOS = 1/1 in DMA under CO**

Similarly performed as Rh/XANTPHOS = 1/1 in DMA under H$_2$/CO by replacing H$_2$/CO with CO.

**Preparation of Rh(acac)(CO)(XANTPHOS)**

To a 50 mL J-Young tube containing Rh(acac)(CO)$_2$ (182 mg, 705 μmol) and XANTPHOS (408 mg, 704 μmol), C$_6$H$_6$ was vacuum-transferred to the tube. After C$_6$H$_6$ melted under argon atmosphere, a rapid generation of CO was observed. Resulting solution was stirred at r.t. for 5 min. After the evaporation of the solvent, the crude orange solid was dissolved in small amount of hot C$_6$H$_6$, and hexane was added to the solution to give an yellow-orange powder of Rh(acac)(CO)(xantphos)•C$_6$H$_6$ (504 mg, 569 μmol, 81.5%). Single crystals for X-ray analysis were obtained via recrystalization from benzene solution with a diffusion of hexane. Crystal graphical data are shown at Figure 4-8. Analytically pure single crystals were obtained by a recrystallization from toluene solution with a diffusion of hexane. $^1$H NMR (CD$_2$Cl$_2$, 400 MHz) δ 0.88 (s, 3H) 1.63 (s, 6H), 2.03 (s, 3H), 5.21 (s, 1H), 6.48 (br t, $J$ = 7 Hz, 2H), 6.99 (t, $J$ = 8 Hz, 2H), 7.06-7.43 (m, 20H), 7.49 (d, $J$ = 8 Hz, 2H); $^{13}$C NMR (CD$_2$Cl$_2$, 101 MHz) δ 26.0 (CH$_3$), 27.5 (CH$_3$), 30.0 (CH$_3$), 35.0 (4°), 100.0 (CH), 122.1 (d, $J$ = 12 Hz, 4°), 123.6 (CH), 126.5 (CH), 128.0 (vt, CH), 128.3 (CH), 129.0 (CH), 131.3 (4°), 131.8 (CH), 134.0 (d, $J$ = 14 Hz, CH), 135.7

(d, $J$ = 18 Hz, 4°), 154.1 (d, $J$ = 12 Hz, 4°), 186.0 (d, $J$ = 32 Hz, 4°), 191.0 (dt, $J$ = 75 Hz, 11 Hz, 4°); $^{31}$P NMR (CD$_2$Cl$_2$, 162 MHz) δ 13.7 (br d, $J$ = 38 Hz); mp 186-190 °C (decomp.); IR (KBr, cm-1): ν(Rh–C≡O) 1965, ν (Rh–O=C) 1578, 1516; Anal. Calced for C$_{45}$H$_{39}$O$_4$P$_2$Rh•C$_7$H$_8$: C, 69.34; H, 5.26. Found: C, 69.23; H, 5.26.
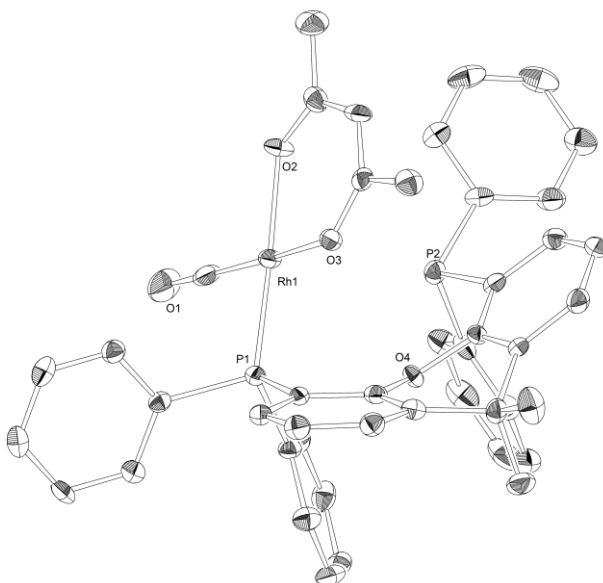


**Figure 4-8.** ORTEP drawing of Rh(acac)(CO)(xantphos) (50% thermal ellipsoid, hydrogen atoms and solvent molecule C$_6$H$_6$ were omitted for clarity)

**X-ray crystallographic data for Rh(acac)(CO)(xantphos)**

Details of the crystal graphical data, and a summary of the intensity data collection parameters for Rh(acac)(CO)(xantphos)·C$_6$H$_6$ are shown in Table 4-6. A suitable crystal was mounted with mineral oil to a glass fiber and transferred to the goniometer of a Rigaku Mercury CCD or VariMax Saturn CCD diffractometer with graphite-monochromated Mo Kα radiation (λ = 0.71070 Å) or . The structures were solved by direct methods with (SIR-97)[26] and refined by full-matrix least-squares techniques against F2 (SHELEXL-97).[27] The intensities were corrected for Lorentz and polarization effects or NUMABA program (Rigaku 2005). The non-hydrogen

atoms were refined anisotropically. Hydrogen atoms were placed using AFIX instructions. All

the resulting CIF files and their checkCIF files are also attached as supporting information.

ORTEP drawings of Rh(acac)(CO)(xantphos)·C$_6$H$_6$ is shown below the Table (Thermal

ellipsoids set at 50% probability; hydrogen atoms except bonded to Ru and solvent molecules are

omitted for clarity.)

**Table 4-6** Crystallographic data and structure refinement details for Rh(acac)(CO)(xantphos)·C$_6$H$_6$

|  | Rh(acac)(CO)(xantphos)·C$_6$H$_6$ |
| --- | --- |
| formula | C$_{51}$H$_{45}$O$_4$P$_2$Rh |
| fw | 886.72 |
| $T$ (K) | 103(2) |
| $\lambda$ (Å) | 0.71070 |
| cryst syst | Triclinic |
| space group | $P$-1 |
| $a$, (Å) | 10.926(3) |
| $b$, (Å) | 12.081(4) |
| $c$, (Å) | 16.732(6) |
| $\alpha$, (°) | 89.729(10) |
| $\beta$, (°) | 83.741(10) |
| $\gamma$, (°) | 73.301(8) |
| $V$, (Å$^3$) | 2102.0(11) |
| $Z$ | 2 |
| D$_{calc}$, (g / cm$^3$) | 1.401 |
| $\mu$ (mm$^{-1}$) | 0.529 |
| F(000) | 916 |
| cryst size (mm) | $0.25 \times 0.20 \times 0.05$ |
| $2\theta$ range, (deg) | 3.06-25.00 |
| reflns collected | 13657 |
| indep reflns/$R_{int}$ | 7189/0.0455 |
| params | 527 |
| GOF on $F^2$ | 1.168 |
| $R_1$, w$R_2$ [I>2$\sigma$(I)] | 0.0610, 0.1444 |
| $R_1$, w$R_2$ (all data) | 0.0733, 0.1502 |

The GC chart showed six peaks around C10 area. Four of six peaks are assignable to 1-decene, n-decane, and (Z)/(E)-2-decene. Remaining two large peaks overlapped with n-decane can be assigned as (Z)/(E)-3-decene as follows. The $^1$H NMR spectrum of the crude product showed two triplet peaks at 0.957 ppm (t, $J$ = 7 Hz) and 0.964 (t, $J$ = 7 Hz), having cross peaks with allylic protons around 2.0 ppm in HH COSY spectrum. Thus, these two peaks are assignable as homoallylic terminal methyl groups in (Z)/(E)-3-decene.
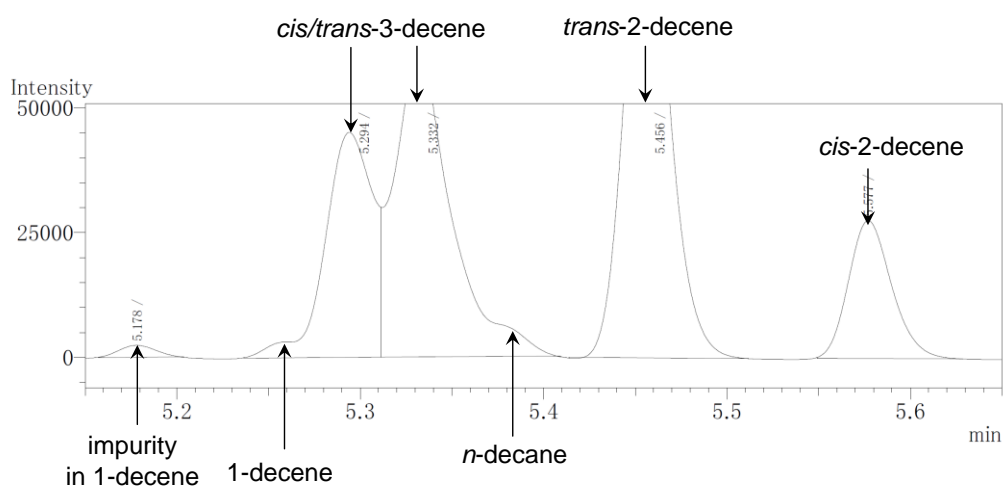


**Figure 4-9.** The GC chart of the reaction mixture around hydrocarbon moiety.
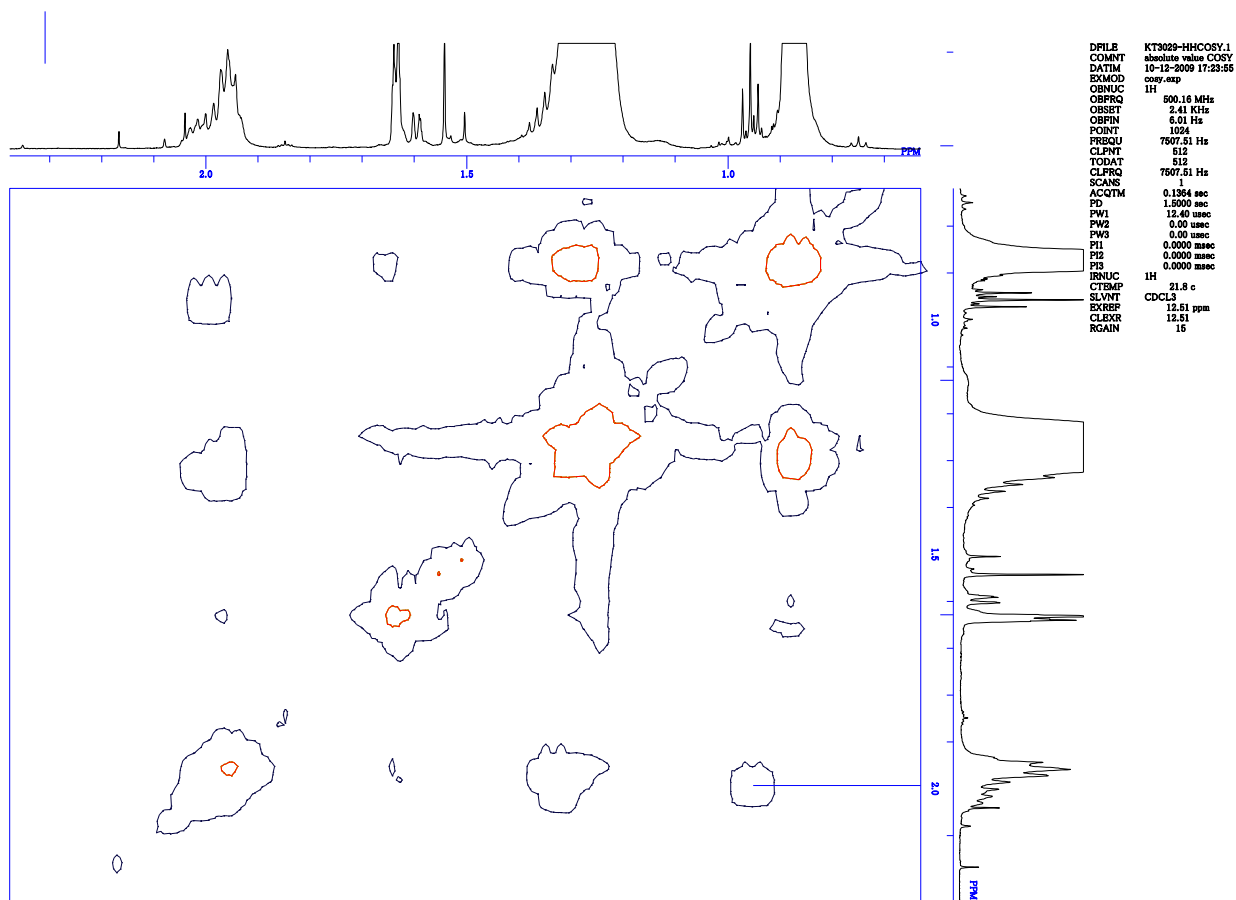
**Figure 4-10.** The $^1$H-$^1$H COSY NMR spectrum of the crude product.

**Preparation of undecyl formate**

To a 100 mL two-necked round-bottomed flask, formic acid (4.51 g, 97.9 mmol) and 1-undecanol (1.72 g, 10.0 mmol) were charged, and the resulting mixture was refluxed for 9 h. After cooling the mixture to room temperature, saturated $NaHCO_3$ aq. was added to neutralize the solution. The solution was extracted with $Et_2O$ (20 mL × 3). Combined organic layer was washed with brine (20 mL × 2), and was dried over $Na_2SO_4$. After filtration, solvent was removed by evaporation. Analytically pure 1-undecyl formate was obtained (1.60 g, 80%, density = 0.870); $^1H$ NMR ($CDCl_3$, 500 MHz) δ 0.87 (3H, t, $J$ = 7 Hz), 1.17-1.41 (16H, m), 1.65 (2H, tt, $J$ = 7 Hz, 7 Hz), 4.16 (2H, t, $J$ = 7 Hz), 8.05 (1H, s), $^{13}C$ NMR ($CDCl_3$, 100 MHz): δ14.33. 22.95, 26.11, 28.81, 29.47, 29.60, 29.78, 29.84, 29.86, 32.18, 64.29, 161.28. IR (KBr, $cm^{-1}$) νCO 1732. Anal. Calcd. for $C_{12}H_{24}O_2$: C, 71.95; H, 12.08. Found: C, 71.75; H, 12.25.

**Real-time IR monitoring of hydroformylation/hydrogenation of 1-decene by Rh(acac)(CO)₂/XANTPHOS/1**

An autoclave (100 mL) equipped with IR probe and high pressure dropping funnel was charged with Rh(acac)(CO)₂ (13.0 mg, 50 μmol), XANTPHOS (57.8 mg, 100 μmol) and magnetic stir bar was flushed with Ar. It was added DMA (2.0 mL) and the resulting mixture was stirred for 5 minutes at room temperature. **1** (67.8 mg, 125 μmol (Ru)) was charged into 20 mL Shlenck under Ar and was dissolved in DMA (3.0 mL). Then the solution was transferred to the autoclave by cannulation, the Schlenk was washed two times with DMA (total 1.0 mL), and they were transferred to the autoclave. At the same time, the dropping funnel was charged with 1-decene (1.0 mL, c.a. 5.3 mmol) and DMA (3.0 mL). The autoclave was pressurized with 2.0 MPa of H₂/CO and stirred at 120 ºC, at 800 rpm, for 1,5 hours. Then the mixture of 1-decene and

DMA in dropping funnel was pressed in to the autoclave with 3 MPa of $H_2$/CO, and the gas pressure was partially released to the value before substrate injection. . The integration of the characteristic peaks for 1-decene (912 cm$^{-1}$, terminal C=C), undecanal (1726 cm$^{-1}$, C=O), and undecanol (1058 cm$^{-1}$, C-O) were monitored during the reaction time. After appropriate reaction time, the autoclave was cooled with water/ice bath for 30 minutes and the pressure was released. Dodecane (500.0 mg, 2.945 mmol) was added to the crude solution. Then the solution was analyzed by GC.

The actual amount of substrate injected into the autoclave was estimated as sum of the observed product with GC analysis. The actual liquid volume was estimated with the following equation

(actual liquid volume) = (initial charge of solvent) + (mixture of solvent and substrate charged via dropping funnel) = 7 + 4 × (mmol of the substrate injected into the autoclave)/(mmol of the substrate charged into the dropping funnel)

Data treatment of IR was as follows. Background was measured before experiment under air. During the reaction, the peak area for 1-decene (912 cm$^{-1}$, terminal C=C), undecanal (1726 cm$^{-1}$, C=O), and undecanol (1058 cm$^{-1}$, C-O) were plotted versus time ($t$) in every 15 sec (64 scans were integrated) for initial 1.5 hours and every 5 minutes (256 scans were integrated) after that time. Signal to noise ratio of these peaks of compounds at concentration of 0.32 M in DMA were c.a. 40, 60, and 70 respectively, which supports the accuracy of the integral value. The consumption of 1-decene until 95% conversion was monitored to confirm the first order kinetics. The obtained pseudo-first order rate constant was multiplied by the selectivity to aldehyde to calculate rate constant for hydroformylation. Since the increase of 1-undecanol was linear versus time, the observed rate constant was calculated from the slope.

As experimental error, the amount of injected substrate ± 5%, $H_2$/CO pressure ± 2.5%, volume of liquid ± 1.0%, the amount of weighed catalyst <0.8%, were considered (± 9.6% in total). Statistical error was respectively determined as standard deviation from obtained data and its least squares fitting curve. The total error (%) was calculated as multiple of experimental and statistical error.

Catalytic species could not be characterized by in-situ infrared spectroscopy because of low intensity of those signals.


**Real-time IR monitoring of hydroformylation of 1-decene by Rh(acac)(CO)$_2$/XANTPHOS**

An autoclave (100 mL) equipped with IR probe and high pressure dropping funnel was charged with Rh(acac)(CO)$_2$ (13.0 mg, 50 μmol), XANTPHOS (57.8 mg, 100 μmol) and magnetic stir bar was flushed with Ar. The IR monitoring was started at this point. It was added DMA (7.0 mL) and the resulting mixture was stirred for 5 minutes at room temperature. At the same time, the dropping funnel was charged with 1-decene (1.0 mL, 5.3 mmol) and DMA (3.0 mL). The autoclave was pressurized with 2.0 MPa of $H_2$/CO and stirred at 120 °C, at 800 rpm, for 1.5 hours. Then the mixture of 1-decene and DMA in dropping funnel was pressed in to the autoclave with 3 MPa of $H_2$/CO, and the gas pressure was partially released to the value before substrate injection. The concentration of 1-decene and undecanal were monitored by the integration of the area at 1-decene (912 cm$^{-1}$, terminal C=C), and undecanal (1726 cm$^{-1}$, C=O) . After appropriate reaction time, the autoclave was cooled with water/ice bath for 30 minutes and the pressure was released. Dodecane (500.0 mg, 2.945 mmol) was added to the crude solution. Then the solution was analyzed by GC. Following data treatments were similar to that mentioned above.

**Real-time IR monitoring of isomerization of 1-decene by 1**

1 (67.8 mg, 125 µmol) was charged into 20 mL Shlenck under Ar and dissolved in DMA (5.0 mL). An autoclave (100 mL) equipped with IR probe and magnetic stir bar was flushed with Ar. IR monitoring was started at this point. Then the solution of **1** was added to the autoclave by cannulation, the Schlenk was washed two times with DMA (total 5.0 mL), and they were transferred to the autoclave. At the same time, the dropping funnel was charged with 1-decene (1.0 mL, c.a. 5.3 mmol) and DMA (3.0 mL). The autoclave was pressurized with 2.0 MPa of $H_2$/CO and stirred at 120 ºC, at 800 rpm for 1.5 hours. Then the mixture of 1-decene and DMA in dropping funnel was pressed in to the autoclave with 3 MPa of $H_2$/CO, and the gas pressure was partially released to the value before substrate injection. The integration of the characteristic peaks for 1-decene (912 $cm^{-1}$, terminal C=C) was monitored during the reaction time. After appropriate reaction time, the autoclave was cooled with water/ice bath for 30 minutes and the pressure was released. Dodecane (500.0 mg, 2.945 mmol) was added to the crude solution. Then the solution was analyzed by GC. Initially the reaction rate was first order on substrate concentration. The rate constant for the consumption of 1-decene until 50% conversion was calculated from the plot of $\ln(1-[1\text{-decene}]/[1\text{-decene}]_0)$ versus time. The rate constant for isomerization was calculated as (rate constant for the consumption of1-decene) × (selectivity to internal alkenes)

**Real-time IR monitoring of hydrogenation of undecanal by 1**

1 (67.8 mg, 125 µmol) was charged into 20 mL Shlenck under Ar and dissolved in DMA (5.0 mL). An autoclave (100 mL) equipped with IR probe and magnetic stir bar was flushed with Ar.

IR monitoring was started at this point. Then the solution of **1** was added to the autoclave by cannulation, the Schlenk was washed two times with DMA (total 5 mL), and they were transferred to the autoclave. At the same time, the dropping funnel was charged with undecanal (1.1 mL, c.a. 5.3 mmol) and DMA (3.0 mL). The autoclave was pressurized with 2.0 MPa of $H_2/CO$ and stirred at 120 ℃, at 800 rpm for 1.5 hours. Then the mixture of 1-decene and DMA in dropping funnel was pressed in to the autoclave with 3 MPa of $H_2/CO$, and the gas pressure was partially released to the value before substrate injection. The integration of the characteristic peaks for undecanal (1726 $cm^{-1}$, C=O), and undecanol (1058 $cm^{-1}$, C-O) were monitored during the reaction time. After appropriate reaction time, the autoclave was cooled with water/ice bath for 30 minutes and the pressure was released. Dodecane (500.0 mg, 2.945 mmol) was added to the crude solution. Then the solution was analyzed by GC. Following data treatments were similar to that mentioned above.

**Stepwise hydroformylation/hydrogenation of 1-decene**

To a stainless autoclave (50 mL) charged with $Rh(acac)(CO)_2$ (5.2 mg, 20 μmol), XANTPHOS (23.1 mg, 40.0 μmol) and magnetic stir bar under Ar, DMA (2.0 mL) was added and the resulting mixture was stirred for 5 minutes at room temperature. 2:1 mole ratio mixture of 1-decene (2.0 mmol) and dodecane (1.0 mmol) was added via syringe. The autoclave was pressurized with 2.0 MPa of $H_2/CO$ and stirred at 120 ℃, at 800 rpm for 1 hour. Then the autoclave was cooled with water/ice bath for 10 minutes, and the pressure was released. **1** (27.1 mg, 50.0 μmol (Ru)) was weighed and dissolved in DMA (2.0 mL) under Ar, which was transferred to the autoclave by cannulation. The autoclave was pressurized with 1.0 MPa of $H_2$ and stirred at 120 ℃, at 800 rpm for 1 hour. Then the autoclave was cooled with water/ice bath

for 30 minutes, the pressure was released, and the solution was analyzed by GC. Obtained products were $n$-alcohol 90%, $i$-alcohol 3.6%, $n$-aldehyde 1.9%, $i$-alcehyde 0.5%, decane 1.0%, undecyl formate 0.6%.

**Real-time IR monitoring of hydrogenation of undecanal by various Ru catalysts under various conditions**

Appropriate amount of Ru catalyst (125, 62.5, or 31.3 µmol) was charged into 20 mL Shlenck under Ar and dissolved in solvent (5.0 mL). An autoclave (100 mL) equipped with IR probe and magnetic stir bar was charged with appropriate amount of XANTPHOS (0, 62.5, 125, or 250 µmol) and flushed with Ar. IR monitoring was started at this point. Then the solution of **1** was added to the autoclave by cannulation, the Schlenk was washed two times with solvent (total 5.0 mL), and they were transferred to the autoclave. A mixture of undecanal and dodecane (2:1 molar ratio, 1.6 mL, 5.0 mmol and 2.5 mmol) was introduced into the autoclave via syringe and it was immediately pressurized with 2.0 MPa of $H_2$/CO and stirred at 120 ºC, at 800 rpm. The integration of the characteristic peaks for undecanol (1058 cm$^{-1}$, C-O) was monitored during the reaction time. After appropriate reaction time, the autoclave was cooled with water/ice bath for 30 minutes and the pressure was released. Dodecane (500.0 mg, 2.945 mmol) was added to the crude solution. Then the solution was analyzed by GC. Following data treatments were similar to that mentioned above except that the rate constants were determined from the time course of alcohol in initial 200 minutes.

As experimental errors, the amount of injected substrate ± 1.0%, $H_2$/CO pressure ± 2.5%, volume of liquid ± 1.0%, the amount of weighed catalyst <0.8%, were considered (± 5.4% in

total). Statistical error was respectively determined as standard deviation from obtained data and its least squares fitting curve.
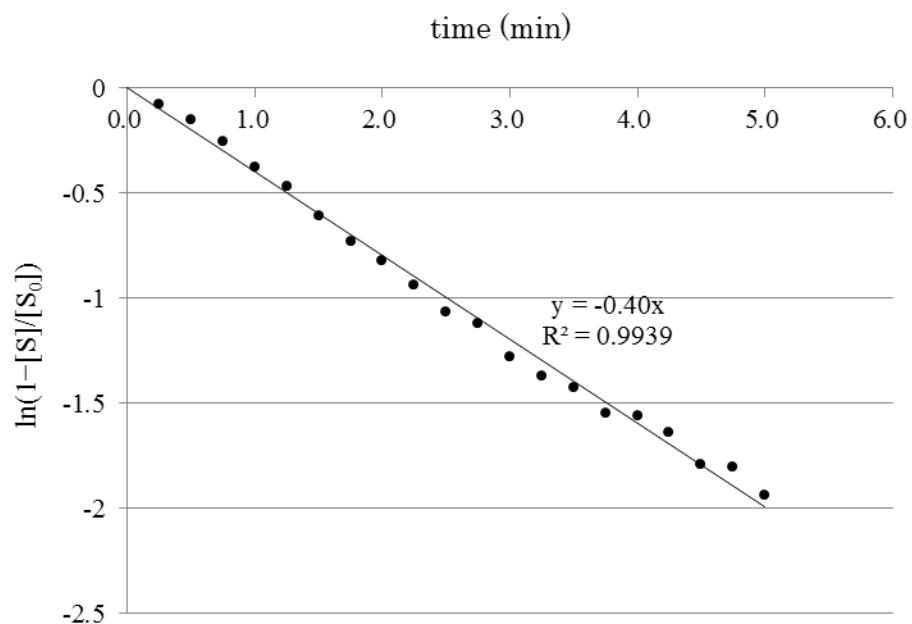


**Figure4-11.** Plot of $\ln(1-[S]/[S_0])$ of hydroformylation/hydrogenation of 1-decene
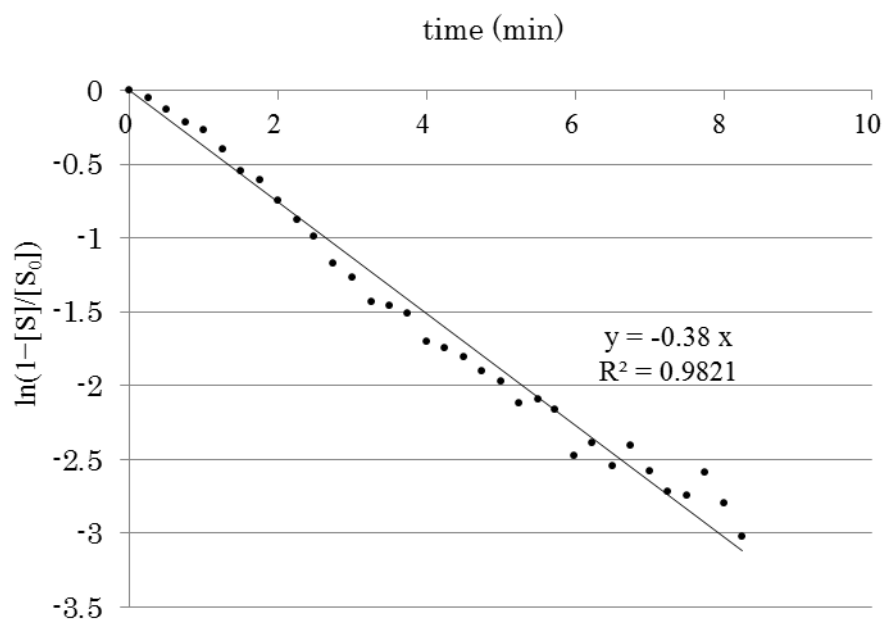


**Figure 4-12.** Plot of $\ln(1-[S]/[S_0])$ of hydroformylation of 1-decene
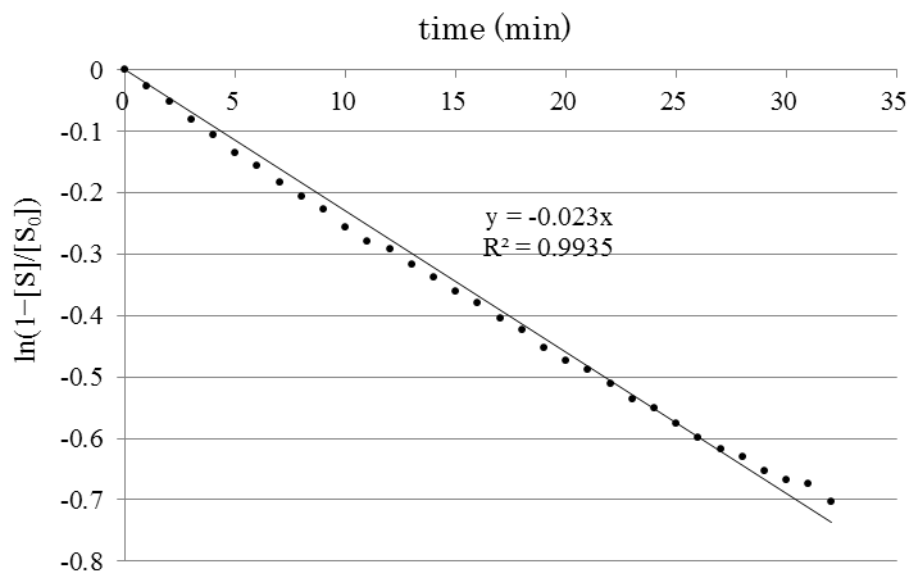
**Figure 4-13.** Plot of $\ln(1-[S]/[S_0])$ of isomerization of 1-decene
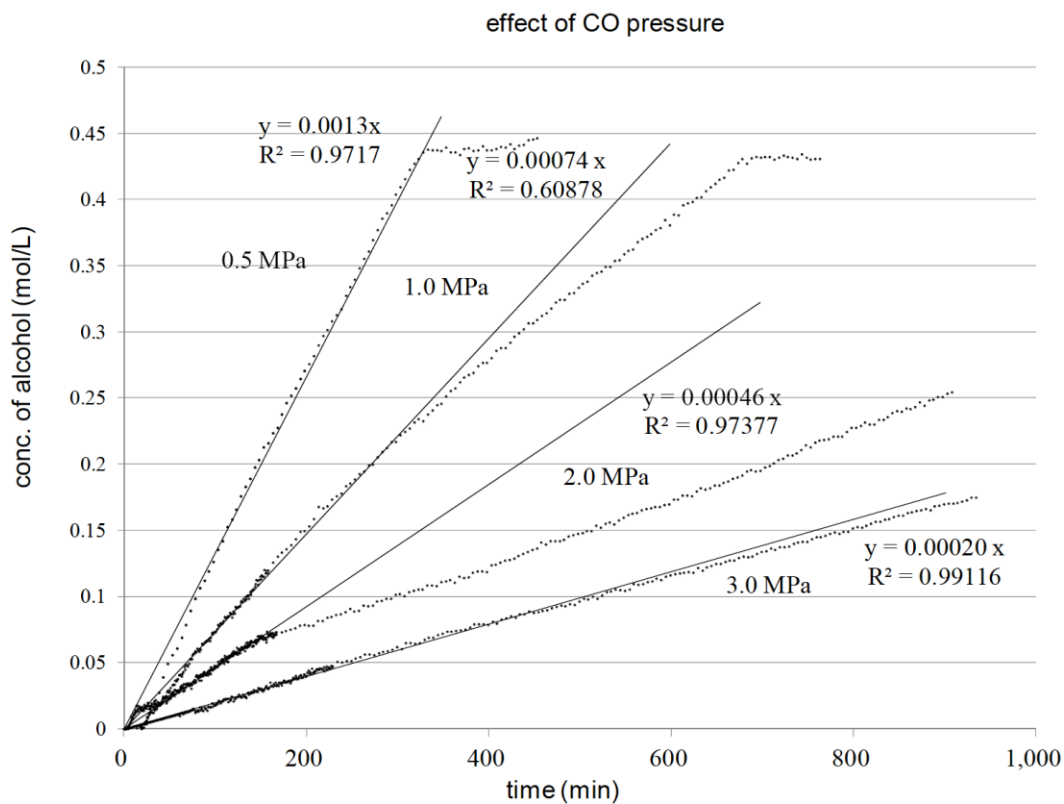


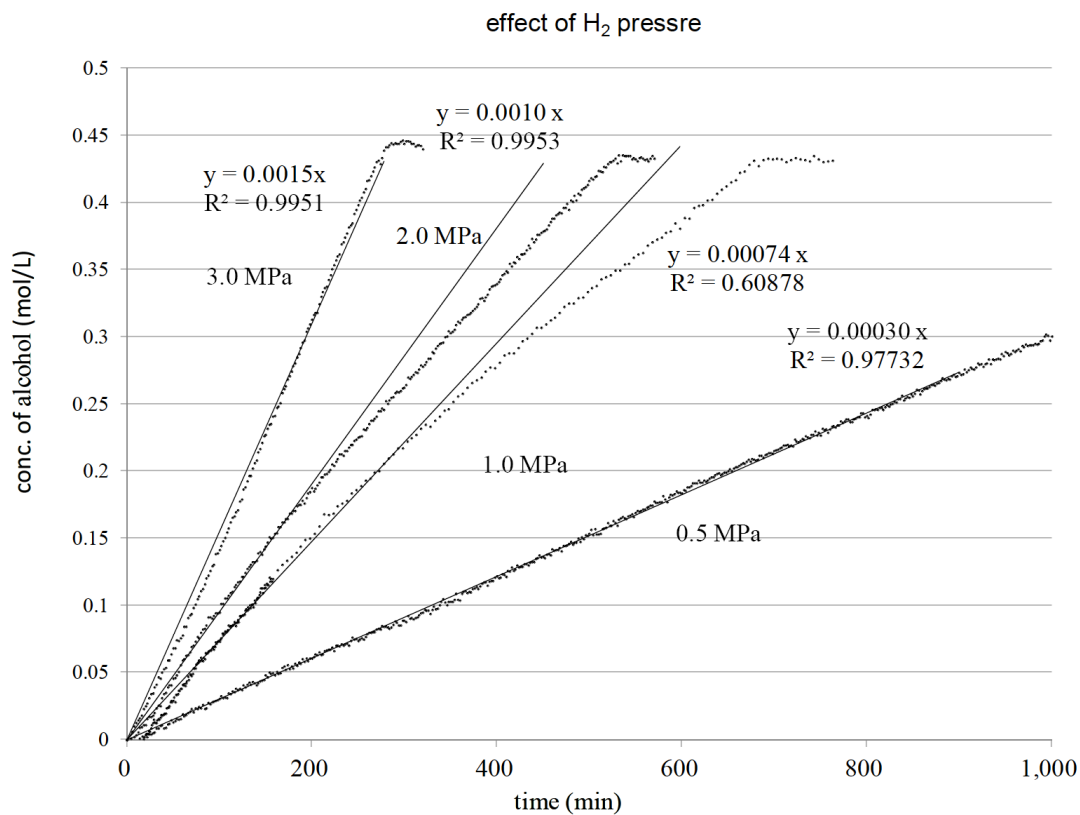**Figure 4-14.** Effect of CO pressure on the rate of hydrogenation fitted as linear line.

143

**Figure 4-15.** Effect of $H_2$ pressure on the rate of hydrogenation
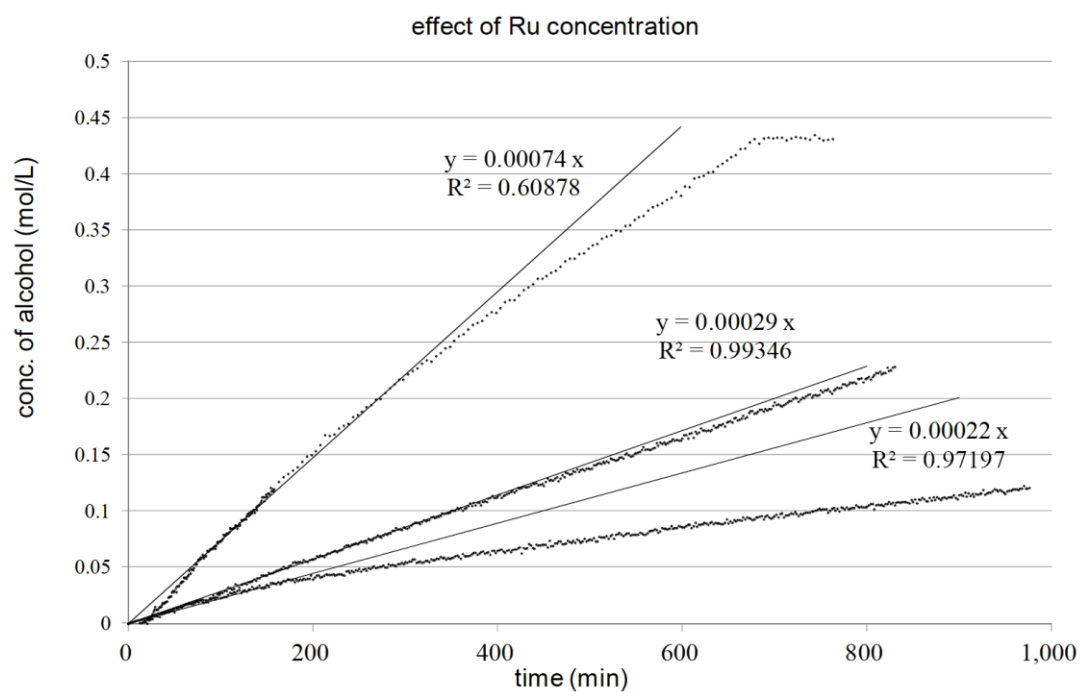


**Figure 4-16.** Effect of Ru concentration on the rate of hydrogenation
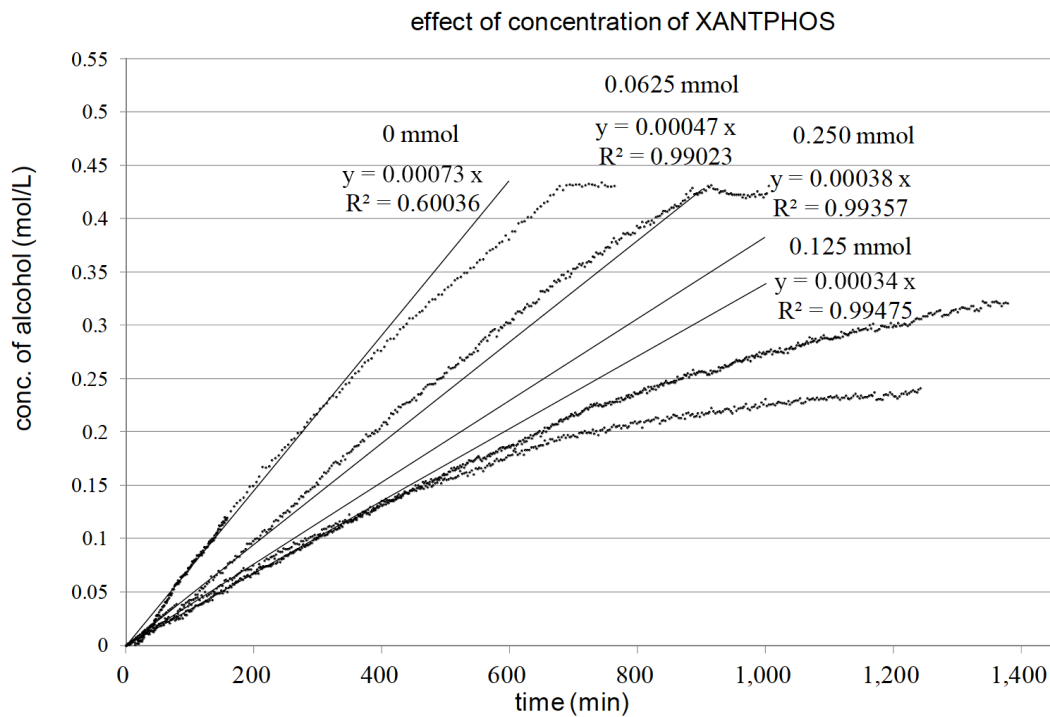
**Figure 4-17.** Effect of XANTPHOS concentration on the rate of hydrogenation

In the presence of more than one equivalent of XANTPHOS, the reaction rate gradually decreased, which could be ascribed to the decomposition of **1**. Possible decomposition pathway induced by XANTPHOS is dissociation of cyclopentadienone with the steric repulsion.

**Treatment of 1 under H$_2$/CO**

   **1** (50 mg, 92 µmol) was charged into autoclave under Ar and dissolved in toluene (2.0 mL). The autoclave was pressurized with 2.0 MPa of H$_2$/CO and stirred at 120 ºC for 2 hours. After cooled to room temperature, the pressure was released and the solution was transferred to glass vial in grove box. Evaporation of the solvent yielded slightly yellowish powder, which was confirmed to be almost pure Ru(CO)$_3$(2,3,4,5-tetraphenylcyclopentadienone) by $^1$H NMR and IR spectroscopy.

## References

1) (a) Lynn H. Slaugh, P. H., and Richard D. Mullineaux US 3239569, 1966; (b) Slaugh, L. H.; Mullineaux, R. D. *J. Organomet. Chem.* **1968**, *13*, 469. (c) John L. Van Winkle, S. L., Rupert C. Morris, Berkeley, and Ronald F. Mason, Mill Valley, Calif. US 3420898, 1969.

2) (a) MacDougall, J. K.; Cole-Hamilton, D. J. *J. Chem. Soc., Chem. Commun.* **1990**, 165. (b) Macdougall, J. K.; Simpson, M. C.; Cole-Hamilton, D. J. *Polyhedron* **1993**, *12*, 2877. (c) MacDougall, J. K.; Simpson, M. C.; Green, M. J.; Cole-Hamilton, D. J. *J. Chem. Soc., Dalton Trans.* **1996**, 1161.

3) Ichihara, T.; Nakano, K.; Katayama, M.; Nozaki, K. *Chem. Asian. J.* **2008**, *3*, 1722.

4) (a) (b) Knifton, J. F. *J. Mol. Cat.* **1988**, 47, 99. (c) Fleischer, I.; Dyballa, K. M.; Jennerjahn, R.; Jackstell, R.; Franke, R.; Spannenberg, A.; Beller, M. *Angew. Chem. Int. Ed.* **2013**, *52*, 2949.

5) (a) Drent, E.; Budzelaar, P. H. M. *J. Organomet. Chem.* **2000**, *593-594*, 211. (b) Konya, D.; Almeida Leñero, K. Q.; Drent, E. *Organometallics* **2006**, *25*, 3166.

6) Diab, L.; Šmejkal, T.; Geier, J.; Breit, B. *Angew. Chem. Int. Ed.* **2009**, *48*, 8022.

7) Boogaerts, I. I. F.; White, D. F. S.; Cole-Hamilton, D. J. *Chem. Commun.* **2010**, *46*, 2194.

8) Fuchs, D.; Rousseau, G.; Diab, L.; Gellrich, U.; Breit, B. *Angew. Chem. Int. Ed.* **2012**, *51*, 2178.

9) Kranenburg, M.; Vanderburgt, Y. E. M.; Kamer, P. C. J.; van Leeuwen P.W. N. M.; Goubitz, K.; Fraanje, J. *Organometallics* **1995**, *14*, 3081.

10) a) Noyori, R.; Ohkuma, T. *Angew. Chem. Int. Ed.* **2001**, *113*, 40. b) Conley, B. L.; Boggio, M. K. P.; Boz, E.; Williams, T. J. *Chem. Rev.* **2010**, *110*, 2294.

11) Vives, A. C.; Ujaque, G.; Lledos, A. *Organometallics* **2007**, *27*, 4854.

12) (a) Blum, Y.; Shvo, Y. *Inorg. Chim. Acta* **1985**, *97*, L25. (b) Shvo, Y.; Czarkie, D. *J. Organomet. Chem.* **1986**, *315*, C25. (c) Shvo, Y.; Czarkie, D.; Rahamim, Y.; Chodosh, D. F. *J. Am. Chem. Soc.* **1986**, *108*, 7400.

13) Choi, J. H.; Kim, Y. H.; Nam, S. H.; Shin, S. T.; Kim, M.-J.; Park, J. *Angew. Chem. Int. Ed.* **2002**, *41*, 2373.

14) Ito, M.; Hirakawa, M.; Osaku, A.; Ikariya, T. *Organometallics* **2003**, *22*, 4190.

15) Haack, K.-J.; Fujii, S. H.; Ikariya, T.; Noyori, R. *Angew. Chem. Int. Ed.* **1997**, *36*, 285.

16) Abdur-Rashid, K.; Guo, R.; Lough, A. J.; Morris, R. H.; Song, D. *Adv. Synth. Catal.* **2005**, *347*, 571.

17) Backvall, J. E.; Andresasson, U.; *Tetrahedron Lett.* **1993**, *34*, 5459.

18) Mays, M. J.; Morris, M. J.; Raithby, P. R.; Shvo, Y.; Czarkie, D., *Organometallics* **1989**, *8*, 1162.

19) (a) Casey, C. P.; Singer S.; Powell, D. R.; Hayashi, R. K.; Kavana, M. *J. Am. Chem. Soc.* **2001**, *123*, 1090. (b) Casey, C. P.; Johnson, J. B.; Singer, W. S.; Cui, Q. *J. Am. Chem. Soc.* **2005**, *127*, 3100. (c) Casey, C. P.; Strotman, N. A.; Beetner, S. E.; Johnson, J. B.; Priebe, D. C.; Guzei, I. A. *Organometallics,* **2006**, *25*, 1236. (d) Casey, C. P.; Beetner, S. E.; Johnson, J. B. *J. Am. Chem. Soc.* **2008**, *130*, 2285.

20) Multiple species are possibly formed under $H_2/CO$. There is a report isolating $H_4Ru_4(CO)_{12}$ by treating $Ru_3(CO)_{12}$ under high $H_2/CO$ pressure: Piacenti, F.; Bianchi, M.; Frediani, P.; Benedetti, E. *Inorg. Chem.* **1971**, *10*, 2759. It was proposed that $Ru(CO)H_2(PPh_3)_3$ is converted to $Ru(CO)_2H_2(PPh_3)_2$ under $H_2/CO$: Delgado, R. A. S.; Bradley, J. S.; Wilkinson, G. *J. Chem. Soc., Dalton Trans.* **1976**, 399.

21) Sabitha, G.; Swapna, R.; Reddy, E. V.; Yadav, J. S. *Synthesis*, **2006**, *24*, 4242.

22) Rawat, V.; Chouthaiwale, P. V.; Suryavanshi, G.; Sdalai, A. *Tetrahedron Asym.* **2009**, *20*, 2173.

23) Rotulo-Sims, D.; Prunet, J. *Org. Lett.* **2002**, *4*, 4701.

24) Lipshutz, B. H.; Ghorai, S.; Leong, W. W. Y.; Taft, B. R. *J. Org. Chem.* **2011**, *76*, 5061.

25) Breit, B.; Seiche, W. *J. Am. Chem. Soc.* **2003**, *125*, 6608.

26) Altomare, A.; Burla, M. C.; Camalli, M.; Cascarano, G. L.; Giacovazzo, C.; Guagliardi, A.; Moliterni, A. G. G.; Polidori, G.; Spagna, R., *J. Appl. Crystallogr.* **1999**, *32*, 115.

27) (a) Sheldrick, G. M. SHELXL-97, Program for the Refinement of Crystal Structures, University of Göttingen: Göttingen, Germany, 1997. (b) Sheldrick, G. M.; Schneider, T. R., SHELXL: High-resolution refinement. In *Macromolecular Crystallography, Pt B*, Academic Press Inc: San Diego, 1997; Vol. 277, 319.

# Chapter 5

# Conclusion

## 5 Conclusion

In this dissertation, the author developed three catalyst systems to solve problems of currently performed hydroformylation process.

1) The author developed cyclopentadienylruthenium/bisphosphine or bisphosphite system for *normal*-selective hydroformylation.

2) The author found hydroxycyclopentadienylruthenium/bisphosphine system for tandem *normal*-selective hydroformylation/hydrogenation.

3) The author established rhodium/ruthenium dual catalyst system for high yielding and more facil tandem *normal*-selective hydroformylation/hydrogenation.

In the first topic, design of new type of catalyst is proposed. When cyclopentadienyl ruthenium/bisphosphine or bisphosphite system for *normal*-selective hydroformylation is compared to the previously reported ruthenium-based systems, *n/i* selectivity was highest level both in propene and 1-decene, selectivity to aldehyde and reaction rate were comparable. When it is compared to representative rhodium or cobalt catalyst, *n/i* ratio is comparable to rhodium, and higher than cobalt. Selectivity to aldehyde and reaction rate were still significantly lower. Cyclopentadienyl was essential for suppressing side reactions such as hydrogenation of alkenes or aldehyde, dimerization of product aldehydes by aldol reaction or acetalization. Existence of bidentate phosphorus ligand was essential for high *n/i* ratio. Although bidentate coordination of the ligand to cyclopentadienylruthenium was confirmed in the catalyst precursor, the true active

species in the catalytic cycle is not clear so far. Further improvement of catalytic activity was achieved by changing pentamethyl cyclopentadienyl to indenyl or 1,2,3-trimethylindenyl. This result suggested $\eta^3$-Cp intermediate is involved in the rate determining step. Therefore, further modification of Cp group might increase the catalytic activity. Considering that the price of ruthenium is roughly 1/10 of rhodium, TOF ~ 100 is a target value, although there are still other problems remaining such as stability, separation, and reuse of catalyst.

When hydroxycyclopentadienylruthenium/bisphosphine system is compared to previously reported tandem hydroformylation/hydrogenation rhodium-based catalyst, $n/i$ ratio is on of the highest, selectivity to alcohol is moderate, and reaction rate is slow. Especially, $n/i$ selectivity is highest as a single metal and single ligand system.

As a tandem hydroformylation/hydrogenation catalyst, rhodium/ruthenium dual catalyst system exhibited highest level of $n/i$ ratio, selectivity to alcohol, and moderate reaction rate. It would be more promising if the slow rate of hydrogenation is overcome. Mechanistic investigation revealed that poisoning of hydrogenation catalyst by the coordination of CO is problematic, and electron poor ruthenium complex was suggested to be effective.

# 6 List of Publications

**Original papers**

1) Takahashi, K.; Yamashita, M.; Ishihara, T.; Nakano, K.; Nozaki, K.

"High-Yielding Tandem Hydroformylation/Hydrogenation of a Terminal Olefin to Produce a

Linear Alcohol Using a Rh/Ru Dual Catalyst System"

*Angew. Chem. Int. Ed.* **2010**, *48*, 4488-4490.


2) Takahashi, K.; Yamashita, M.; Tanaka, Y.; Nozaki, K.

"Ruthenium/$C_5Me_5$/Bisphosphine- or Bisphosphite-Based Catalysts for normal-Selective

Hydroformylation"

*Angew. Chem. Int. Ed.* **2012**, *51*, 4383-4387.


3) Takahashi, K.; Yamashita, M.; Nozaki, K.

"Tandem Hydroformylation/Hydrogenation of Alkenes to Normal Alcohols Using Rh/Ru Dual

Catalyst or Ru Single Component Catalyst"

*J. Am. Chem. Soc.* **2012**, *134*, 18746-18757.


**Other publication that are not included in this thesis**

1) Yuki, Y.; Takahashi, K.; Nozaki, K. "Tandem Isomerization/Hydroformylation/

Hydrogenation of Internal Alkenes to *normal*-Alcohols Using Rh/Ru Dual or Ternary Catalyst

Systems", submitted for publication.

**Review**

1) Takahashi, K.; Nozaki, K.

"ヒドロホルミル化"

*触媒調製ハンドブック*, NTS Inc. **2011**, 第 4 編, 第 9 章, 370-374.


2) Takahashi, K.; Nozaki, K.

"Hydroformylation of epoxide"

*Science of synthesis*,

in press

# 7 Acknowledgement